NASA TECHNICAL NOTE

NASA TN D-2205

C. 1

NASA TN D-2205

LOW-SPEED CHARACTERISTICS OF A 1/20-SCALE FOUR-ENGINE TRANSPORT MODEL WITH LARGE BODIES MOUNTED ABOVE THE FUSELAGE

by Vernard E. Lockwood

Langley Research Center
Langley Station, Hampton, Va.

NATIONAL AERONAUTICS AND SPACE ADMINISTRATION • WASHINGTON, D. C. • MARCH 1964

LOW-SPEED CHARACTERISTICS OF A

1/20-SCALE FOUR-ENGINE TRANSPORT MODEL WITH LARGE BODIES

MOUNTED ABOVE THE FUSELAGE

By Vernard E. Lockwood

Langley Research Center
Langley Station, Hampton, Va.

NATIONAL AERONAUTICS AND SPACE ADMINISTRATION

For sale by the Office of Technical Services, Department of Commerce,
Washington, D.C. 20230 -- Price $1.75

LOW-SPEED CHARACTERISTICS OF A 1/20-SCALE FOUR-ENGINE TRANSPORT MODEL WITH LARGE BODIES MOUNTED ABOVE THE FUSELAGE

By Vernard E. Lockwood

SUMMARY

An investigation was made at a Mach number of 0.2 to determine the aerodynamic characteristics of a 1/20-scale model of a transport airplane having bodies with diameters greater than the fuselage mounted above the fuselage. The bodies represented were the Saturn first stage, a Saturn upper stage, and a capsule large enough to contain either stage. All bodies had nose and tail fairings.

The addition of bodies to the airplane model resulted in a large loss of directional stability. The airplane-capsule configuration required a vertical-tail area about $2\frac{1}{2}$ times the original area to provide satisfactory directional characteristics. Although the bodies had a detrimental effect on the longitudinal stability, the modifications to the vertical and horizontal tails that were necessary for directional stability resulted in the combinations having greater longitudinal stability than the basic model. The minimum drag of the airplane-body combinations were 50 to 70 percent greater than that of the original airplane configuration.

INTRODUCTION

This investigation was made to explore the possibility of transporting large booster rockets such as the Saturn by airplane. One method proposed by an aircraft company was a "pickaback" arrangement of booster rocket and transport. The proposal called for mounting a streamlined version of the Saturn upper stage booster rocket above the wing of a transport airplane. Additional proposals were made for carrying the full-size Saturn booster or a capsule large enough to contain either stage. Because of the size of these bodies, which have a diameter considerably greater than the airplane fuselage, it would be expected that the aerodynamics of the combination would be materially altered. Also it might be reasoned from the length of the capsule and its nearness to the vertical tail that the directional stability of the model might be seriously impaired. It is the purpose of this investigation to determine how the aerodynamic characteristics of the airplane would be affected by the addition of the bodies and what modifications might be made to the model in order to retain a desired level of stability. Emphasis was placed on finding tail configurations which would not entail large and costly modifications to the airplane. With this in mind, many horizontal- and vertical-tail combinations related to the original tail were tested. The vertical-tail configurations varied in size, aspect ratio, shape, and number.

Results are presented for a 1/20-scale model of a transport airplane and for combinations of the model with the Saturn upper stage, the Saturn first stage, or a capsule large enough to contain either stage. For all tests the model propellers were removed. Rudder, elevator, and flap effectiveness was determined for some airplane-body configurations. The model was tested at a sideslip angle of 0° over an angle-of-attack range from -8° to 13° and at an angle of attack of about 0° over a sideslip range from -8° to 16°. In addition, a few tests were made over an angle-of-attack range from -8° to 13° at a sideslip angle of 5°. The tests were made at a Mach number of 0.2 which corresponds to a Reynolds number of about 1,390,000 per foot. The results are presented without extensive analysis.

SYMBOLS

The force and moment coefficients are referred to the stability-axis system, which is shown in figure 1. The reference dimensions used for reducing the data are those of a 1/20-scale model of the airplane shown in figure 2. The moment reference point was located at a position 810 inches behind the nose of the airplane and 234 inches above the bottom of the fuselage which corresponds to the center of gravity of the proposed airplane-body combinations shown in figures 3 to 5.

b span of model, 8.983 ft

$\bar{c}$ mean aerodynamic chord of model, 0.843 ft

C_D drag coefficient, $\frac{\text{Longitudinal force}}{qS}$

C_L lift coefficient, $\frac{\text{Lift}}{qS}$

C_l rolling-moment coefficient, $\frac{\text{Rolling moment}}{qSb}$

C_{l_β} effective dihedral parameter, $\frac{\partial C_l}{\partial \beta}$, per deg

C_m pitching-moment coefficient, $\frac{\text{Pitching moment}}{qS\bar{c}}$

C_n yawing-moment coefficient, $\frac{\text{Yawing moment}}{qSb}$

C_{n_β} directional-stability parameter, $\frac{\partial C_n}{\partial \beta}$, per deg

C_Y side-force coefficient, $\frac{\text{Side force}}{qS}$

C_{Y_β} side-force parameter, $\frac{\partial C_Y}{\partial \beta}$, per deg

q free-stream dynamic pressure, lb/sq ft

S wing area, 6.683 sq ft

α angle of attack of fuselage reference line, deg

β angle of sideslip, deg

δ surface deflection, deg

Subscripts:

e elevator

f flap

r rudder

MODEL DESCRIPTION

Airplane

A 1/20-scale model of the Douglas C-133 airplane which is a high-wing, four-engine turboprop transport was used as the carrier vehicle in the wind-tunnel investigation reported herein. A three-view drawing of the full-scale airplane is given in figure 2 and a photograph of the 1/20-scale model in combination with one of the bodies tested is presented in figure 6. Dimensions of the basic model are also given in table I. Although the wing of the model was equipped with engine nacelles no propellers were used in the investigation.

Three body configurations were tested in combination with the airplane model; they are the Saturn first-stage booster, a Saturn upper stage, and a cylinder or capsule large enough to contain either stage.

Capsule

The capsule which had a diameter 268.0 inches and overall length of 1404.0 inches (full scale) was made up of three sections, a hemispherical nose, a cylindrical midsection, and a tail fairing. Two tail fairings were used on the capsule, one having a circular cross section and the other having an elliptical cross section as shown in figures 3 and 4, respectively. Initially the capsule was supported by four airfoil-shape struts but during the investigation the forward struts were replaced by round ones. The capsule was tested in two positions on the fuselage, the "basic position" and the "rear position." In these two positions different shrouds were used. The long rear shrouds were used with the capsule in the basic position in figure 3 and the short forward shrouds when the capsule was mounted in the rear position in figure 4.

Saturn First Stage

The Saturn first stage, which is referred to as S-I, is a body with the same overall dimensions as the capsule. In order to simulate the S-I a section of the cylinder of the capsule was replaced by eight smaller cylinders arranged in a circle as shown in the upper sketch of figure 4. A fairing at each end of the eight cylinders completed the configuration. The S-I model was tested in only the rear position and with only the round support strut.

Saturn Upper Stage

A sketch of the Saturn upper stage booster (S-IV) which had a diameter of 220 inches (full scale) and an overall length of 837 inches is given in figure 5. The booster was mounted on a bracket called a test bed which in turn was mounted above the wing of the airplane. The booster was detachable so that the bed could be tested in combination with the airplane model.

Tail Configurations

The various tail configurations used on the model are shown in figure 7. Several of these configurations made use of the basic stabilizer as shown in figures 7(a) to 7(d). Other configurations used a constant-chord stabilizer with the vertical tails as shown in figures 7(e), 7(f), and 7(g). The dimensions shown in figure 7 are full scale; the figures in parentheses associated with each surface are the area in square feet and the aspect ratio. The data from a particular tail configuration are also identified in a like manner on the data plots. The vertical tail of the basic configuration is referred to as the fin on the data plots and the auxiliary vertical surfaces are referred to as end plates. If both end plates and fin are off, the horizontal tail is also off.

TESTS AND CORRECTIONS

The investigation was made in the Langley 300-MPH 7- by 10-foot tunnel at a Mach number of 0.2 which corresponds to a dynamic pressure of 57.5 pounds per square foot. The Reynolds number of the tests was approximately 1,390,000 per foot of length. Transition strips approximately 1/8 inch wide of No. 100 carborundum grit were placed on bodies and surfaces at approximately 10 percent of their length to insure turbulent flow over the model.

The forces and moments were measured on the mechanical balance system which surrounds the tunnel test section.

Blockage corrections determined by the method of reference 1 have been applied to the dynamic pressure and drag, and jet-boundary corrections determined by the method of reference 2 have been applied to the angle of attack and the pitching-moment and drag coefficients. Drag coefficients have also been corrected for tunnel buoyancy effects.

PRESENTATION OF DATA

An index of data figures 8 to 31 is presented in table II. A summary of the aerodynamic characteristics is presented in figures 32 and 33 for some model configurations.

SUMMARY OF RESULTS

The addition of the bodies to the airplane model resulted in a large loss of directional stability (see fig. 8) which could be overcome by the addition of a large amount of vertical-tail area. Several configurations involving end plates and the original vertical tail gave marginal directional stability but only the twin vertical tails with an area about $2\frac{1}{2}$ times the original area gave a large degree of directional stability with no appreciable nonlinearities in the curve for yawing-moment coefficient as a function of sideslip angle (fig. 32). The combination of the airplane model and the S-IV booster required the addition of end plates with a total area about equal to that of the center fin to give directional stability equivalent to that of the basic airplane configuration (fig. 32). The modifications to the vertical and horizontal tails that were necessary for directional stability resulted in the model having greater longitudinal stability than with the basic tail configuration. Addition of the S-IV or the capsule increased the minimum drag about 50 and 70 percent, respectively, over that for the basic model (fig. 33).

Langley Research Center,
National Aeronautics and Space Administration,
Langley Station, Hampton, Va., December 11, 1963.

REFERENCES

1. Herriot, John G.: Blockage Corrections for Three-Dimensional-Flow Closed-Throat Wind Tunnels, With Consideration of the Effect of Compressibility. NACA Rep. 995, 1950. (Supersedes NACA RM A7B28.)

2. Gillis, Clarence L., Polhamus, Edward C., and Gray, Joseph L., Jr.: Charts for Determining Jet-Boundary Corrections for Complete Models in 7- by 10-Foot Closed Rectangular Wind Tunnels. NACA WR L-123, 1945. (Formerly NACA ARR L5G31.)

TABLE I.- BASIC DIMENSIONS OF 1/20-SCALE MODEL OF AIRPLANE

Wing:	
Area, sq ft	6.683
Span, ft	8.983
Mean aerodynamic chord, ft	0.843
Aspect ratio	12.07
Taper ratio	0.228
Airfoil section:	
Root	Modified NACA 23017
Tip	Modified NACA 23015
Total flap area aft of hinge, sq ft	1.239
Flap mean chord aft of hinge line, ft	0.222
Maximum cross-sectional area of engine nacelle:	
Inboard, sq ft	0.072
Outboard, sq ft	0.071
Horizontal tail:	
Area, sq ft	2.002
Span, ft	3.000
Mean aerodynamic chord, ft	0.722
Aspect ratio	4.50
Taper ratio	0.348
Airfoil section:	
Root	NACA 64_1A012
Tip	NACA 64A010.7
Elevator area, sq ft	0.301
Elevator mean chord aft of hinge line, ft	0.239
Vertical tail:	
Area, sq ft	1.342
Span, ft	1.575
Mean aerodynamic chord, ft	0.923
Aspect ratio	1.85
Taper ratio	0.345
Airfoil section:	
Root	NACA 64_1A012
Tip	NACA 64A010.7
Rudder area aft of hinge line, sq ft	0.343
Rudder mean chord aft of hinge line, ft	0.289

TABLE II.- INDEX OF FIGURES

Body	Stabilizer	Fin	End plate	Capsule position	Tail fairing	Strut shape	α, deg	β, deg	δ_r, deg	δ_e, deg	δ_f, deg	Figure
Capsule[a]	Basic[a]	[a](537-1.85)	[a](266-1.73)	Basic	Circular	Airfoil	0.42	-8 to 16	0	0	0	8
Capsule[a]	Basic[a]	[a](537-1.85)	[a](266-1.73)	Basic	Circular	Airfoil	-8 to 13	0, 5	0			9
Capsule	Basic	(537-1.85)	(266-1.73)	Basic	Both	Airfoil	0.43	-8 to 16	0	0	0	10
Capsule	Basic	(537-1.85)	(266-1.73)	Basic	Circular	Both	0.43	-8 to 16	0	0	0	11
Capsule	Basic	(537-1.85)	(266-1.73)	Basic	Circular	Round	0.44	0	-8 to 20	0	0	12
Capsule[a]	Basic[a]	[a](537-1.85)	[a](266.173)	Basic	Circular	Airfoil	-8 to 13	0	0	0	0	13
Capsule	Basic	Various	(420-2.08)	Rear	Elliptical	Round	0.44	-8 to 16	0	0	0	14
S-I or capsule	Basic	(591-2.68)	(420-2.08)	Rear	Elliptical	Round	0.43	-8 to 16	0	0	0	15
Capsule[a]	Basic	(591-2.68)	(420-2.08)	Rear	Elliptical	Round	0.42	-8 to 16	0, 20	0	0	16
S-I[a] or capsule[a]	Basic	Various	(420-2.08)	Rear	Elliptical	Round	-8 to 13	0	0	0	0	17
Capsule	Constant chord[a]	Various[a]	[a](420-2.08)	Rear	Elliptical	Round	0.44	-8 to 16	0	0	0	18
Capsule[a]	Constant chord	(588-2.48)	(420-2.08)	Rear	Elliptical	Round	0.42	-8 to 16	0	0	0	19
Capsule[a]	Constant chord[a]	[a](588-2.48)	[a](420-2.08)	Rear	Elliptical	Round	-8 to 13	0, 5	0	0	0	20
Capsule[a]	Constant chord	Off	(420-2.08)	Rear	Elliptical	Round	0.42	-8 to 16	0	0	0	21
Capsule	Constant chord	Off	(420-2.08)	Both	Both	Round	0.43	-8 to 16	0	0	0	22
Capsule[a]	Constant chord[a]	Off	[a](420-2.08)	Rear	Elliptical	Round	-8 to 13	0	0	0	0	23
Capsule[a]	Constant chord	Off	(663-2.31)	Rear	Elliptical	Round	0.42	-8 to 16	0	0	0	24
Capsule[a]	Constant chord	Off	(663-2.31)	Rear	Elliptical	Round	1.20	-8 to 16	0	0	40	25
Capsule[a]	Constant chord	Off	(663-2.31)	Rear	Elliptical	Round	-8 to 13	0	0	0	0	26
Capsule[a]	Constant chord	Off	(663-2.31)	Rear	Elliptical	Round	-10 to 7	0	0	0, 5	40	27
S-IV[a]	Basic[a]	[a](537-1.85)	Various[a]	-----	-----------	-------	0.41	-8 to 16	0	0	0	28
S-IV	Basic	(537-1.85)	(266-1.73)	-----	-----------	-------	0.41	-8 to 16	0, 10	0	0	29
S-IV[a]	Basic[a]	[a](537-1.85)	[a](266-1.73)	-----	-----------	-------	-8 to 13	0	0	0	0	30
S-IV bed[a]	Basic	(537-1.85)	(266-1.73)	-----	-----------	-------	-8 to 13	0	0	0	0	31

[a]Figures also include data with component off.

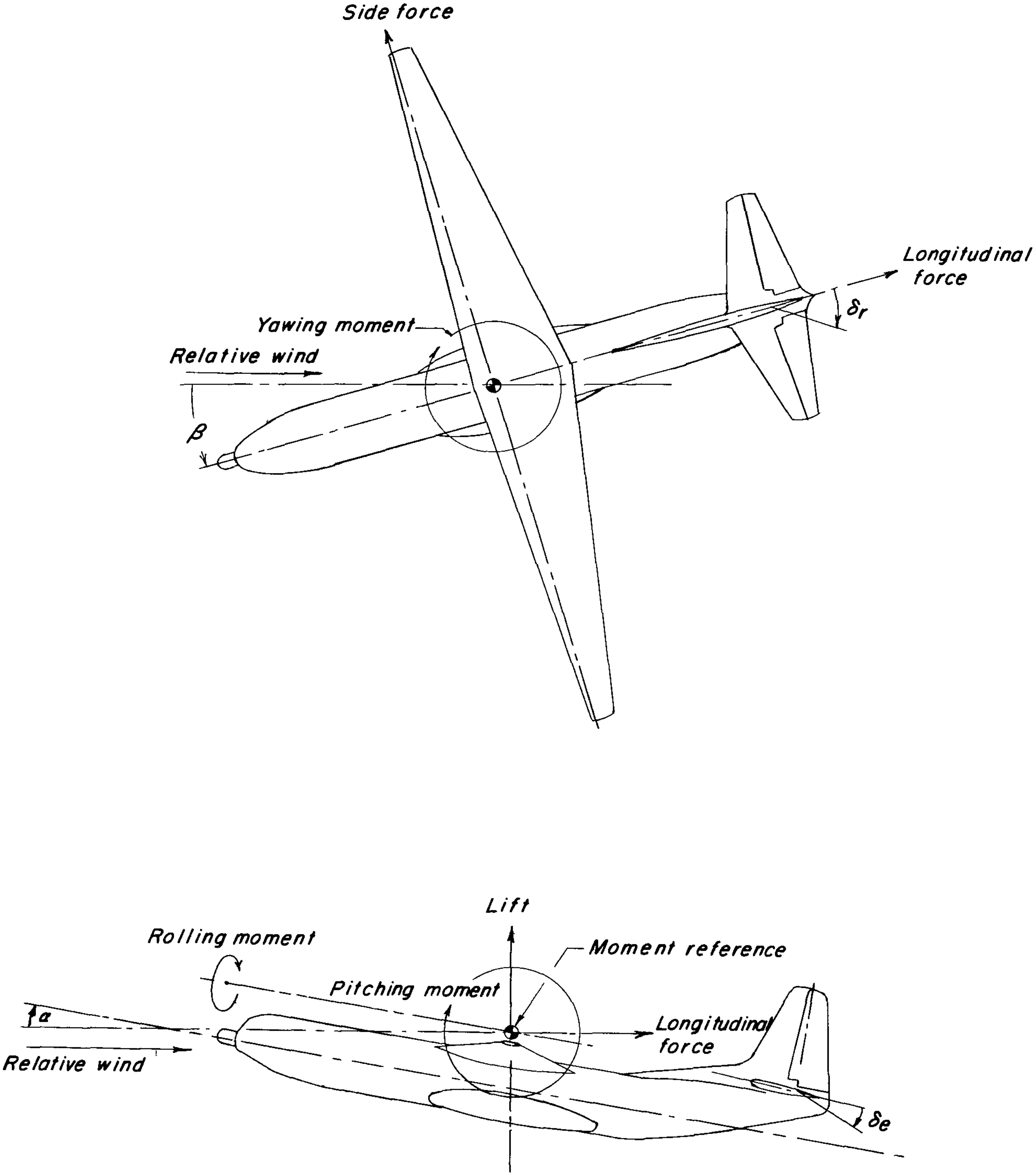

Figure 1.- Stability-axis system.

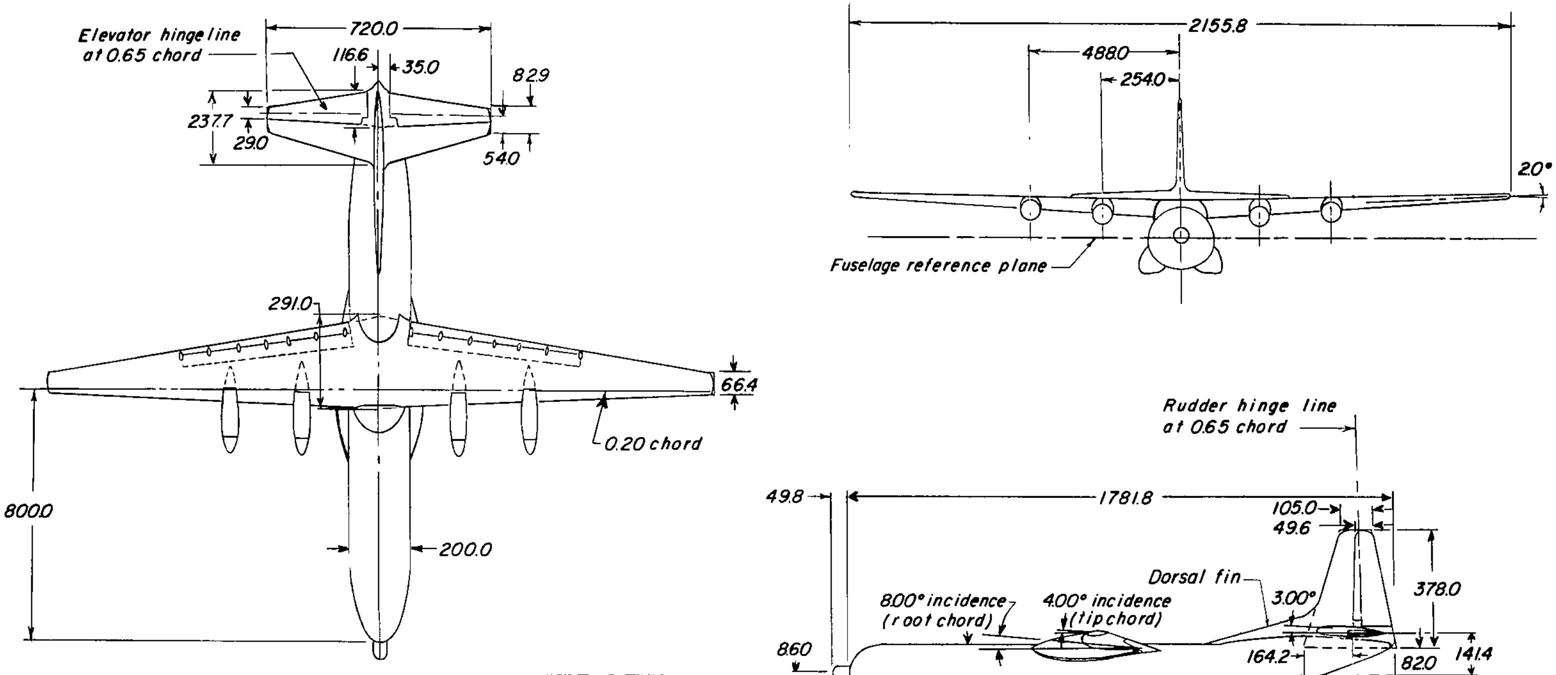

Reference dimensions

	Airplane	Model
Wing area, sq ft	2673.2	6.683
Mean aerodynamic chord, ft	16.86	.843
Span, ft	179.66	8.983

Figure 2.- Three-veiw drawing of basic airplane. All linear dimensions are in inches unless otherwise indicated.

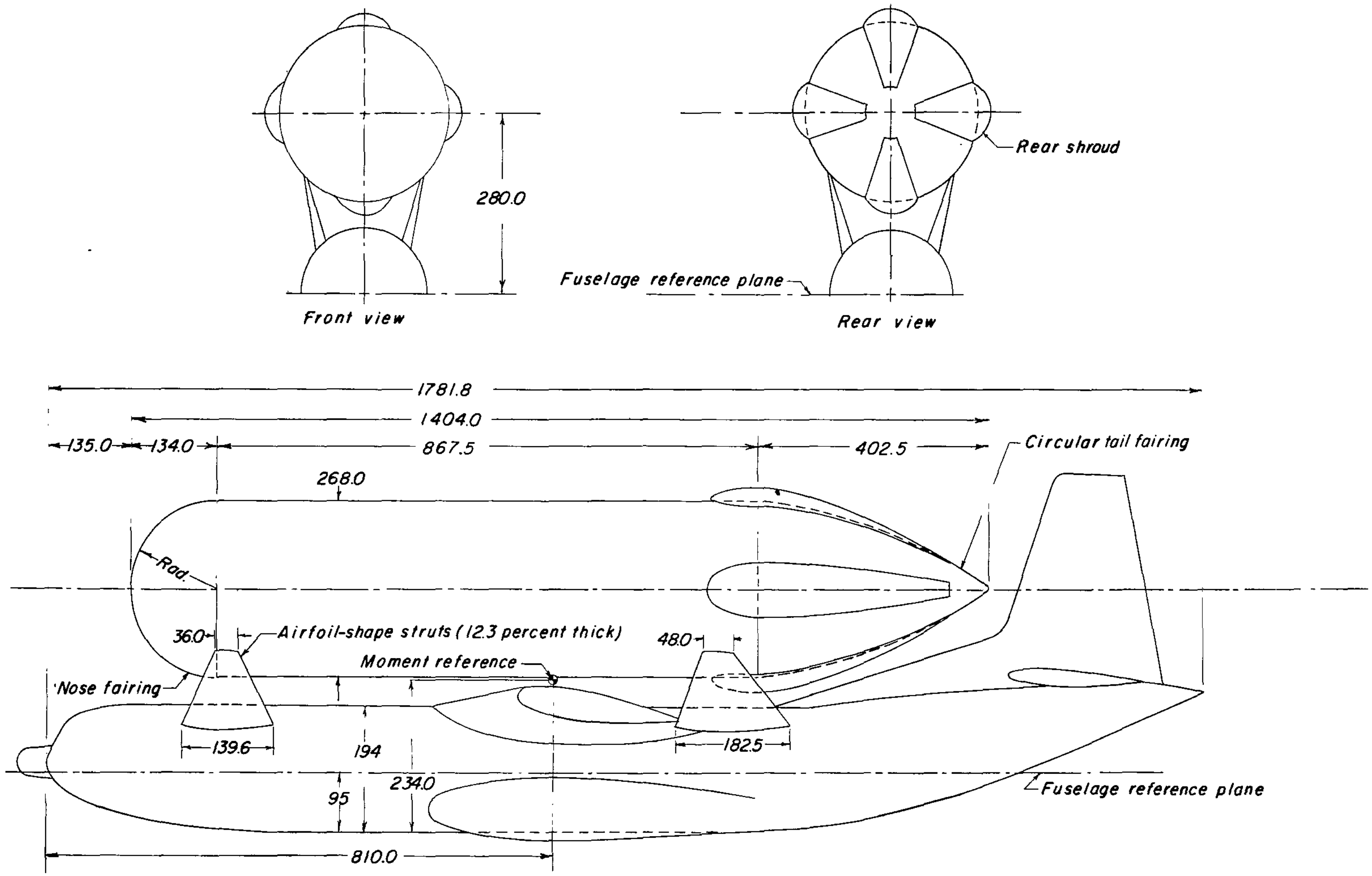

Figure 3.- Capsule mounted on airplane in basic position. Linear dimensions are in inches.

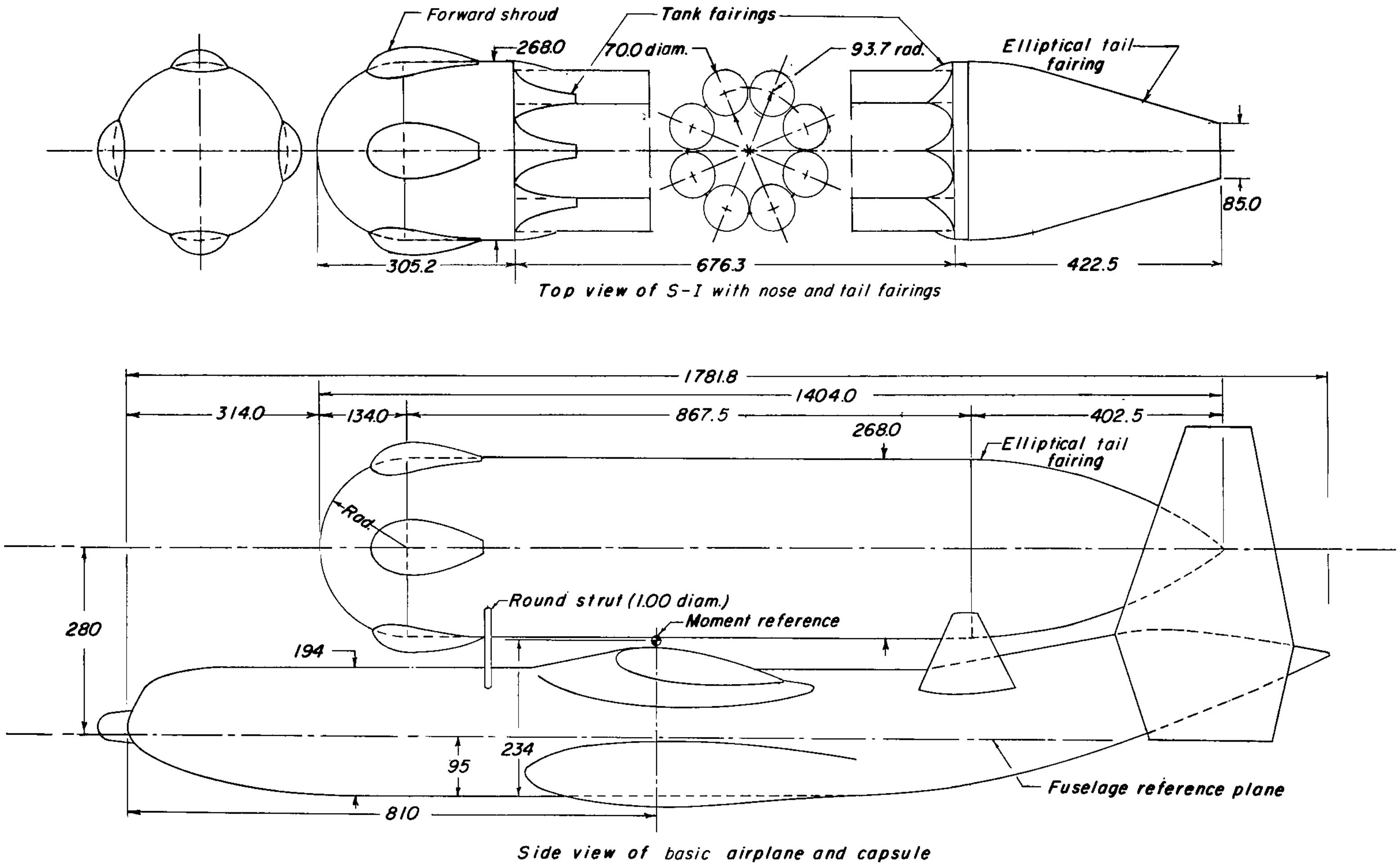

Figure 4.- Capsule and S-I mounted on airplane in rear position. Linear dimensions are in inches.

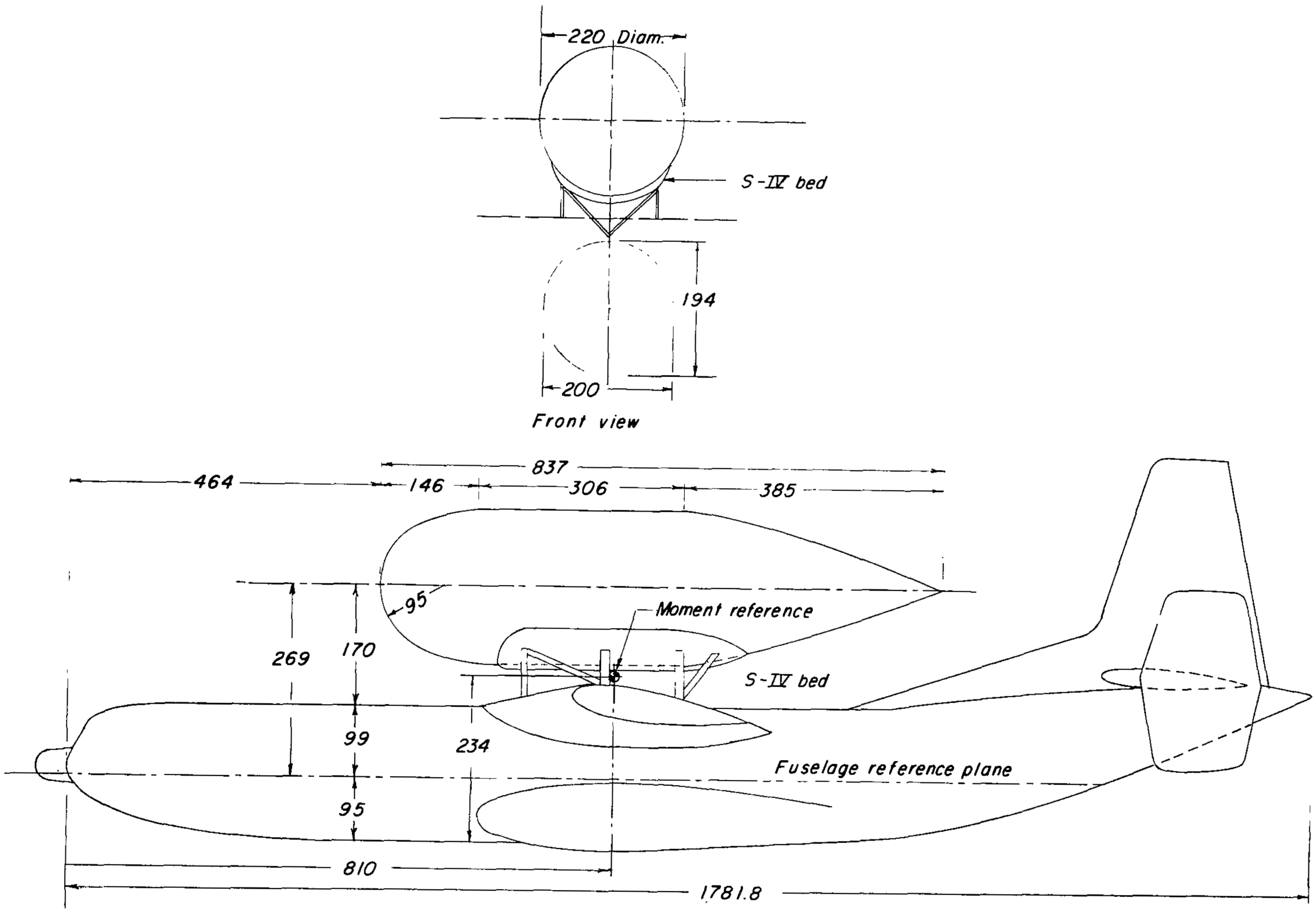

Figure 5.- S-IV booster mounted on airplane. Linear dimensions are in inches.

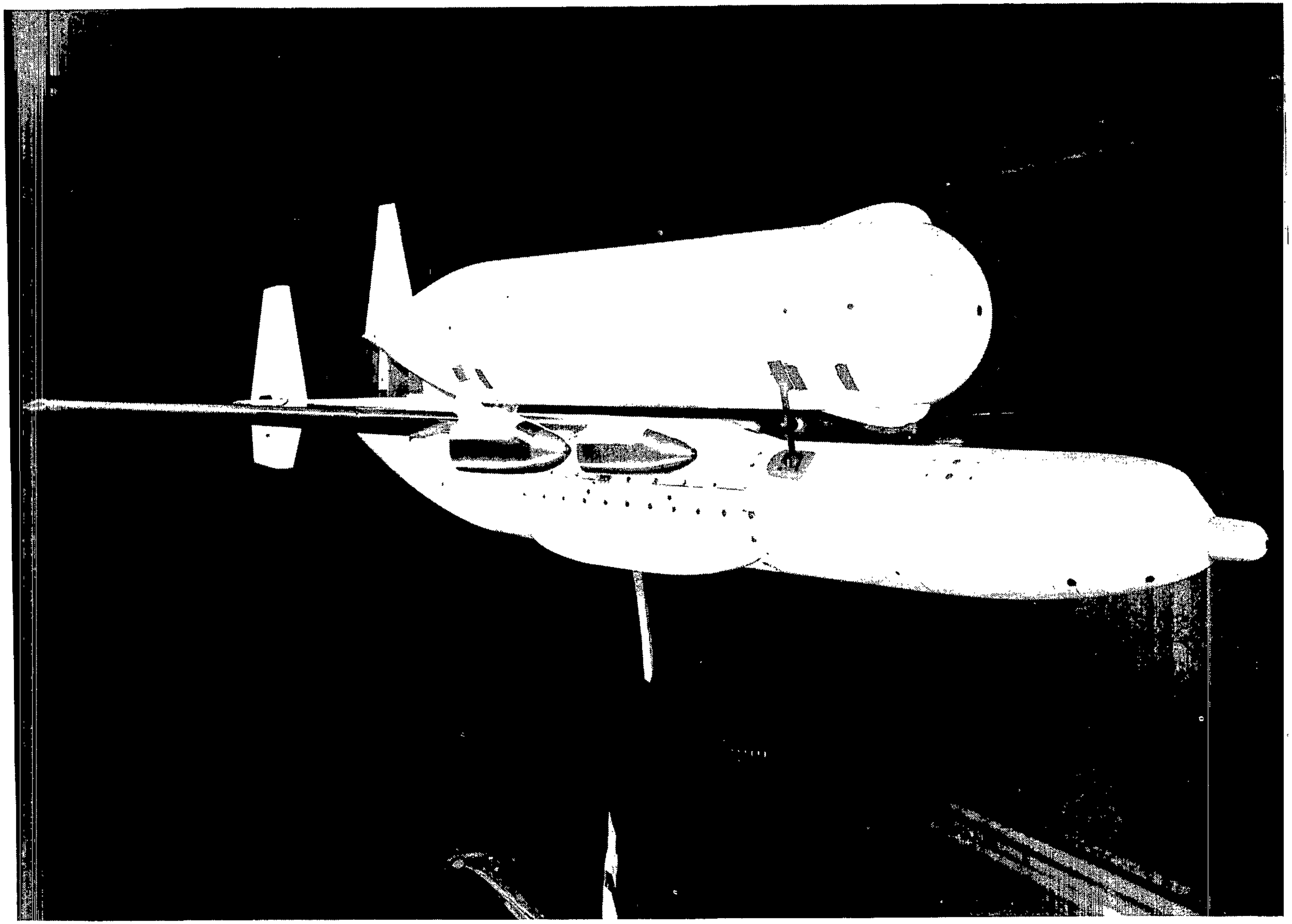

L-61-1729

Figure 6.- Photographs of 1/20-scale model of capsule and basic airplane configuration mounted in Langley 300-MPH 7- by 10-foot tunnel. Inset end plates (420-2.08) on basic stabilizer (591-2.68); elliptical tail fairing; rear capsule position; round support struts.

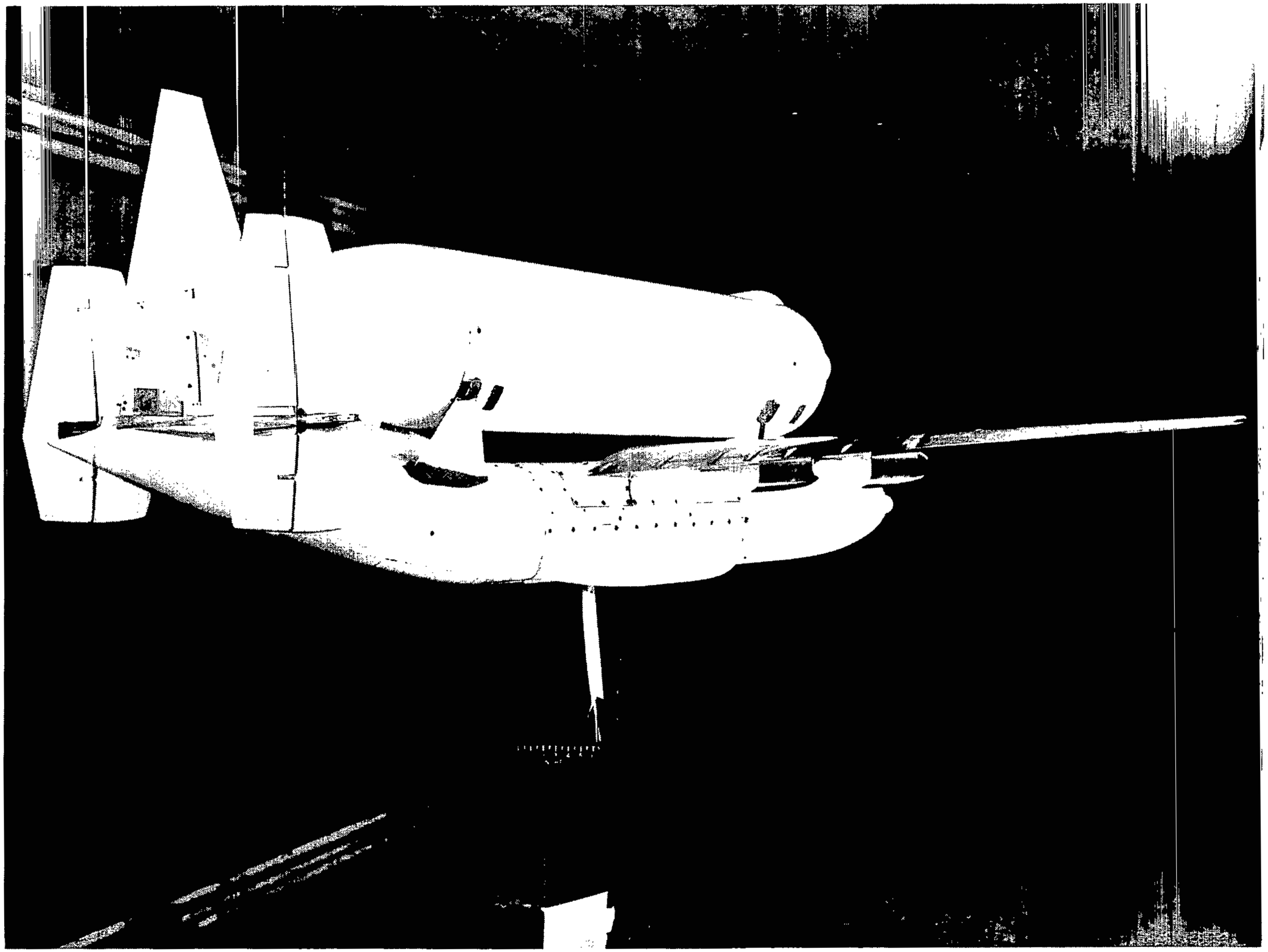

Figure 6.- Concluded. L-61-1730

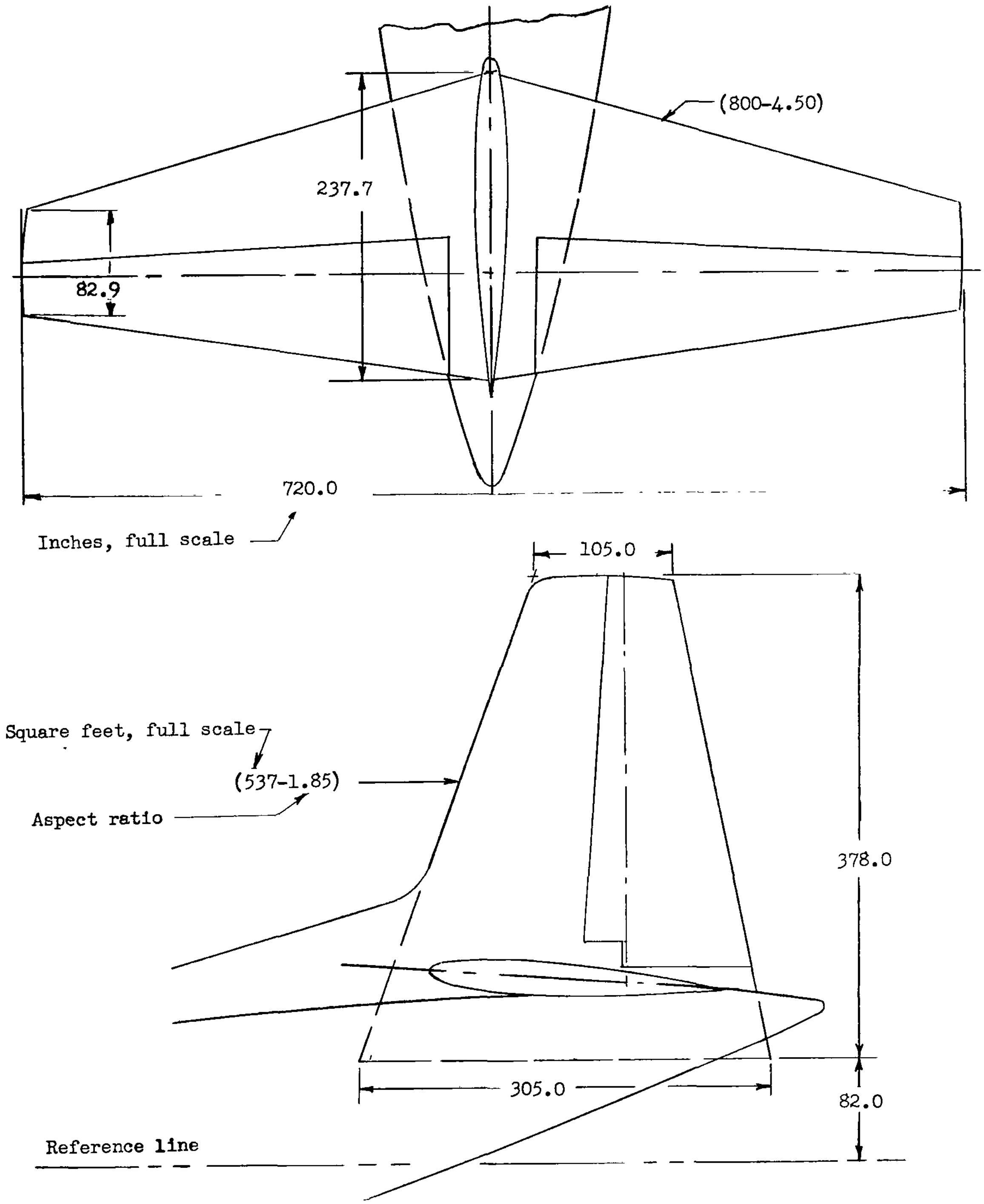

(a) Basic tail.

Figure 7.- Drawings of tail assemblies on model.

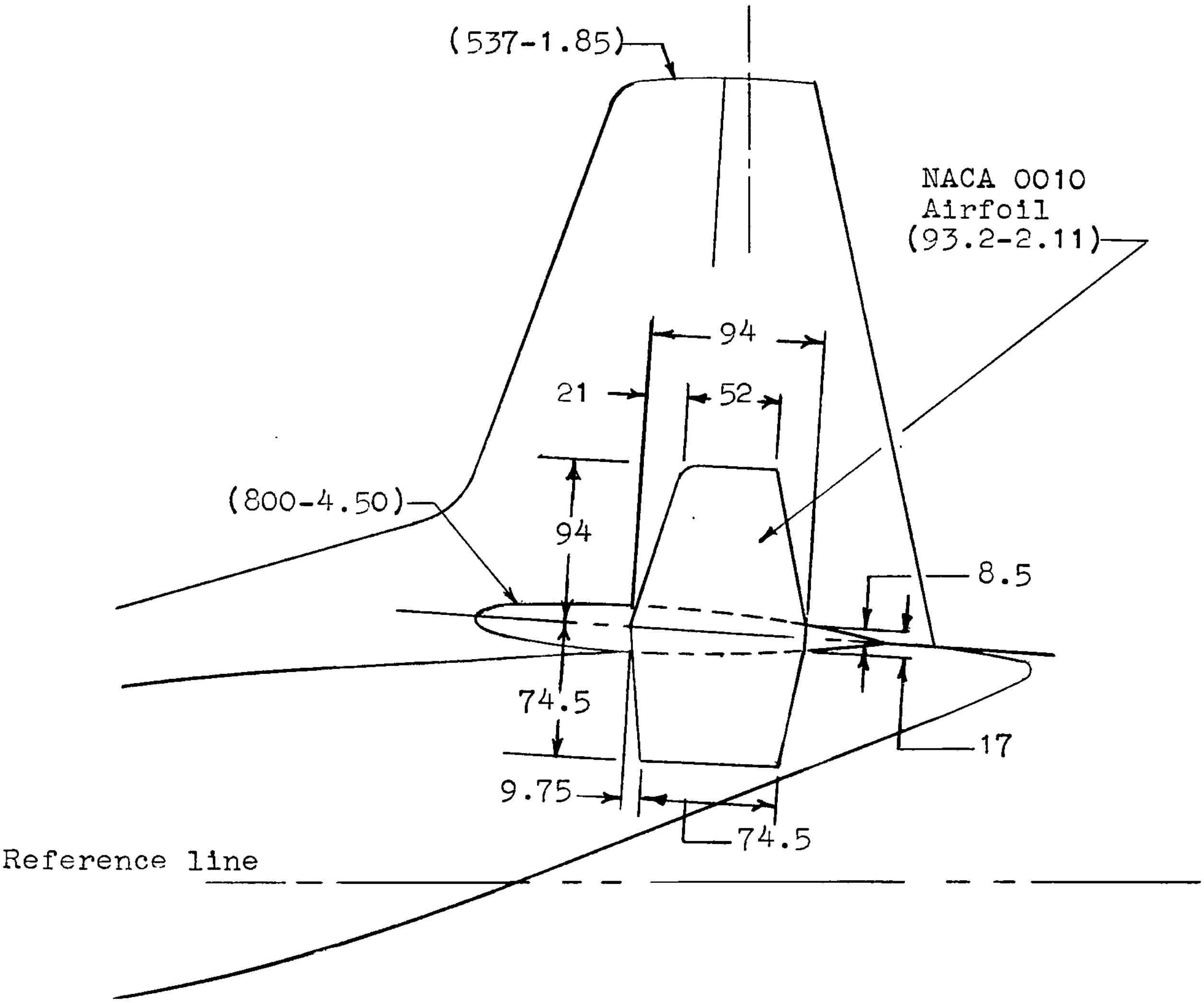

(b) End plates (93.2-2.11) on basic tail.

Figure 7.- Continued.

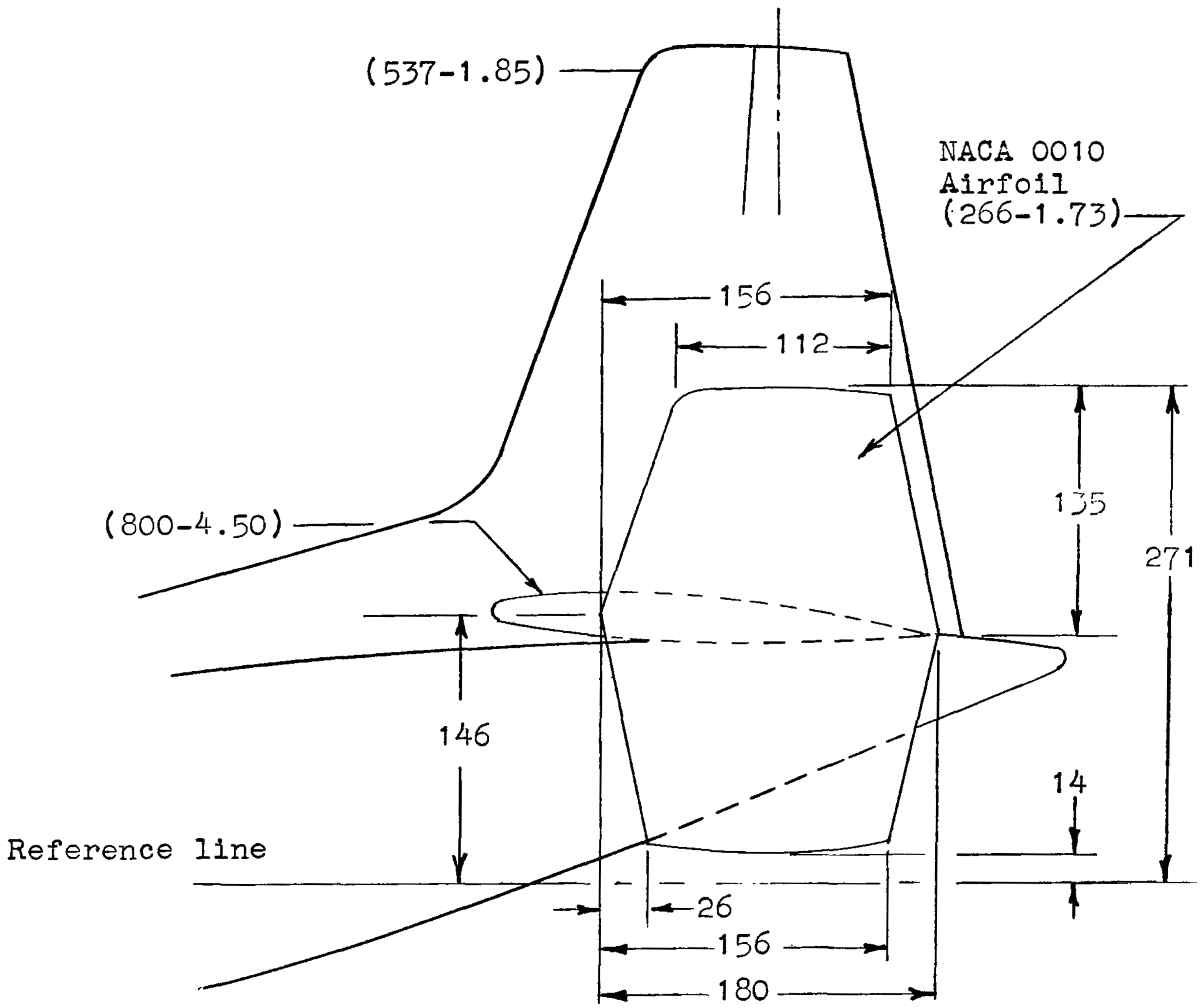

(c) End plates (266-1.73) on basic tail.

Figure 7.- Continued.

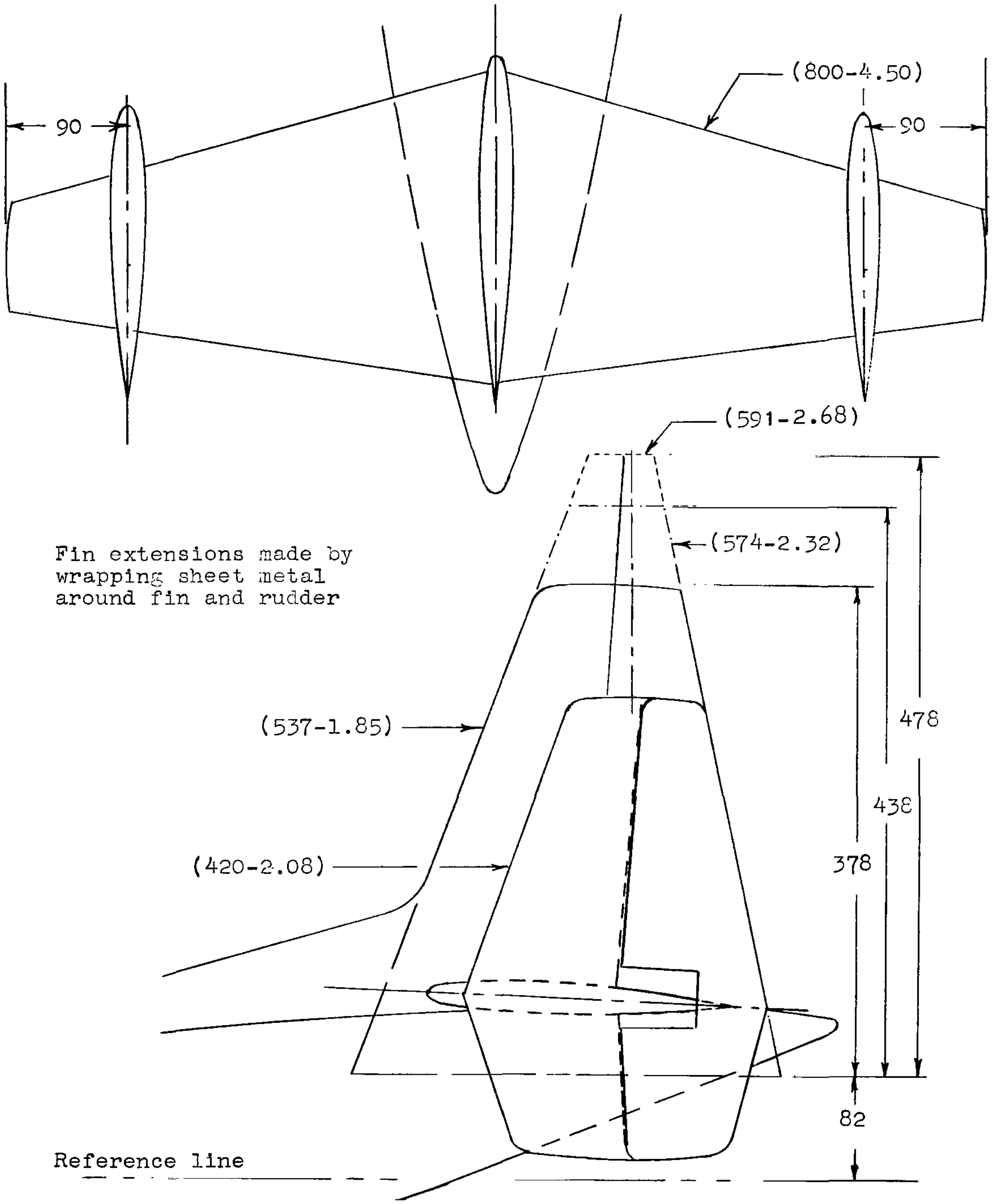

(d) Inset end plates (420-2.08) on basic tail.

Figure 7.- Continued.

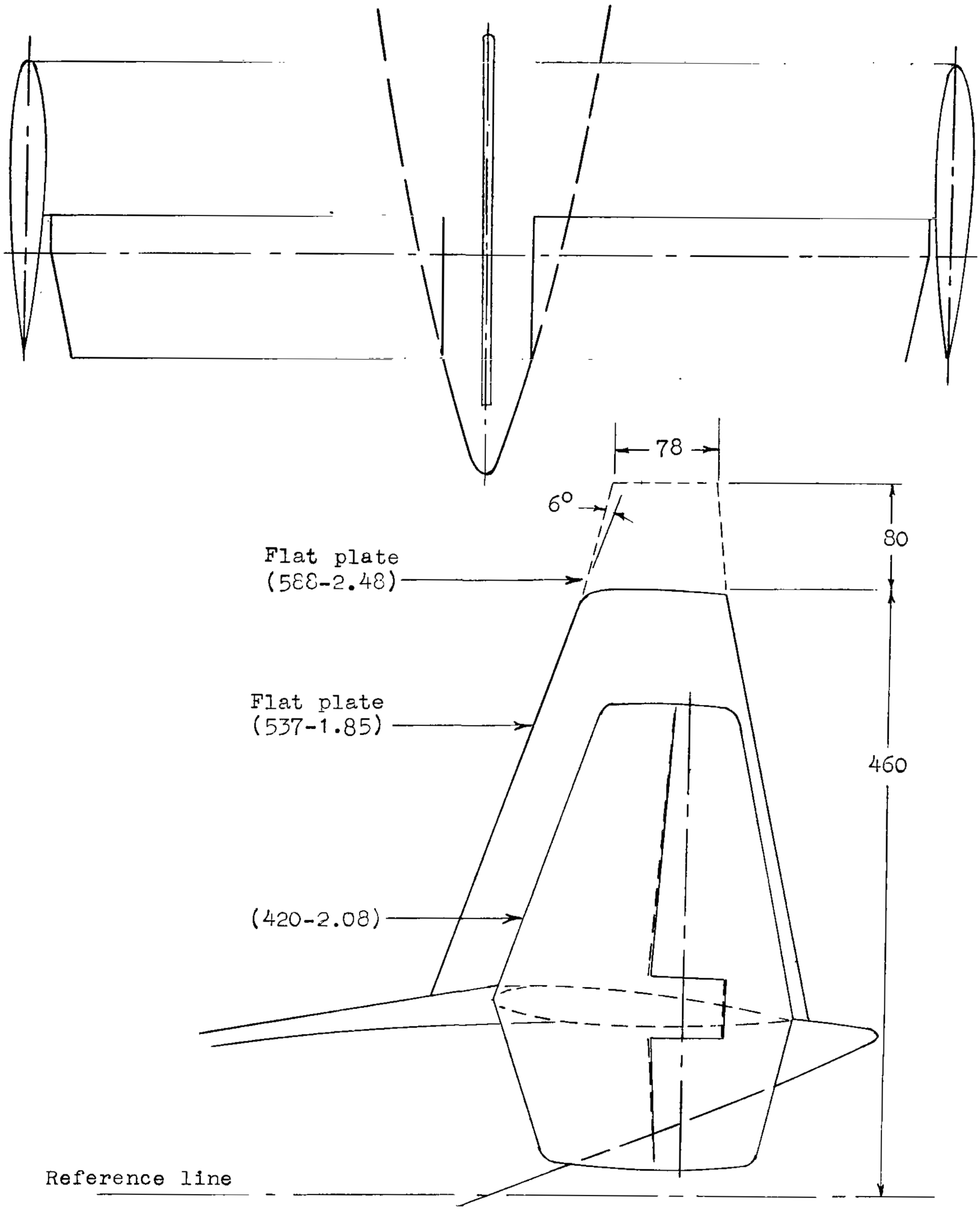

(e) End plates (420-2.08) and center fin on constant-chord stabilizer.

Figure 7.- Continued.

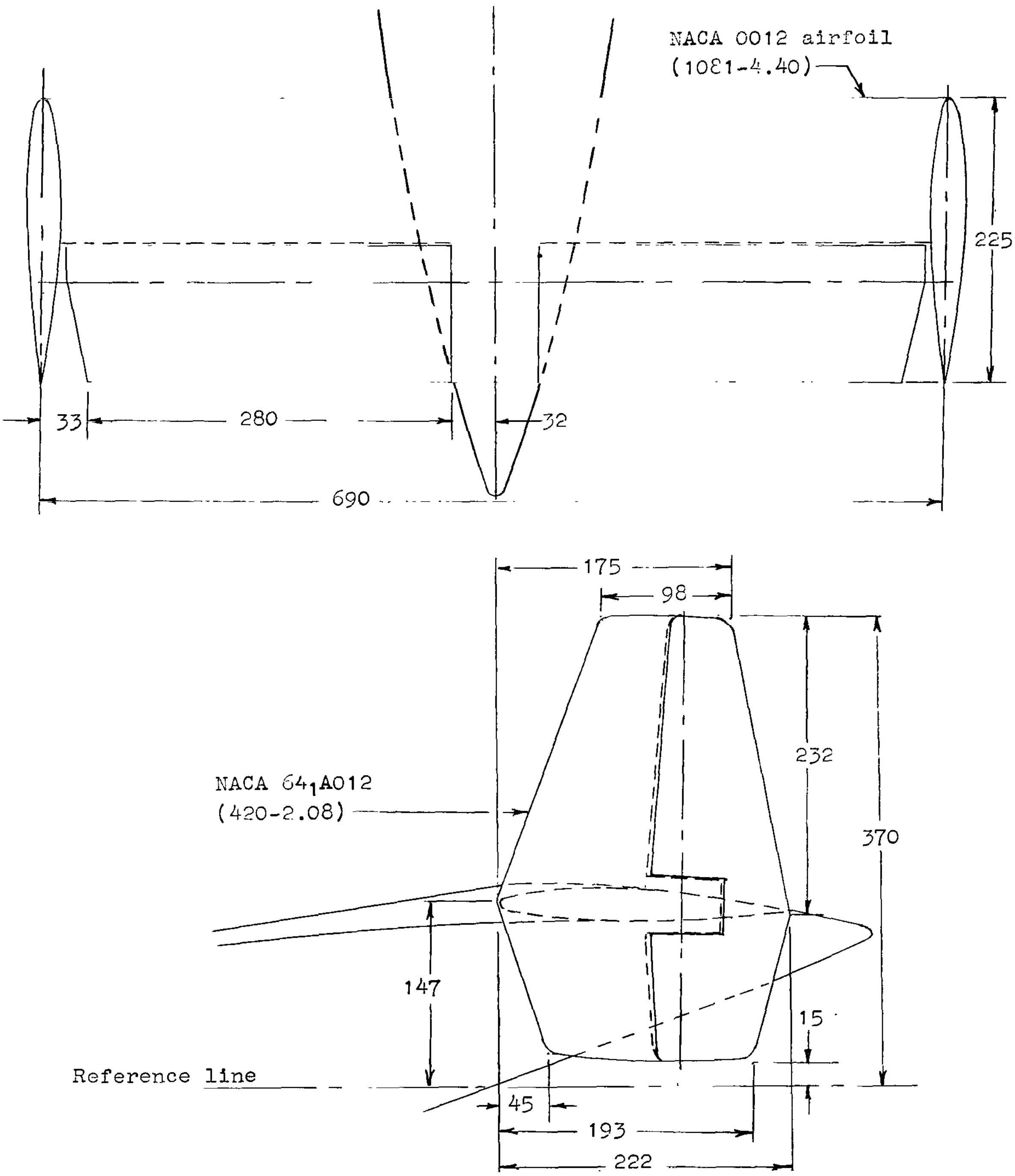

(f) Details of end plates (420-2.08) on constant-chord stabilizer.

Figure 7.- Continued.

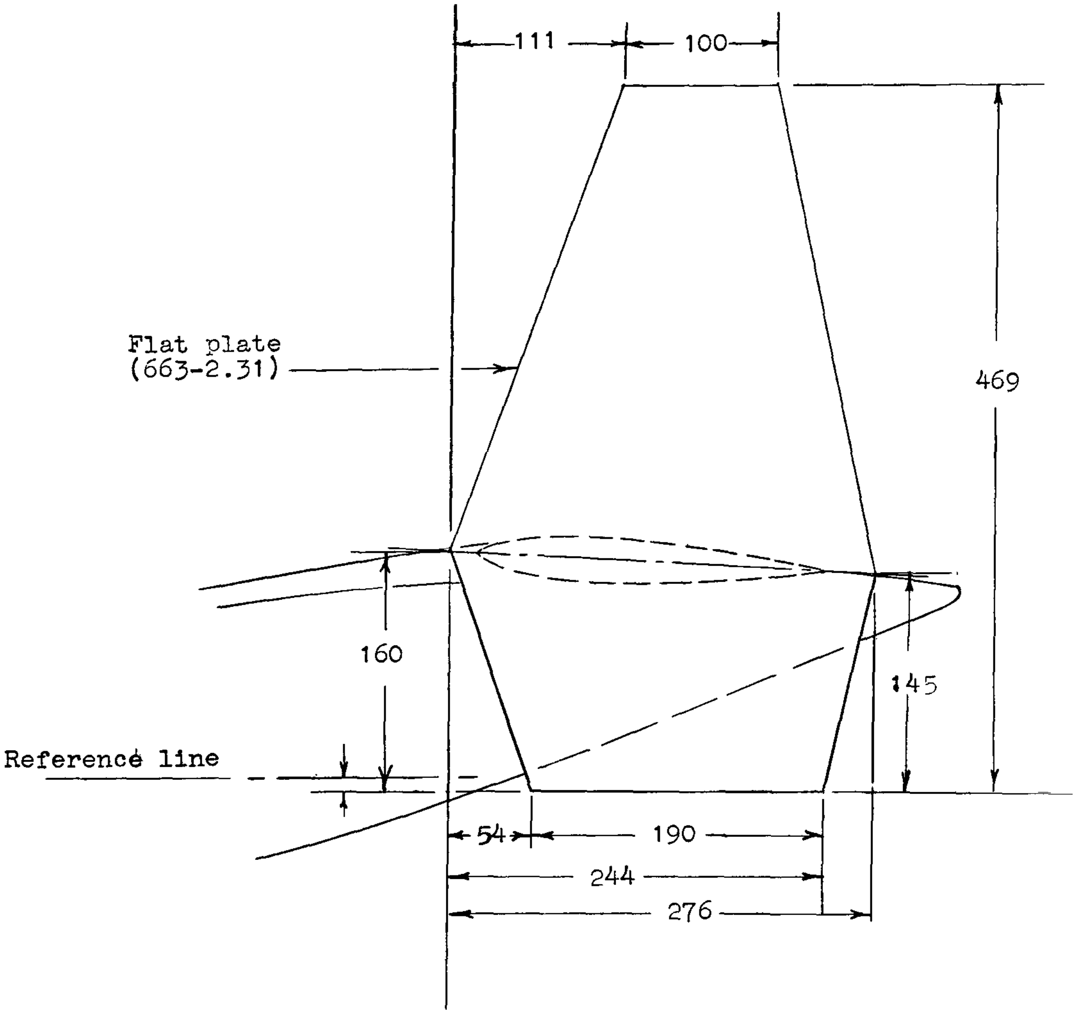

(g) Details of end plates (663-2.31) on constant-chord stabilizer.

Figure 7.- Concluded.

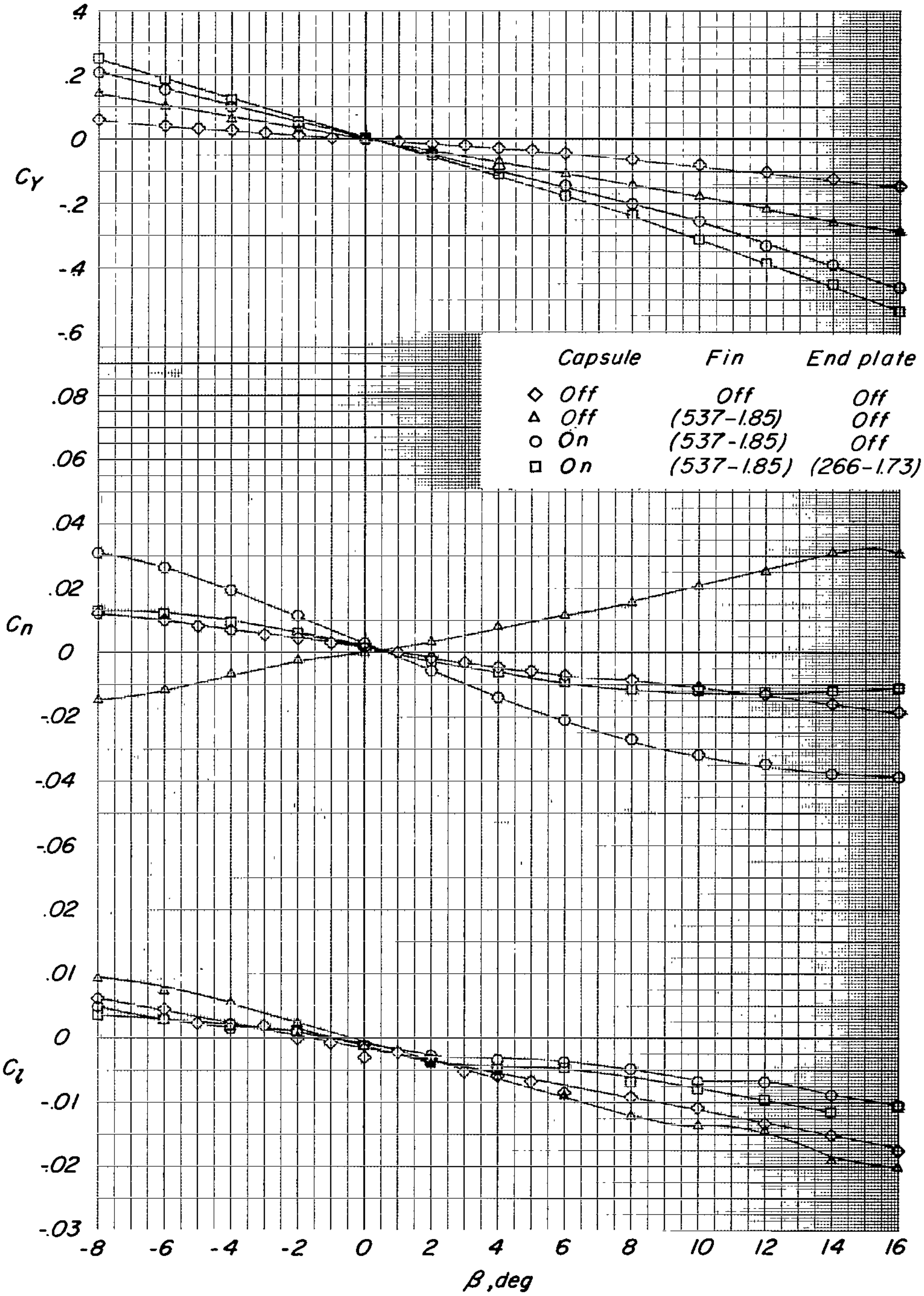

Figure 8.- Effect of vertical-tail configuration and capsule on aerodynamic characteristics in sideslip. Basic stabilizer; circular tail fairing; basic capsule position; airfoil-shape struts; $\alpha = 0.42^{\circ}$.

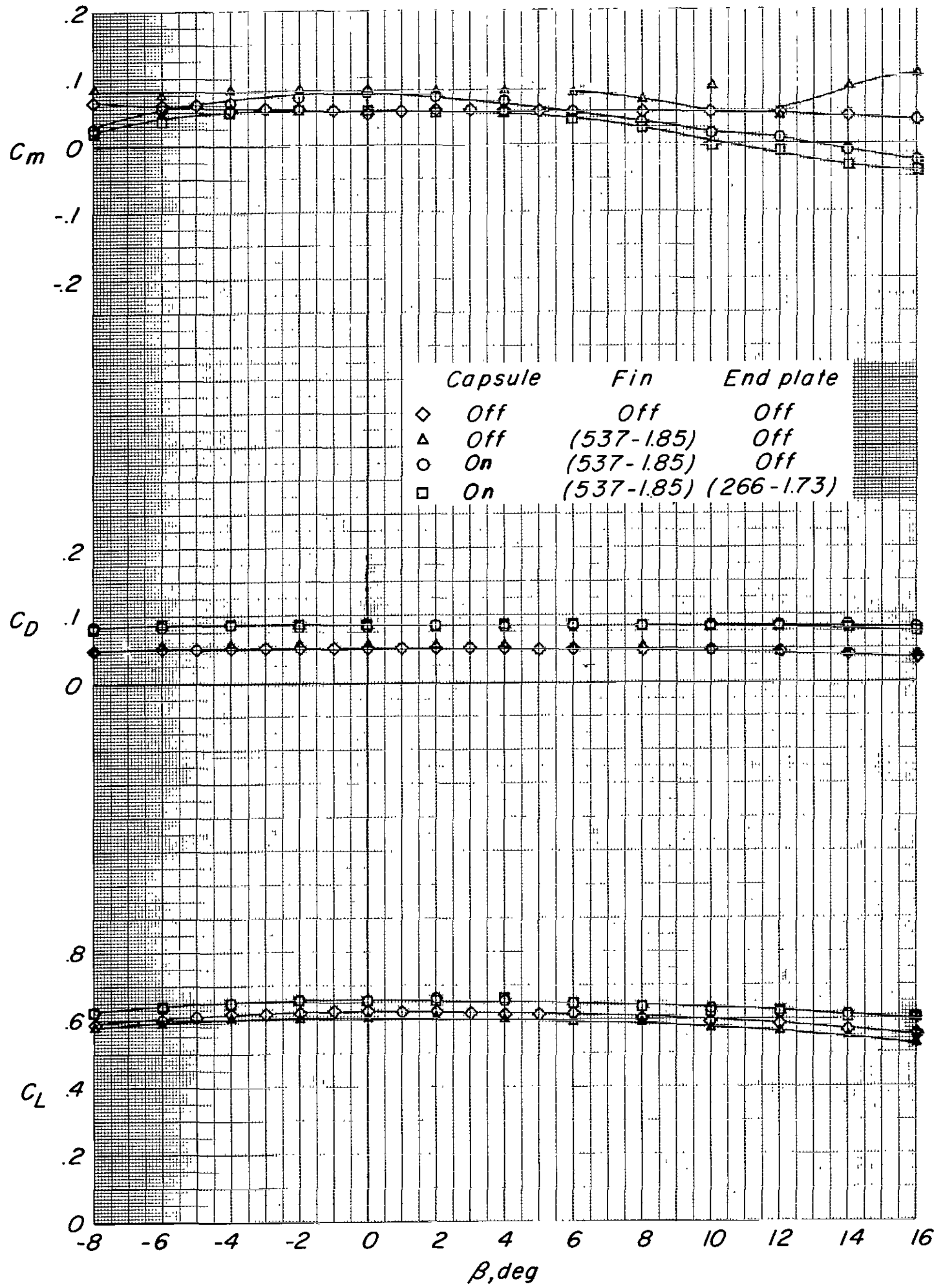

Figure 8.- Concluded.

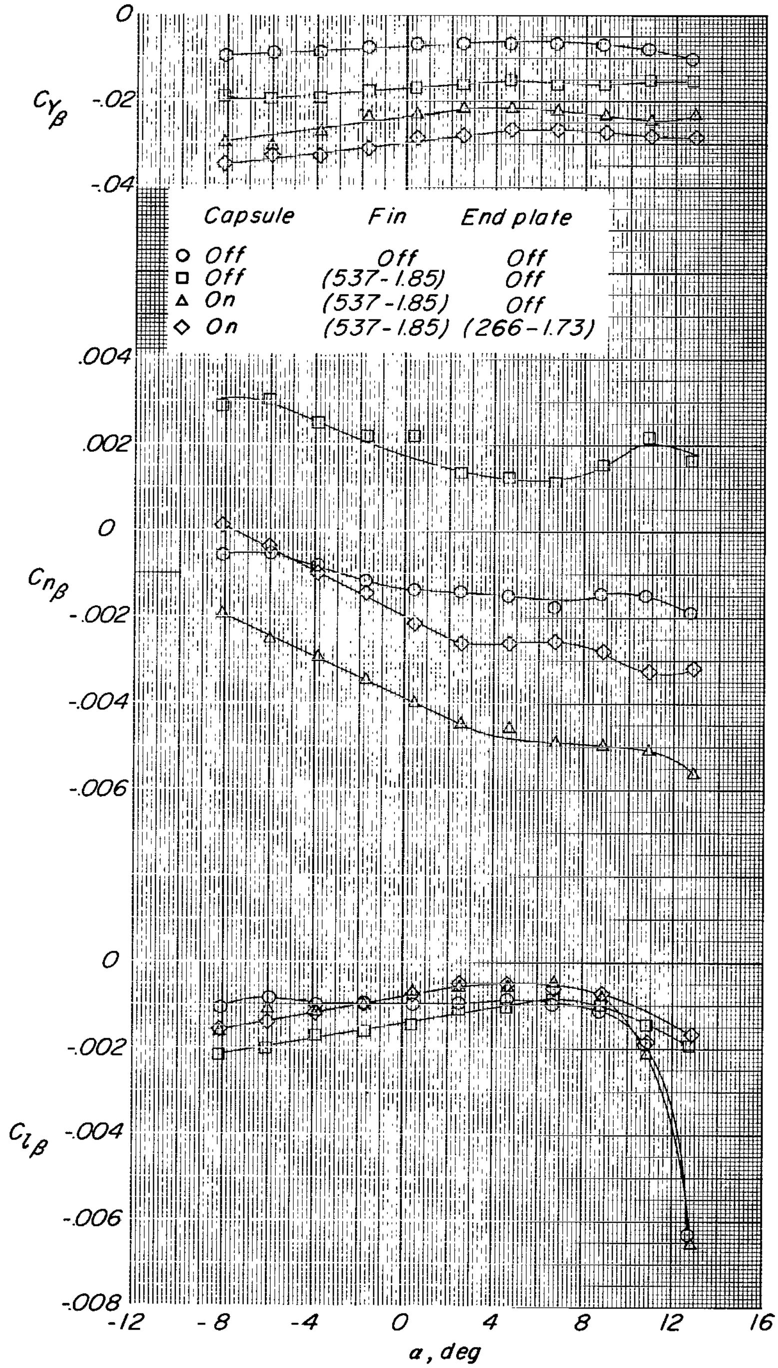

Figure 9.- Effect of vertical-tail configuration and capsule on lateral stability parameters. Basic stabilizer; circular tail fairing; basic capsule position; airfoil-shape struts.

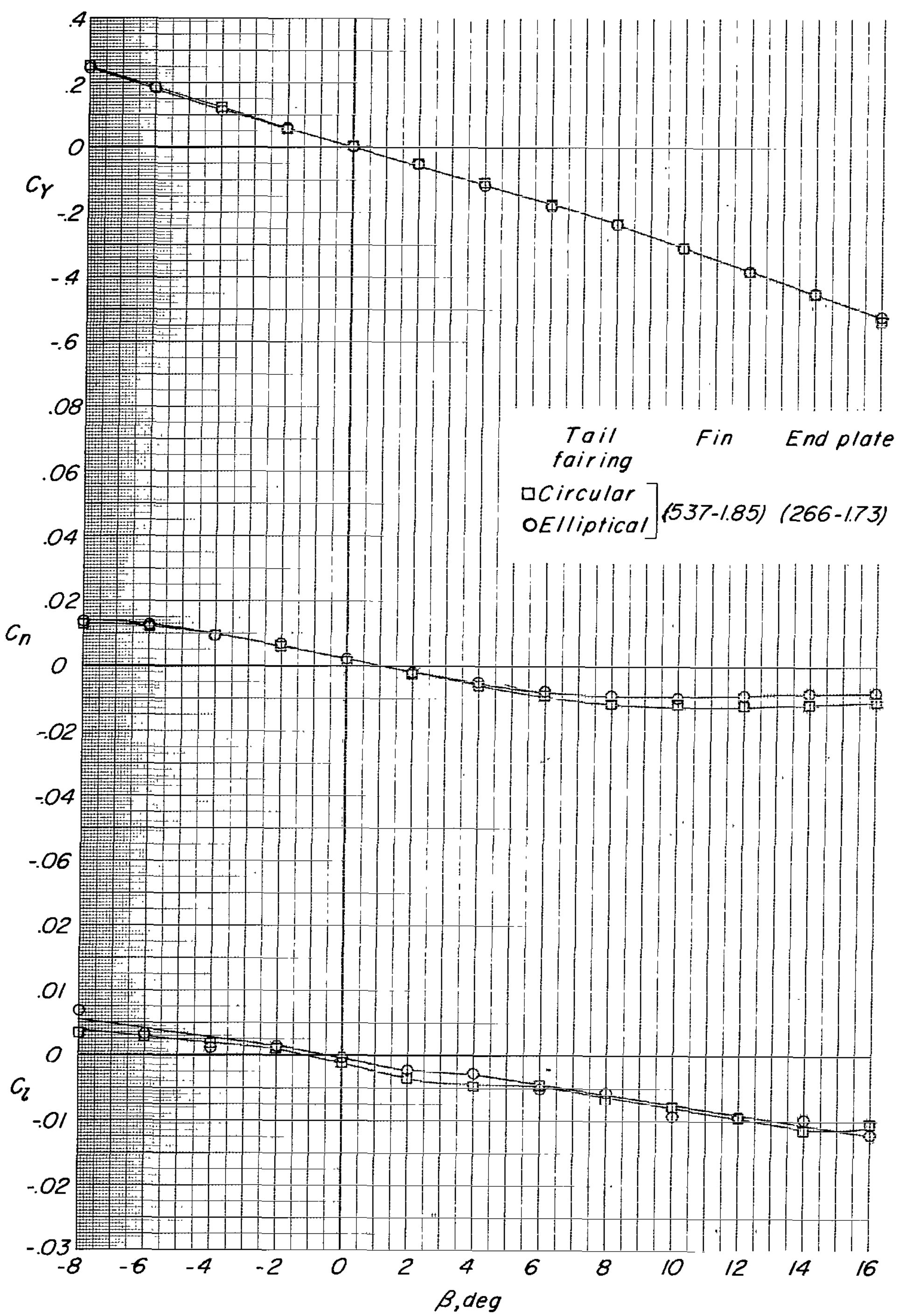

Figure 10.- Effect of tail fairing on aerodynamic characteristics in sideslip. Basic stabilizer; basic capsule position; airfoil-shape struts; $\alpha = 0.43^{\circ}$.

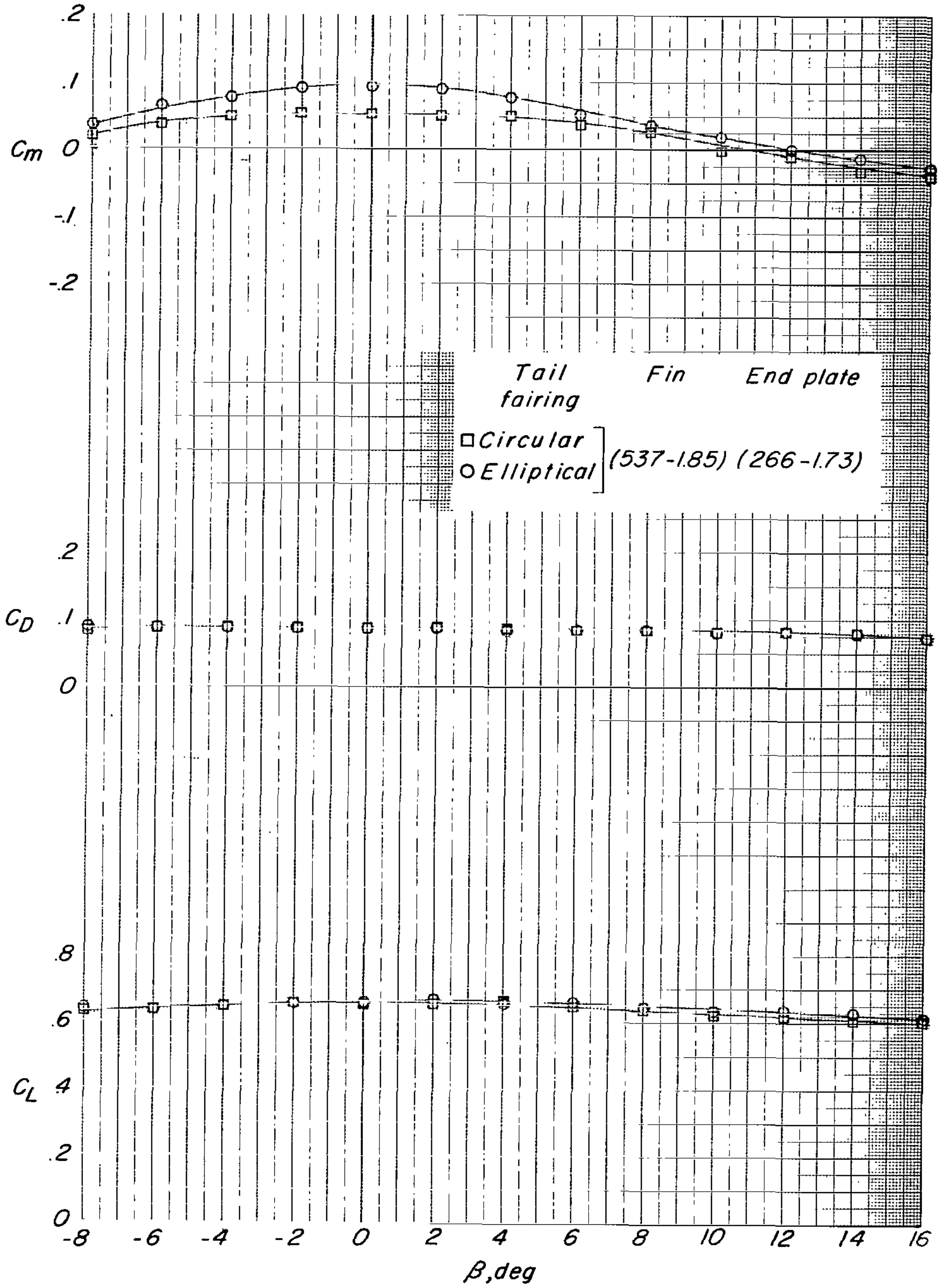

Figure 10.- Concluded.

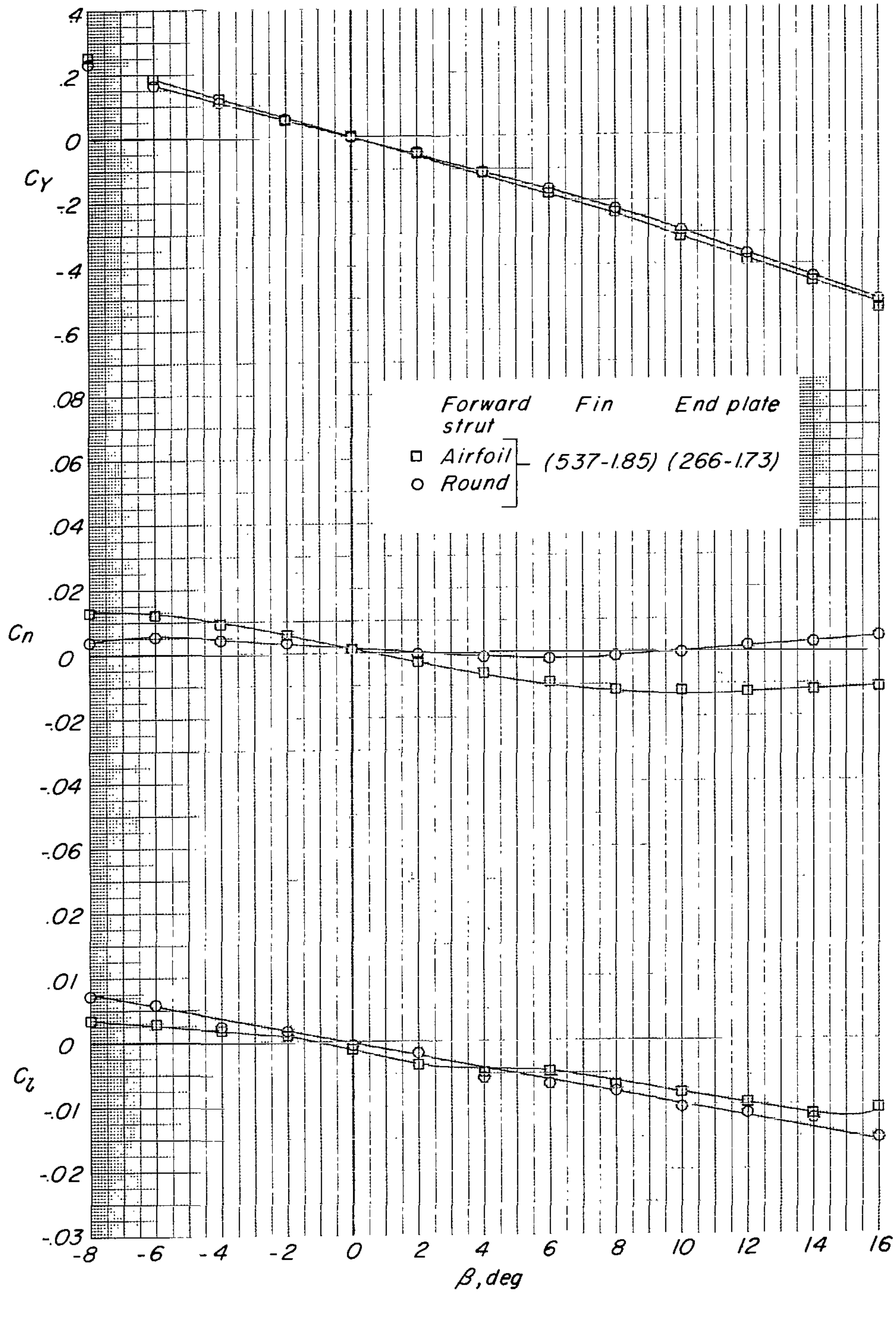

Figure 11.- Effect of shape of forward support strut on aerodynamic characteristics in sideslip. Basic stabilizer; circular tail fairing; basic capsule position; $\alpha = 0.43^{\circ}$.

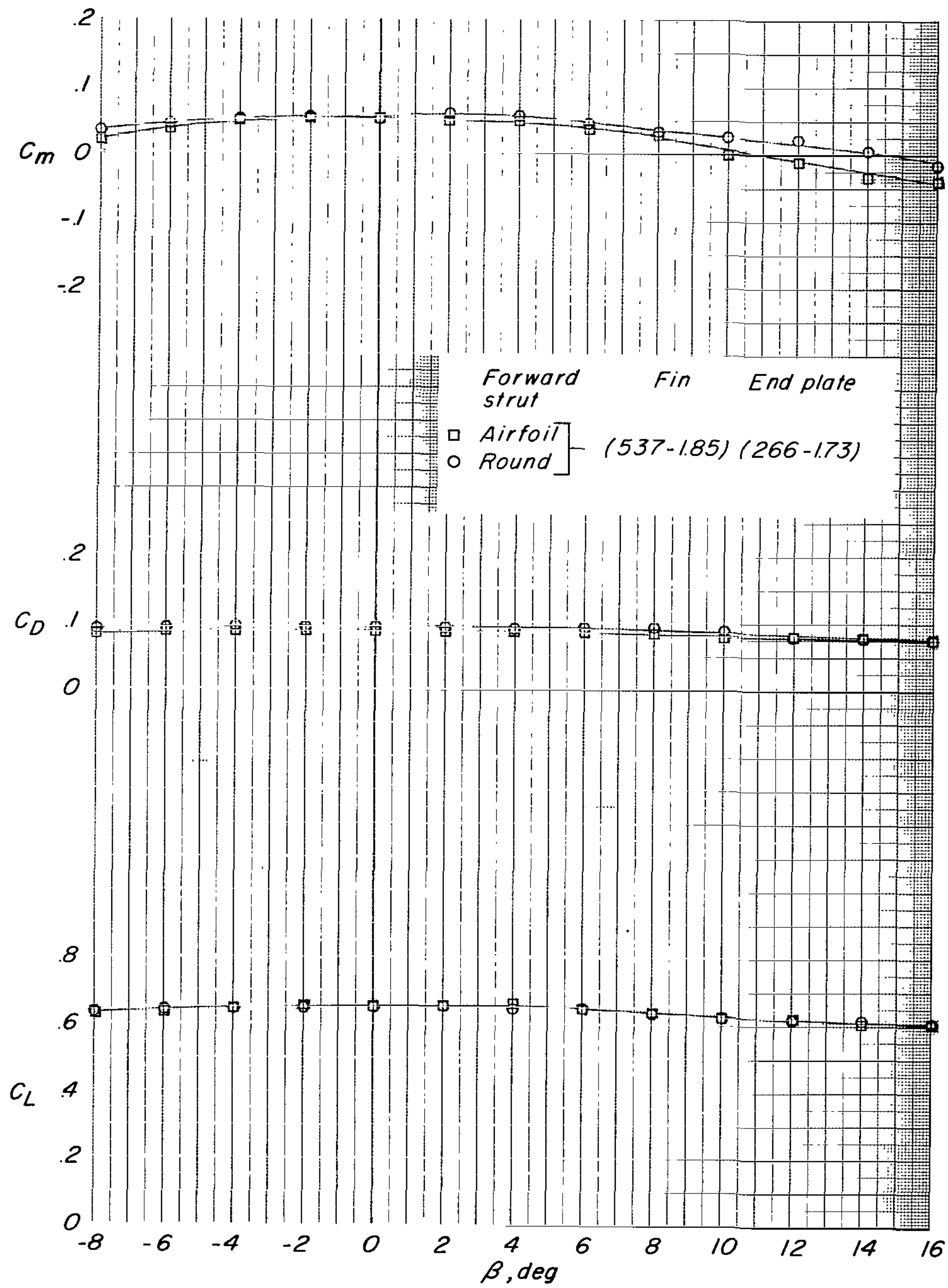

Figure 11.- Concluded.

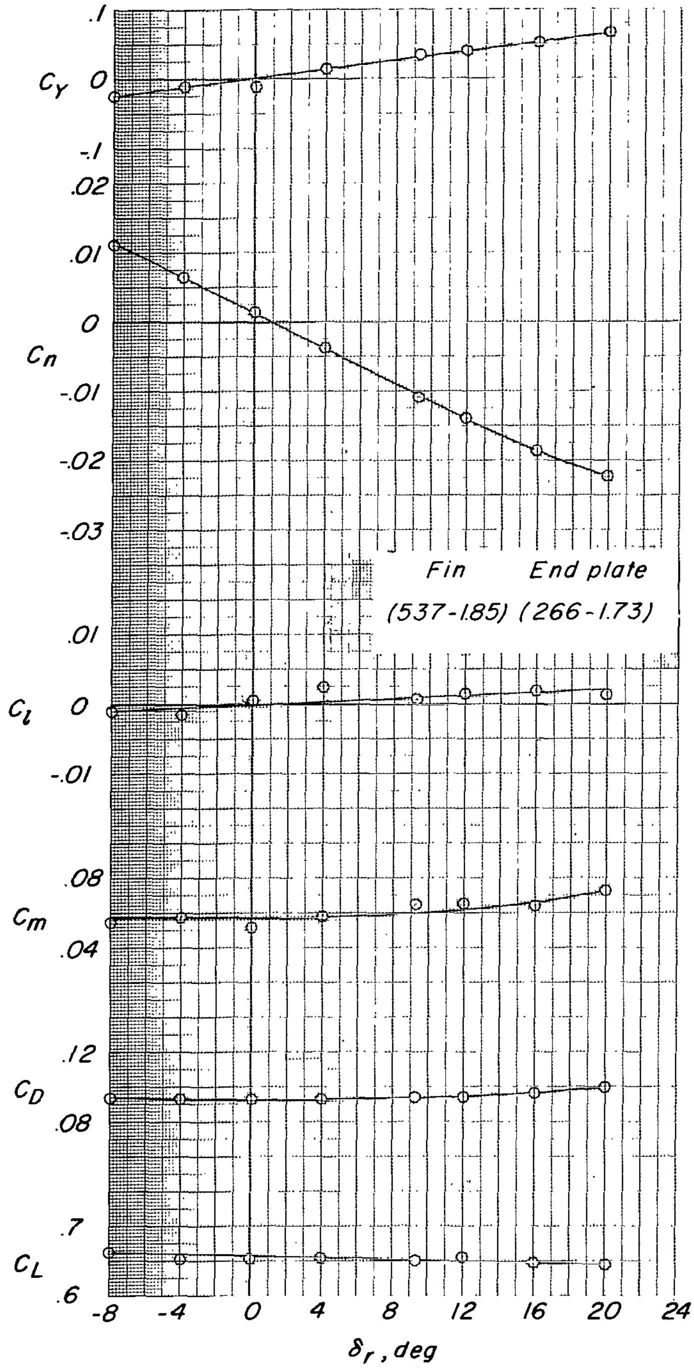

Figure 12.- Effect of rudder deflection on aerodynamic characteristics. Basic stabilizer; circular tail fairing; basic capsule position; round struts; $\alpha = 0.44^{\circ}$; $\beta = 0^{\circ}$.

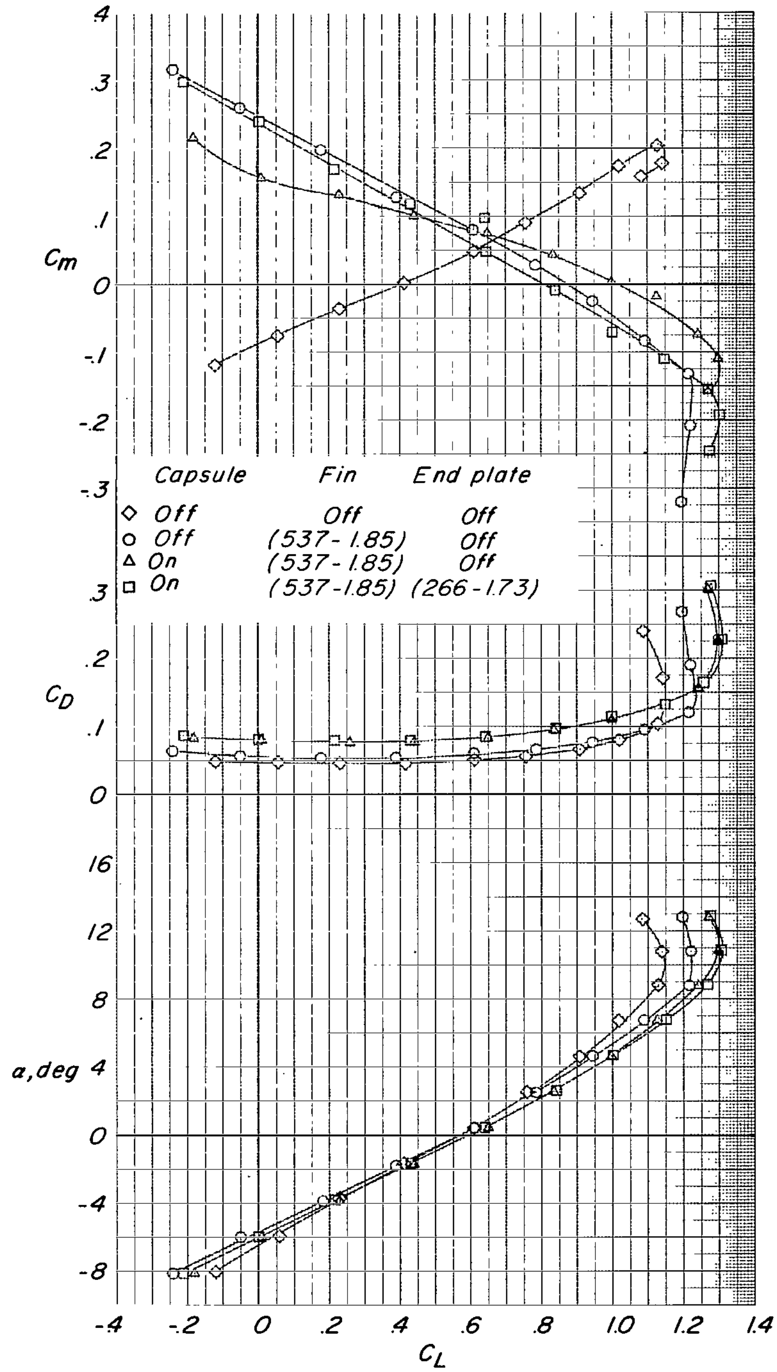

Figure 13.- Effect of vertical-tail configuration and capsule on longitudinal characteristics in pitch. Basic stabilizer; circular tail fairing; basic capsule position; airfoil-shape struts.

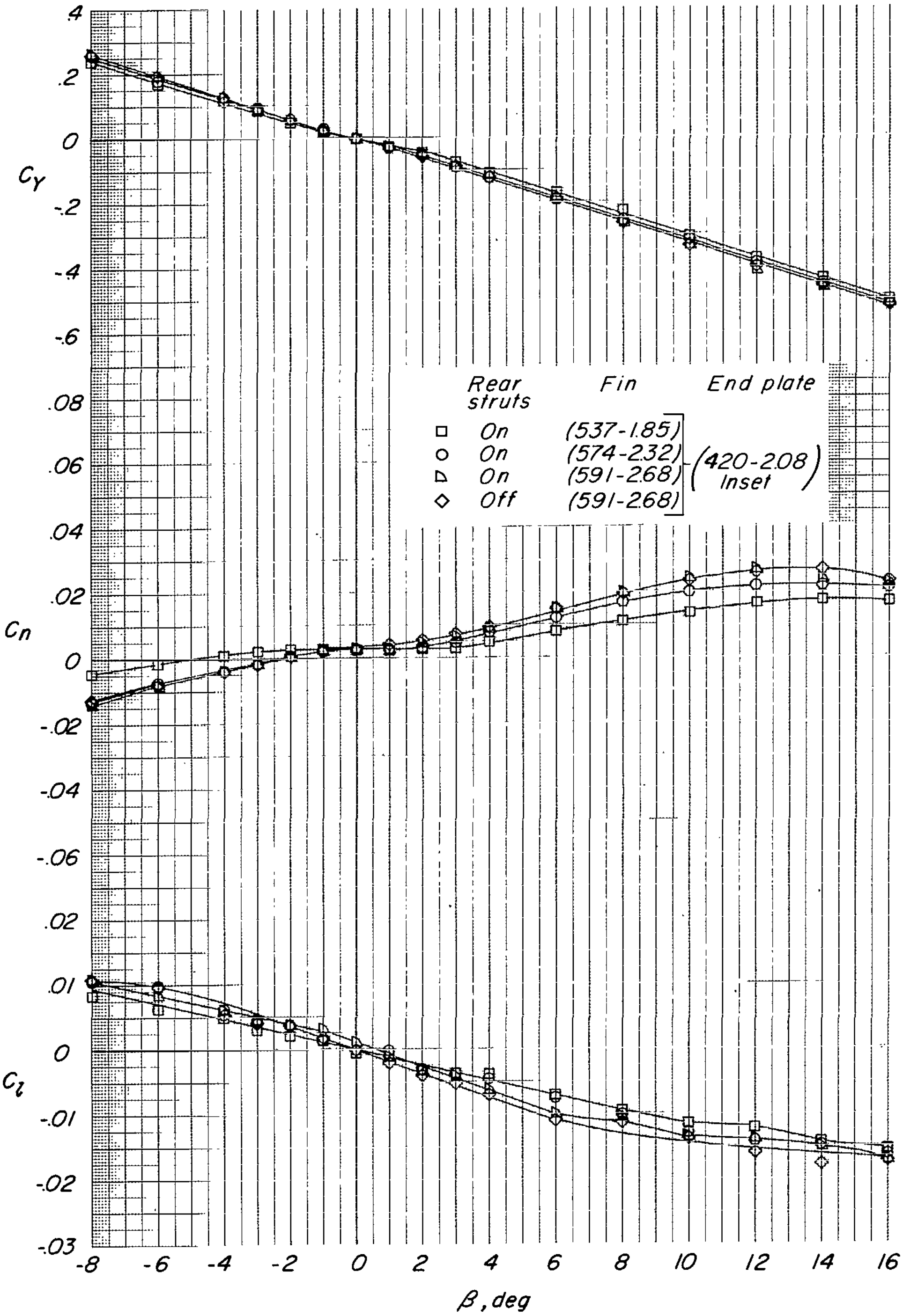

Figure 14.- Effect of fin size and rear struts on aerodynamic characteristics in sideslip. Basic stabilizer; elliptical tail fairing; rear capsule position; round struts; $\alpha = 0.44^\circ$.

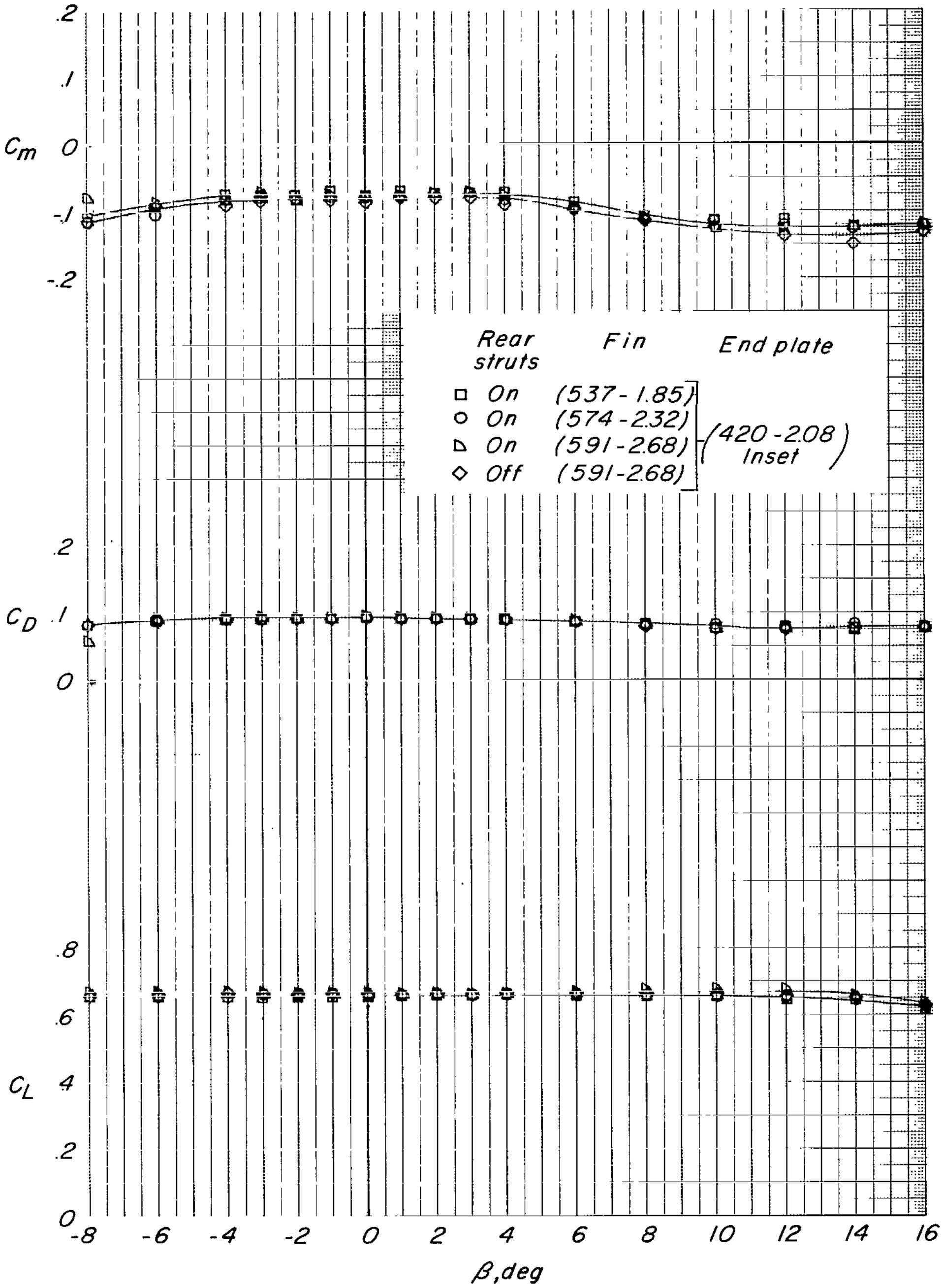

Figure 14.- Concluded.

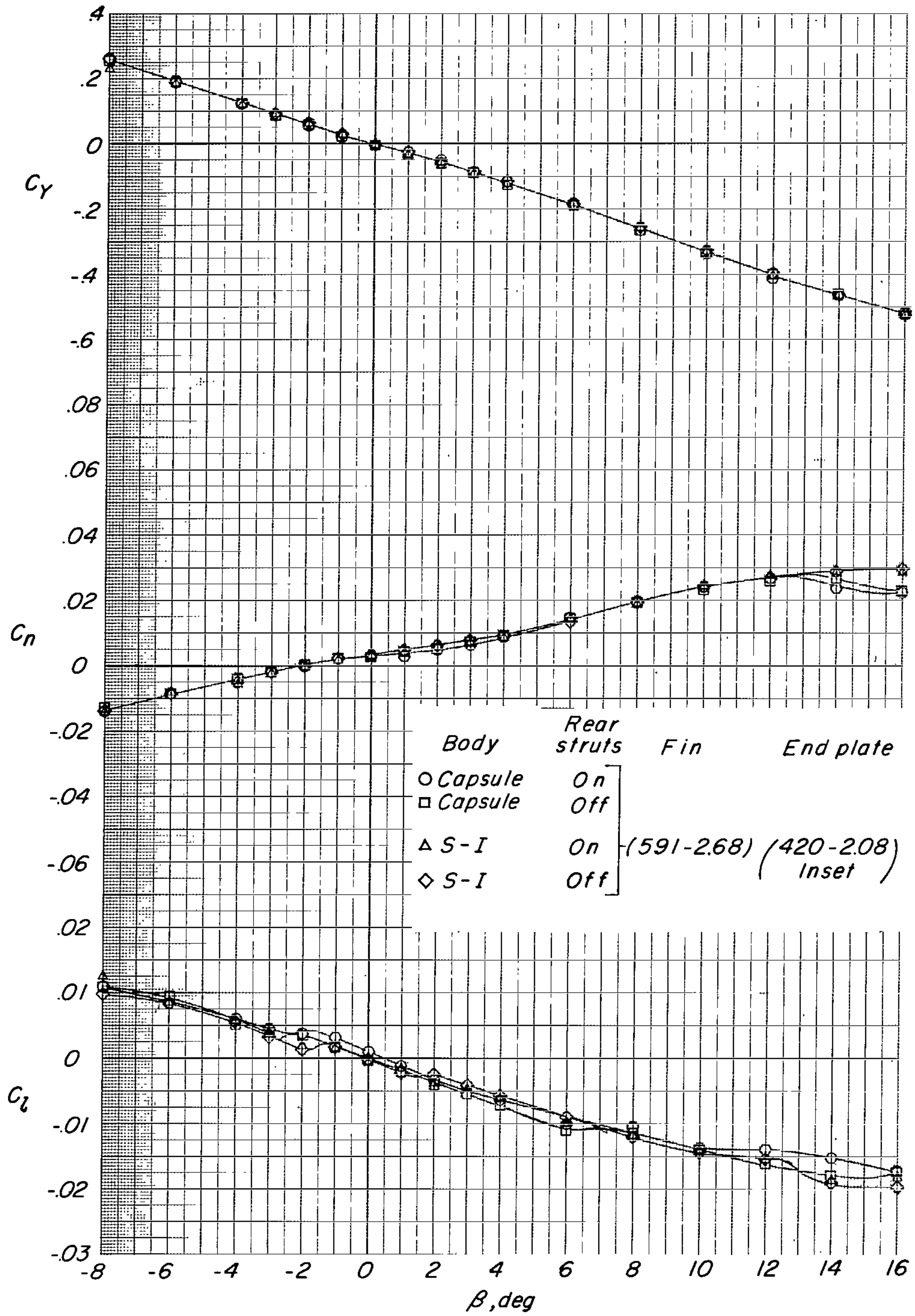

Figure 15.- Effect of body and rear struts on aerodynamic characteristics in sideslip. Basic stabilizer; elliptical tail fairing; rear capsule position; round struts; $\alpha = 0.43^{\circ}$.

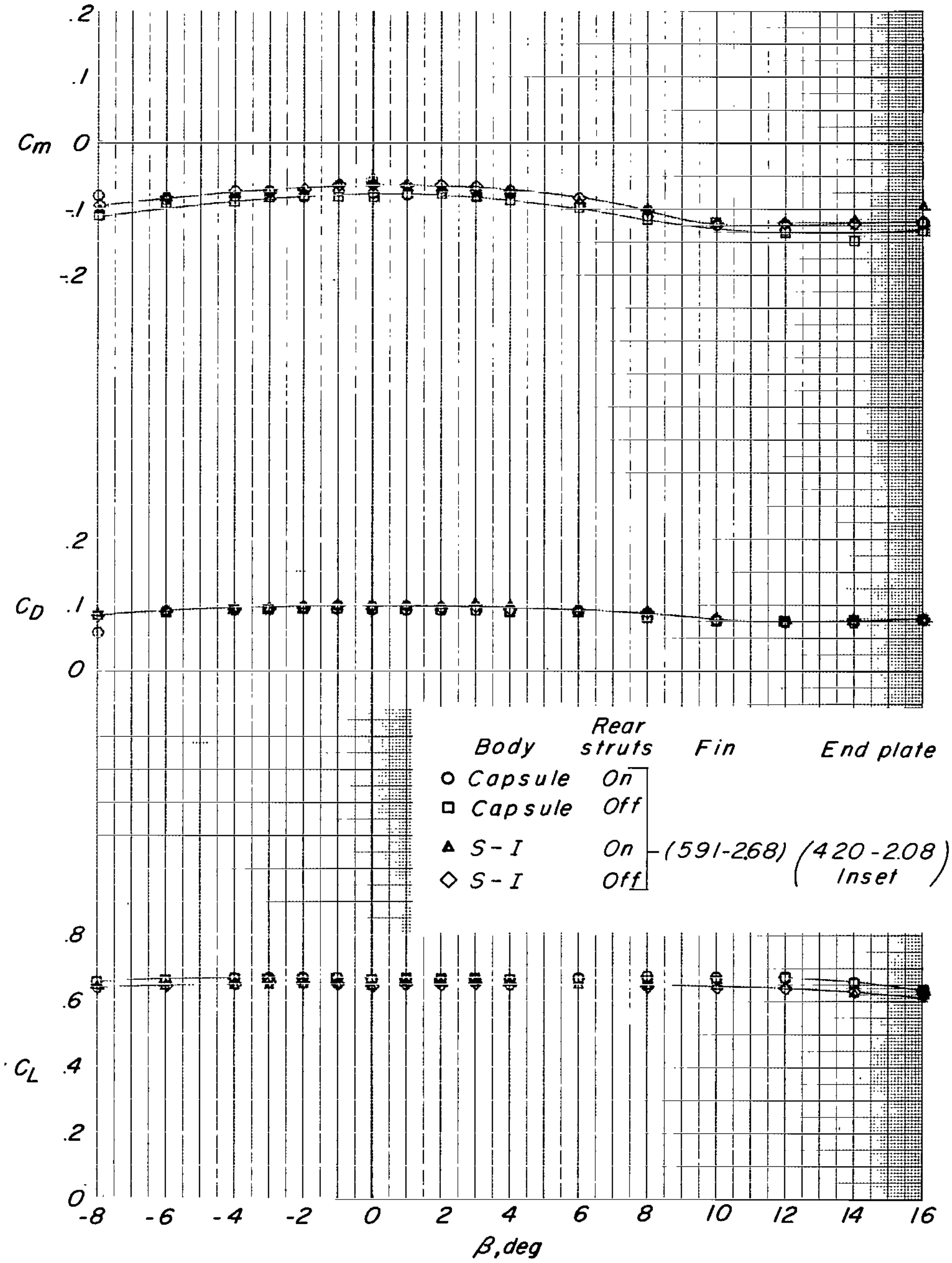

Figure 15.- Concluded.

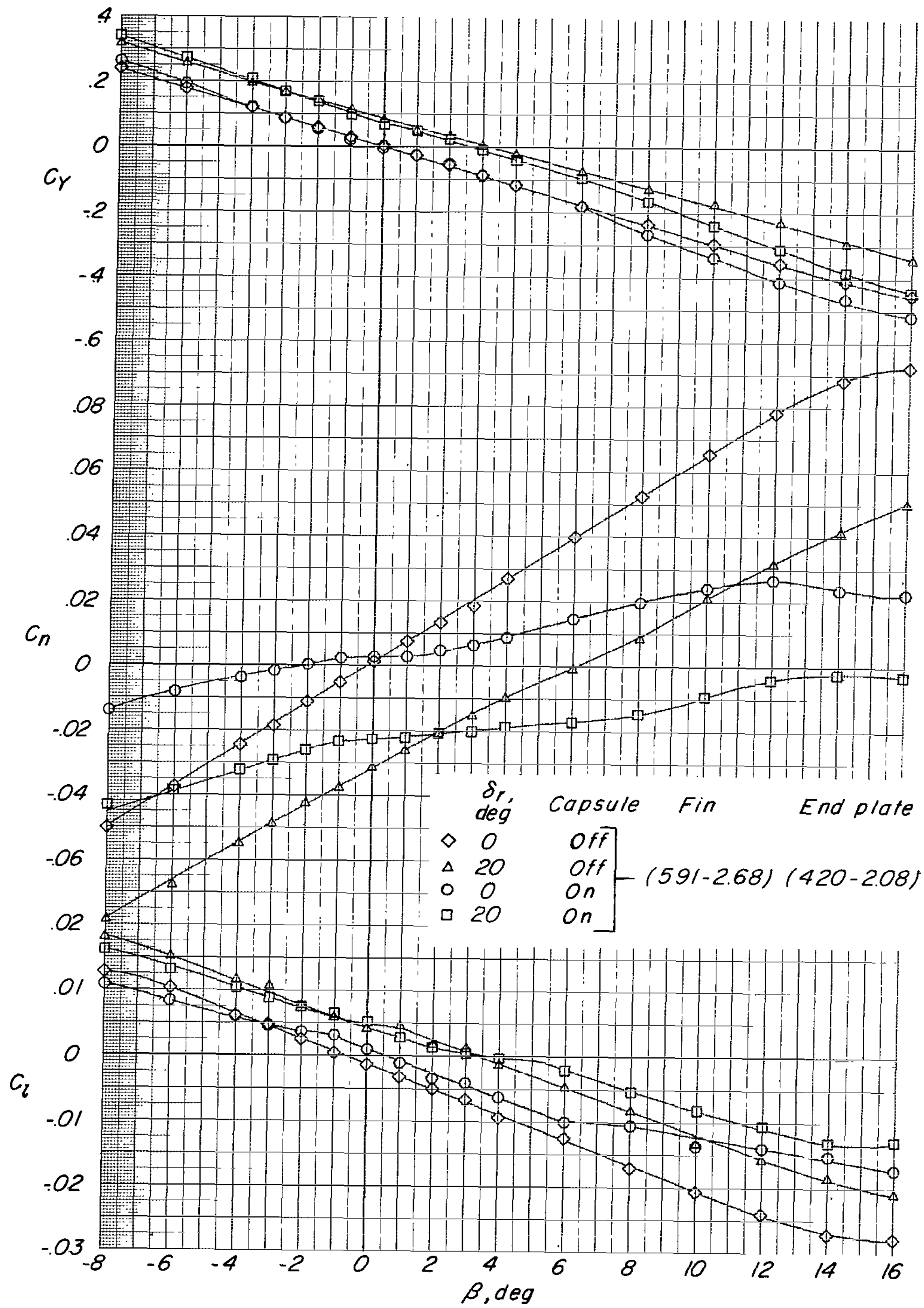

Figure 16.- Effect of rudder deflection on aerodynamic characteristics in sideslip. Basic stabilizer; elliptical tail fairing; rear capsule position; round struts; $\alpha = 0.42^{\circ}$.

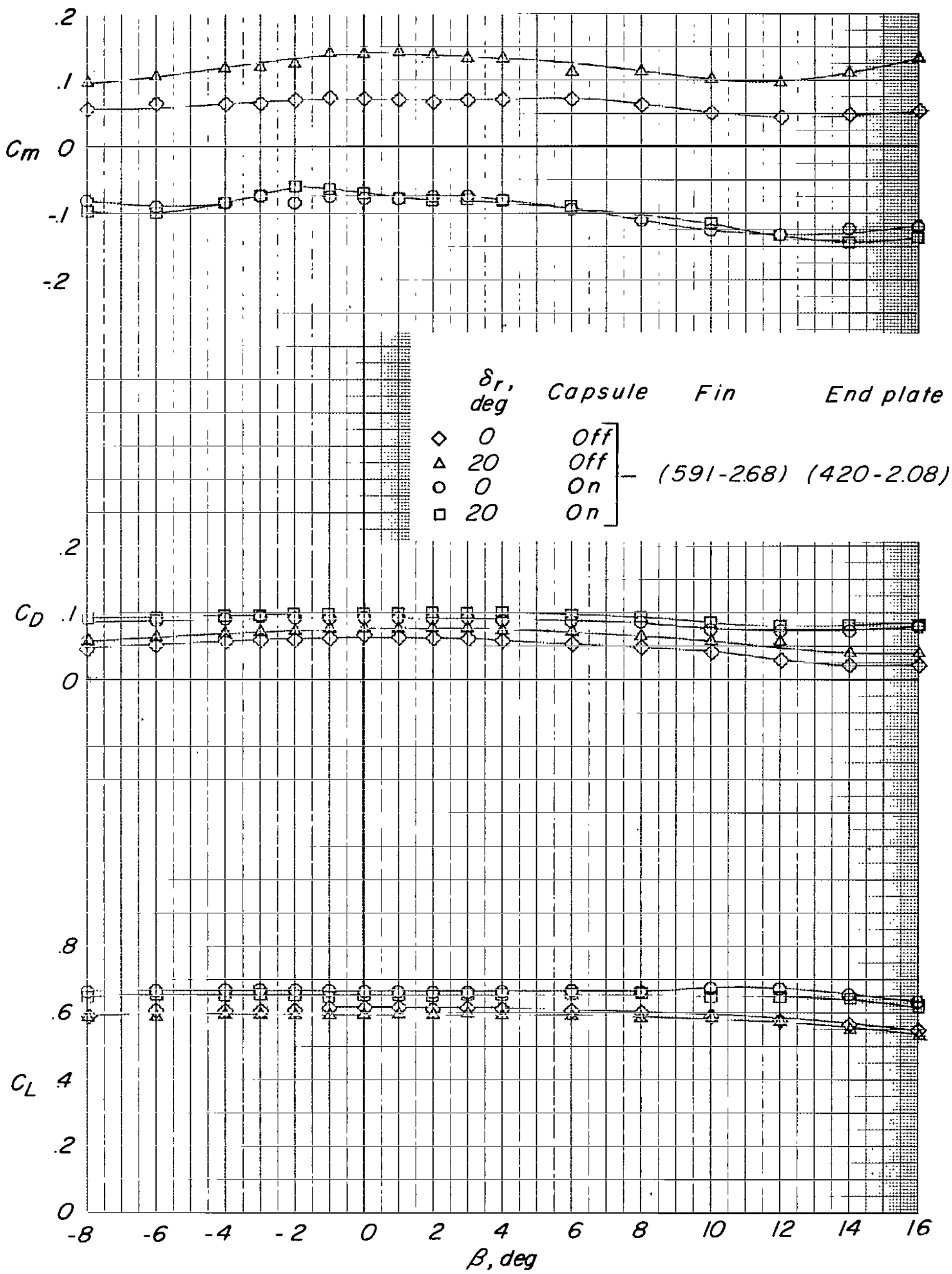

Figure 16.- Concluded.

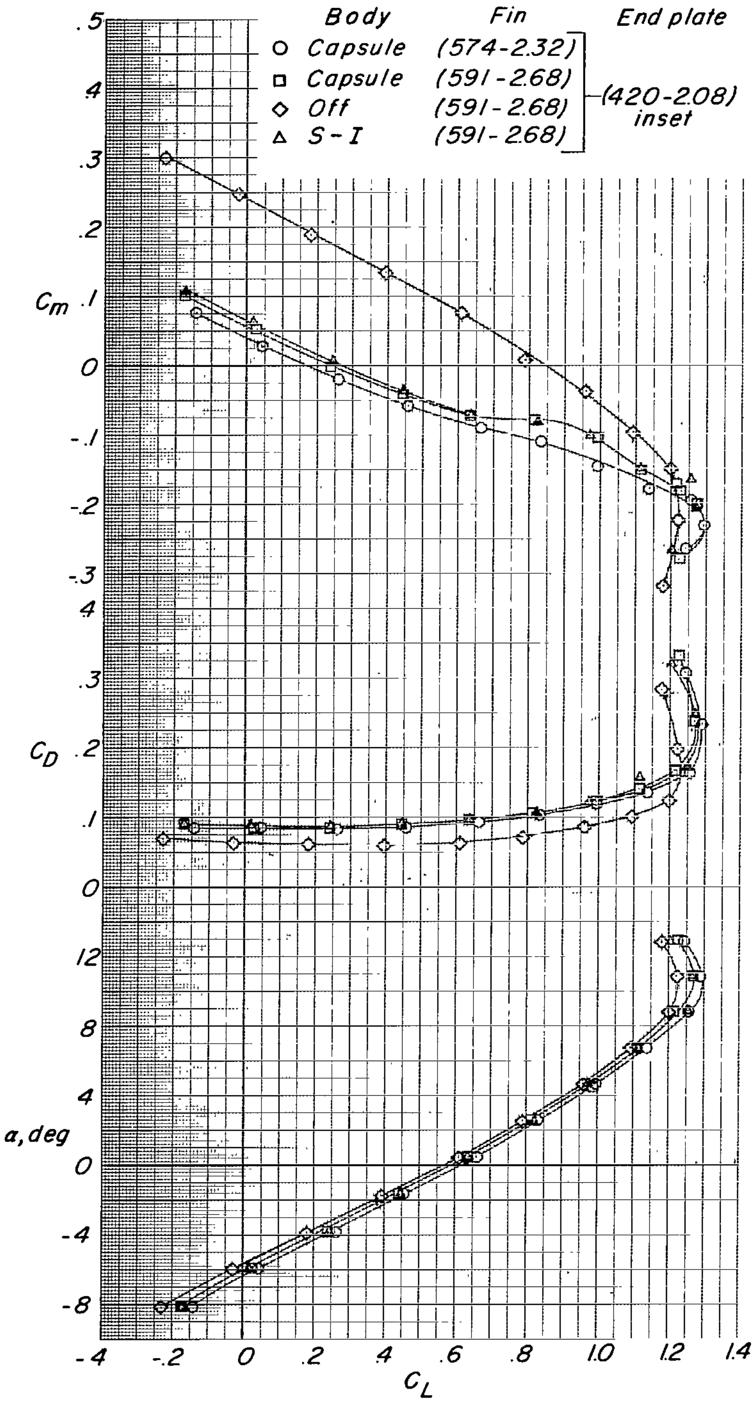

Figure 17.- Effect of body on aerodynamic characteristics in pitch. Basic stabilizer; elliptical tail fairing; rear capsule position; round struts.

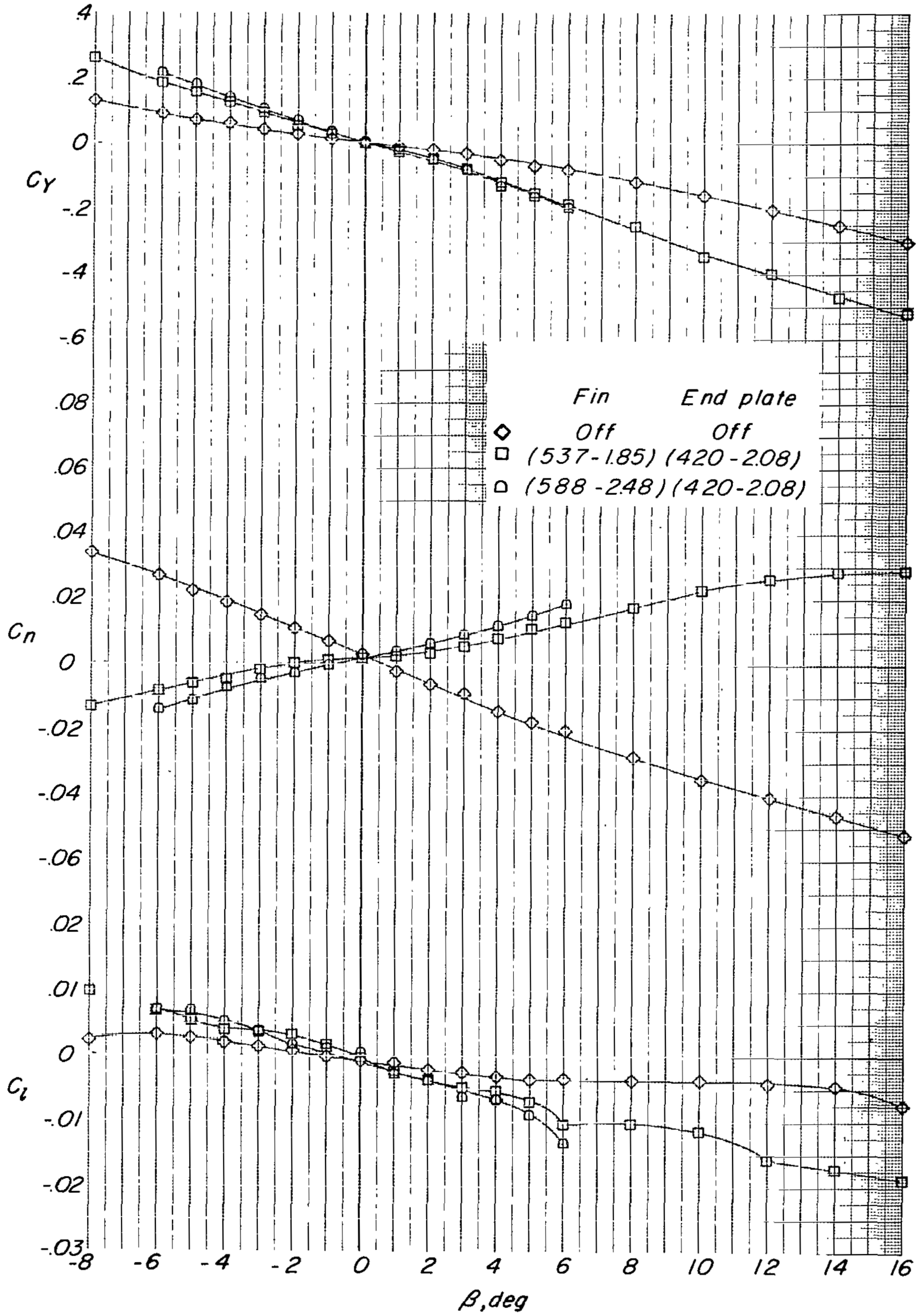

Figure 18.- Effect of fin size on aerodynamic characteristics in sideslip. Constant-chord stabilizer; elliptical tail fairing; rear capsule position; round struts; $\alpha = 0.44^{\circ}$.

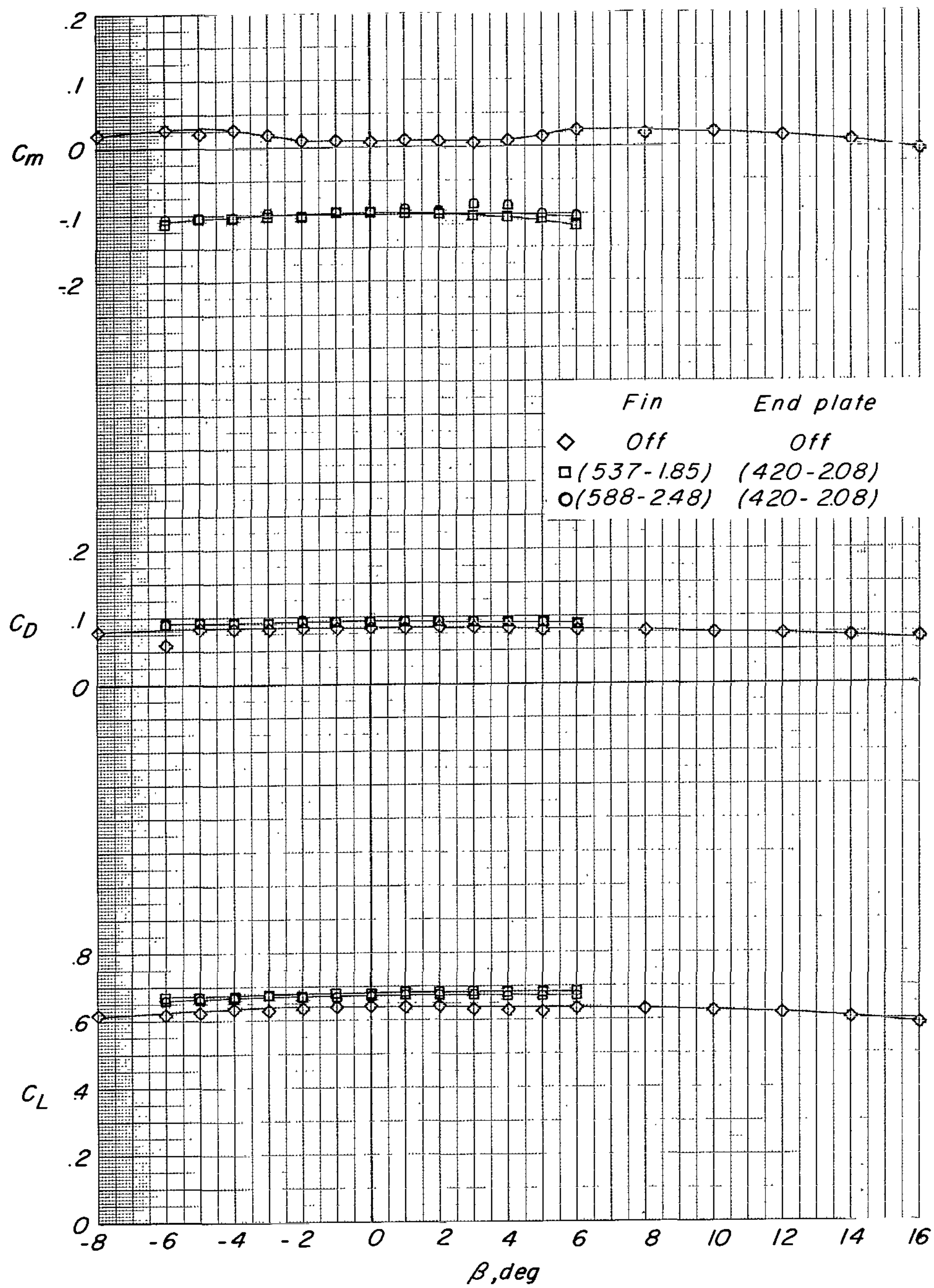

Figure 18.- Concluded.

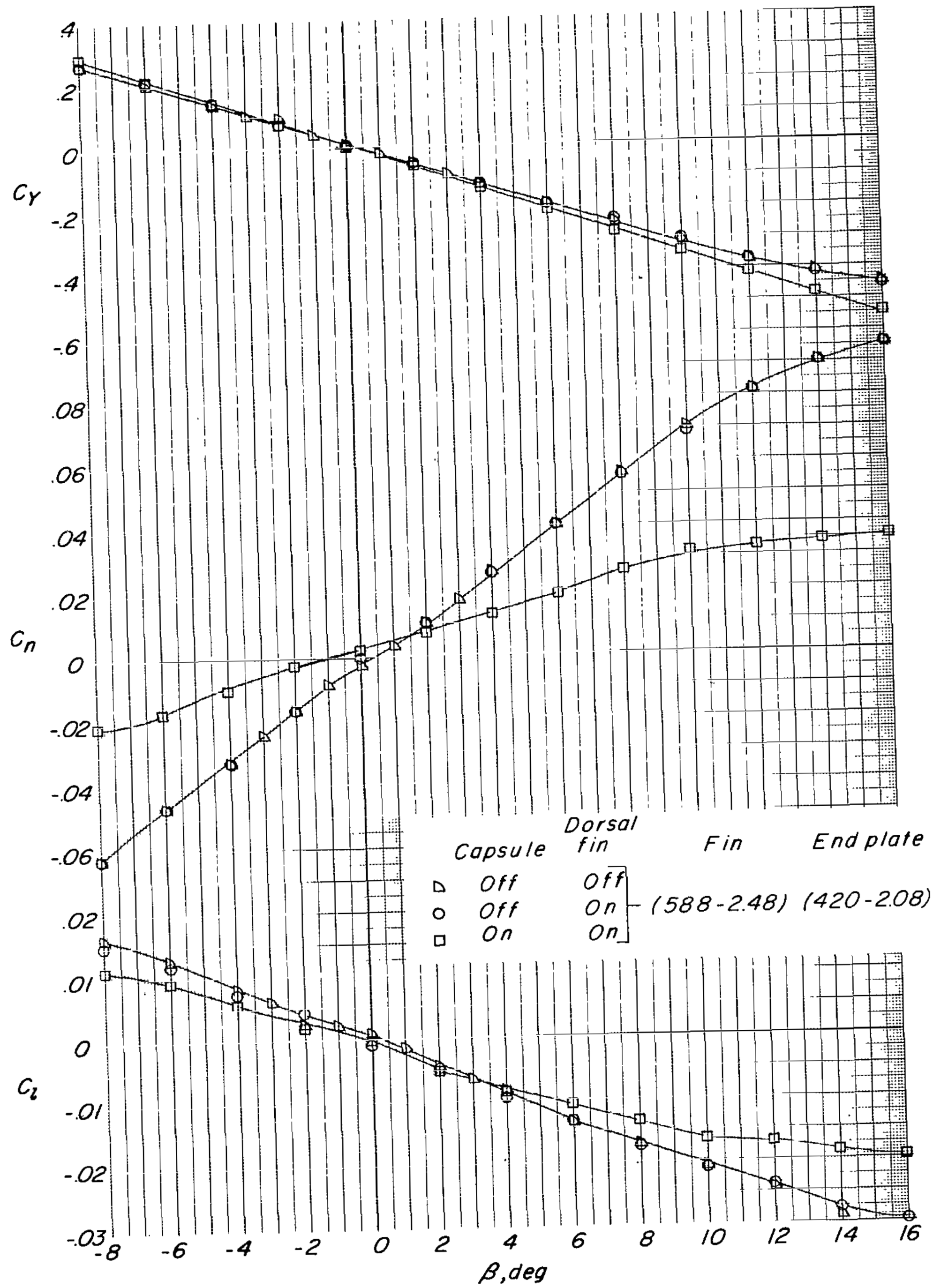

Figure 19.- Effect of capsule and dorsal fin on aerodynamic characteristics in sideslip. Constant-chord stabilizer; elliptical tail fairing; rear capsule position; round struts; $\alpha = 0.42^{\circ}$.

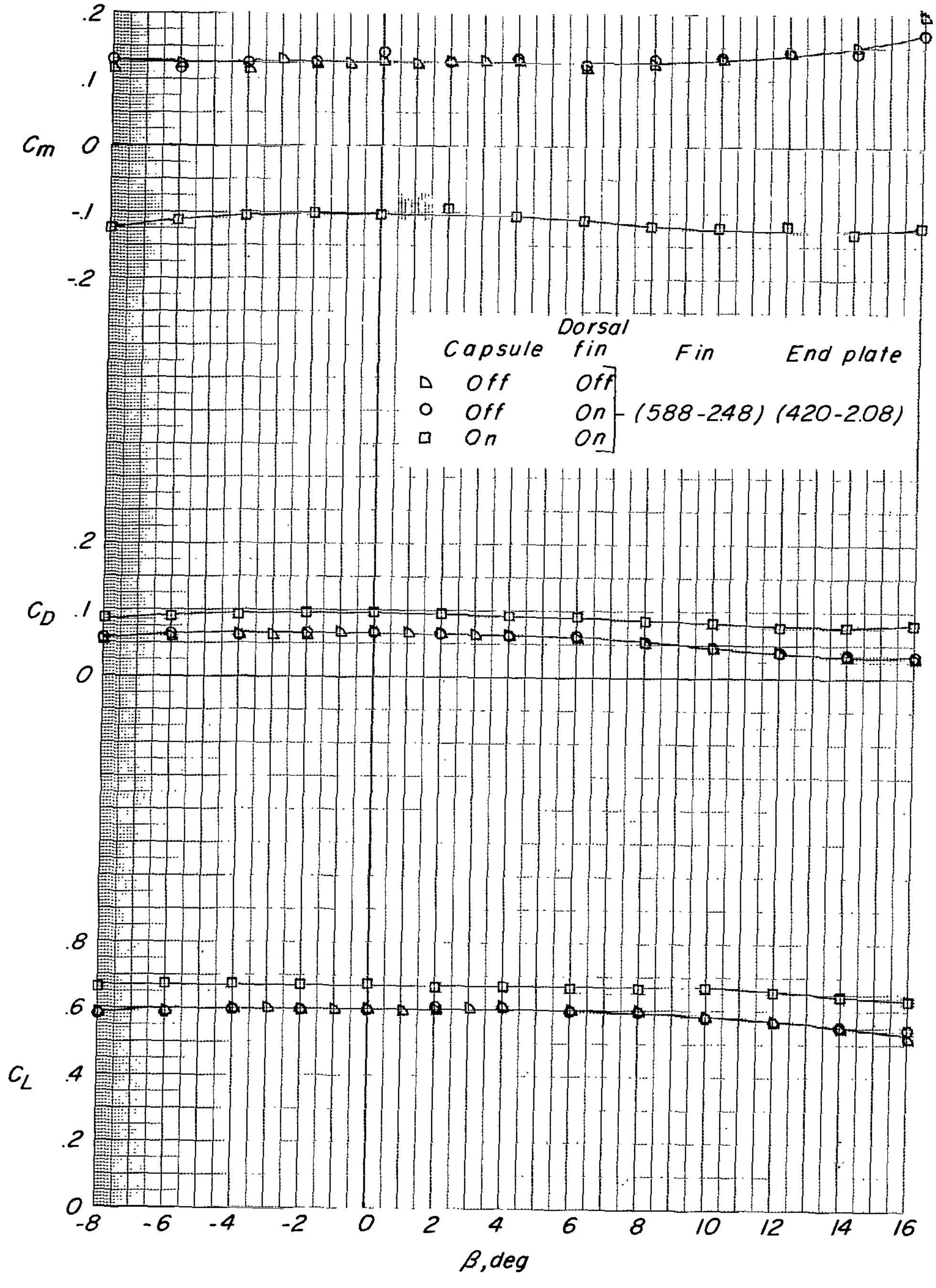

Figure 19.- Concluded.

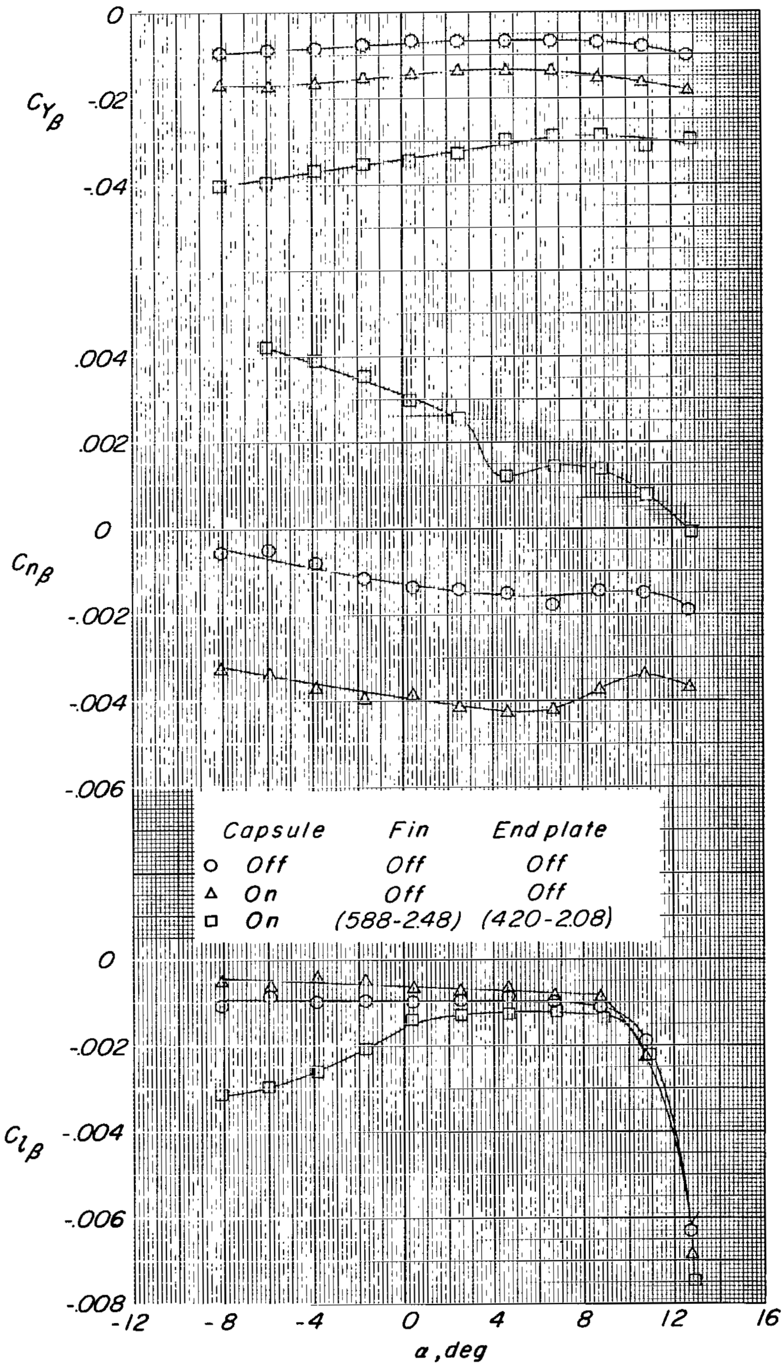

Figure 20.- Effect of capsule and vertical-tail configuration on lateral stability parameters. Constant-chord stabilizer; elliptical tail fairing; rear capsule position; round struts.

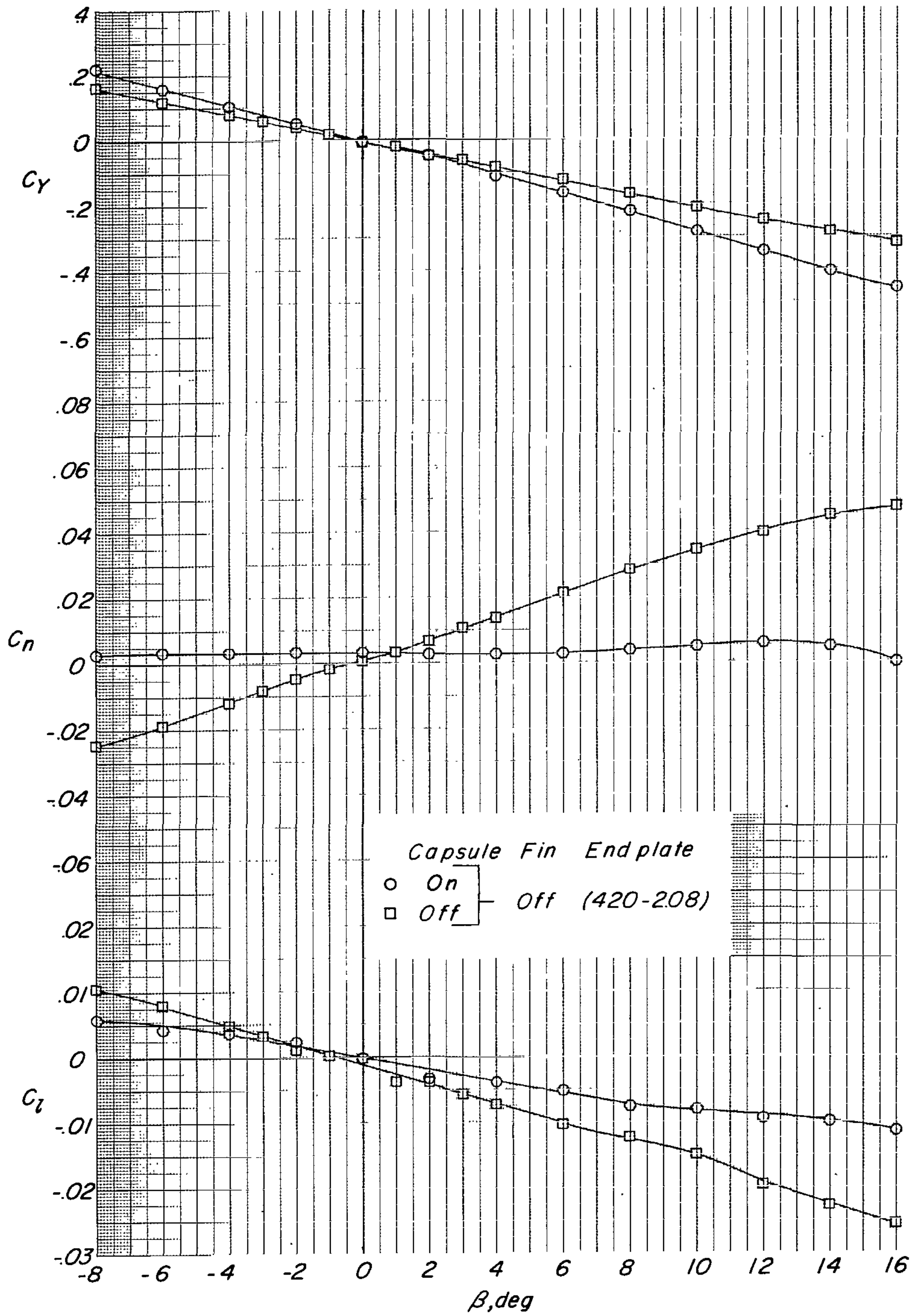

Figure 21.- Effect of capsule on aerodynamic characteristics in sideslip. Constant-chord stabilizer; elliptical tail fairing; rear capsule position; round struts; $\alpha = 0.42^{\circ}$.

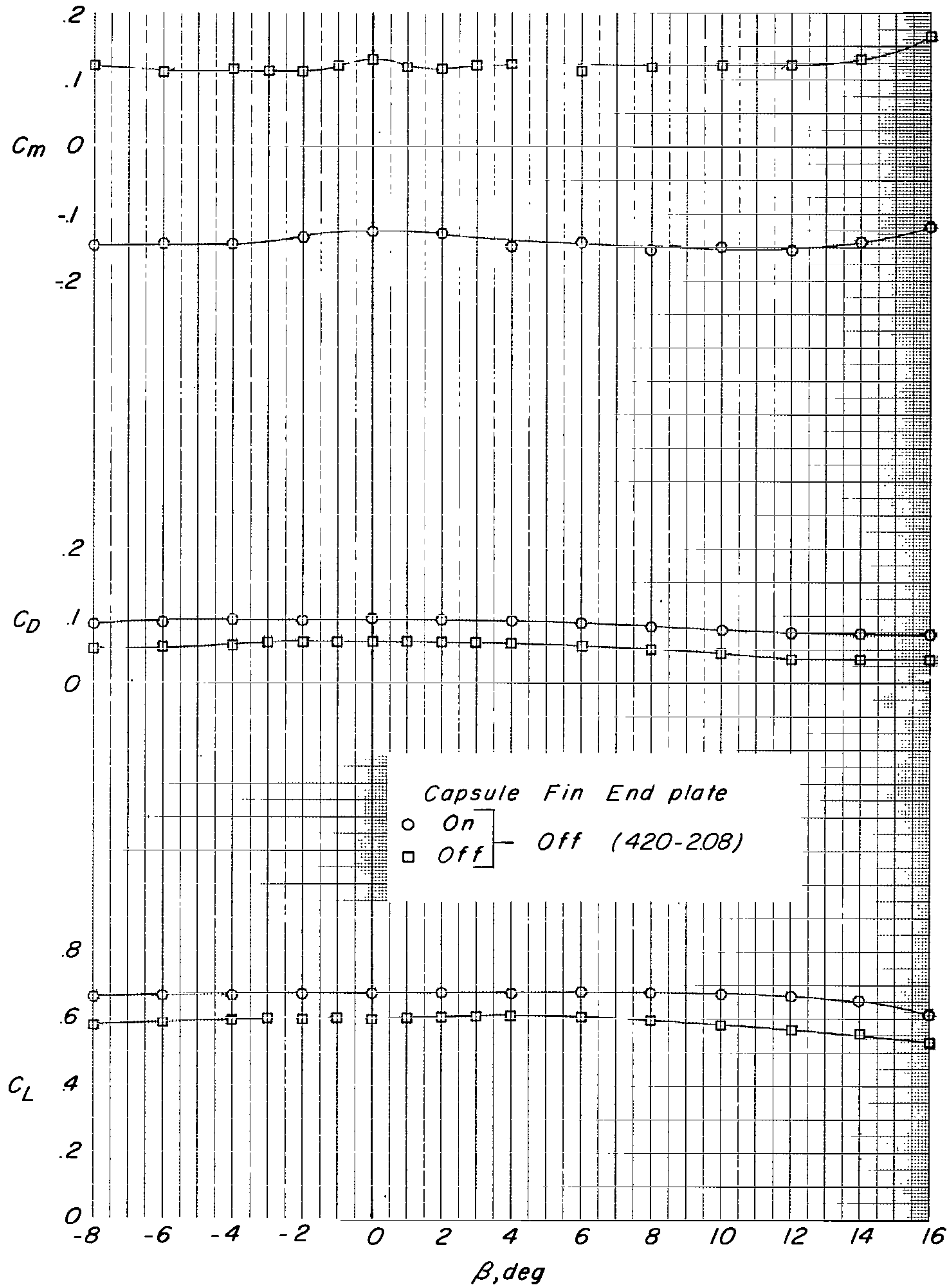

Figure 21.- Concluded.

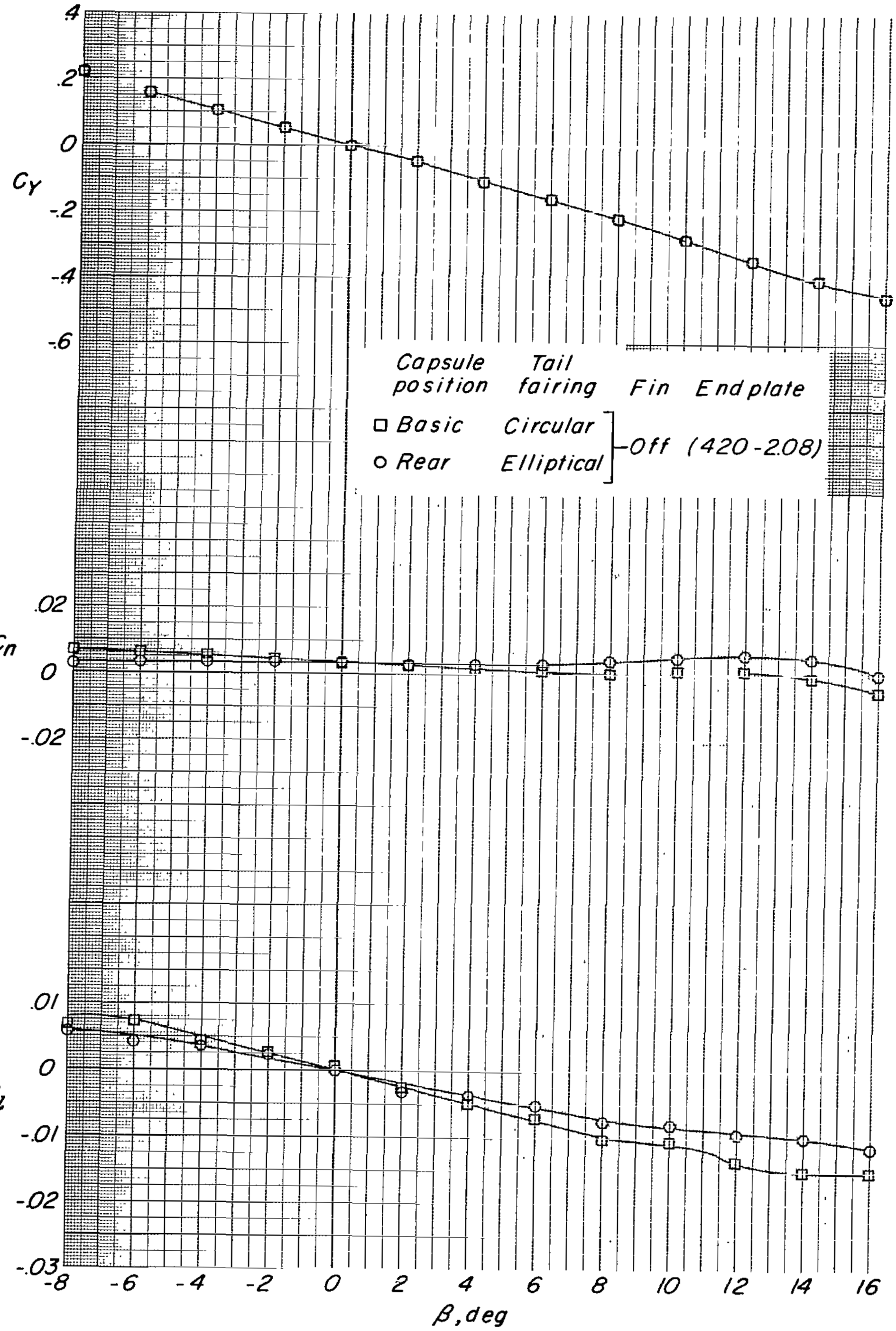

Figure 22.- Effect of capsule position on aerodynamic characteristics in sideslip. Constant-chord stabilizer; round struts; $\alpha = 0.43^{\circ}$.

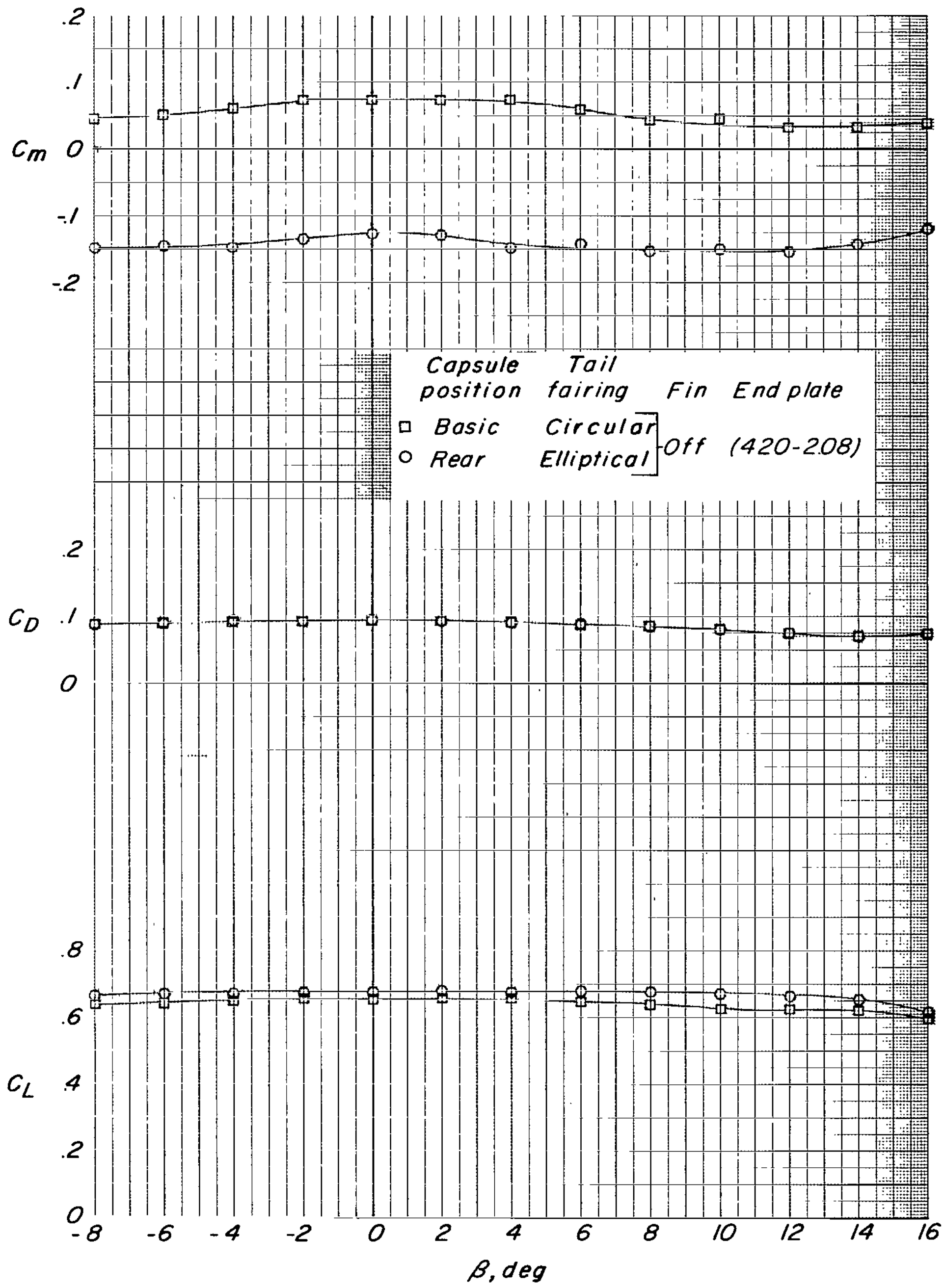

Figure 22.- Concluded.

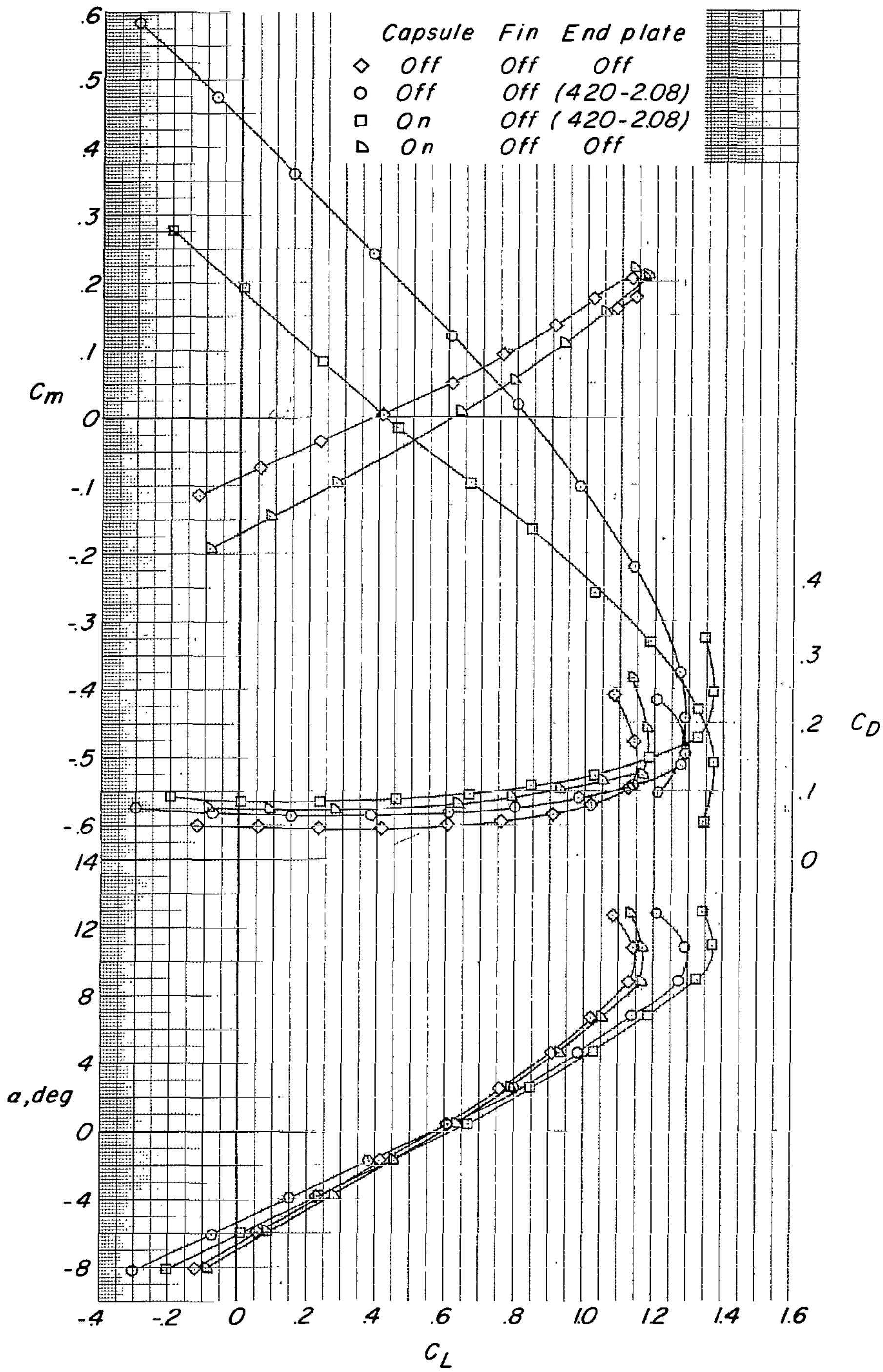

Figure 23.- Effect of capsule and end plate on aerodynamic characteristics in pitch. Constant-chord stabilizer; elliptical tail fairing; rear capsule position; round struts.

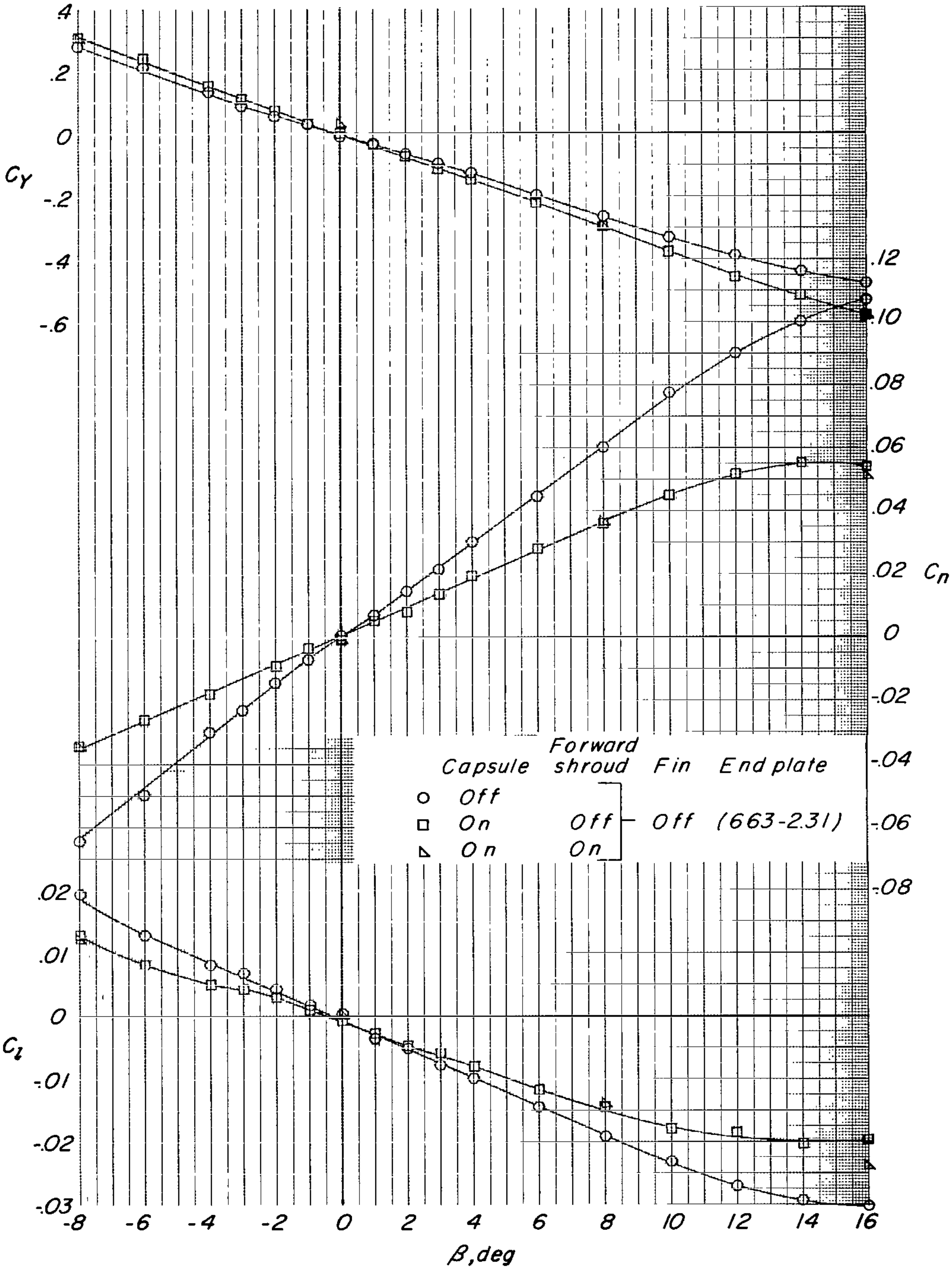

Figure 24.- Effect of capsule and nose fairings on aerodynamic characteristics in sideslip. Constant-chord stabilizer; elliptical tail fairing; rear capsule position; round struts; $\alpha = 0.42^{\circ}$.

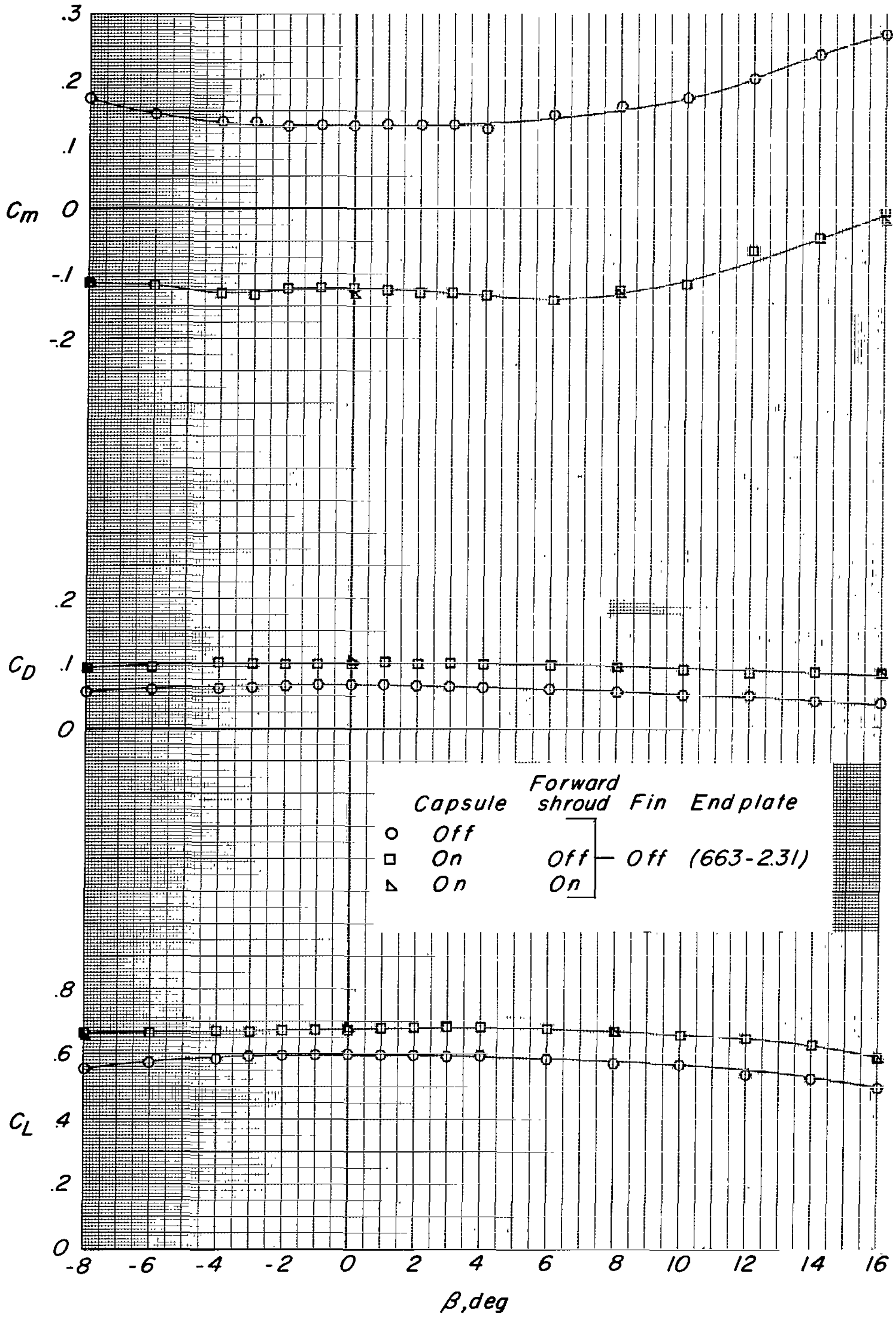

Figure 24.- Concluded.

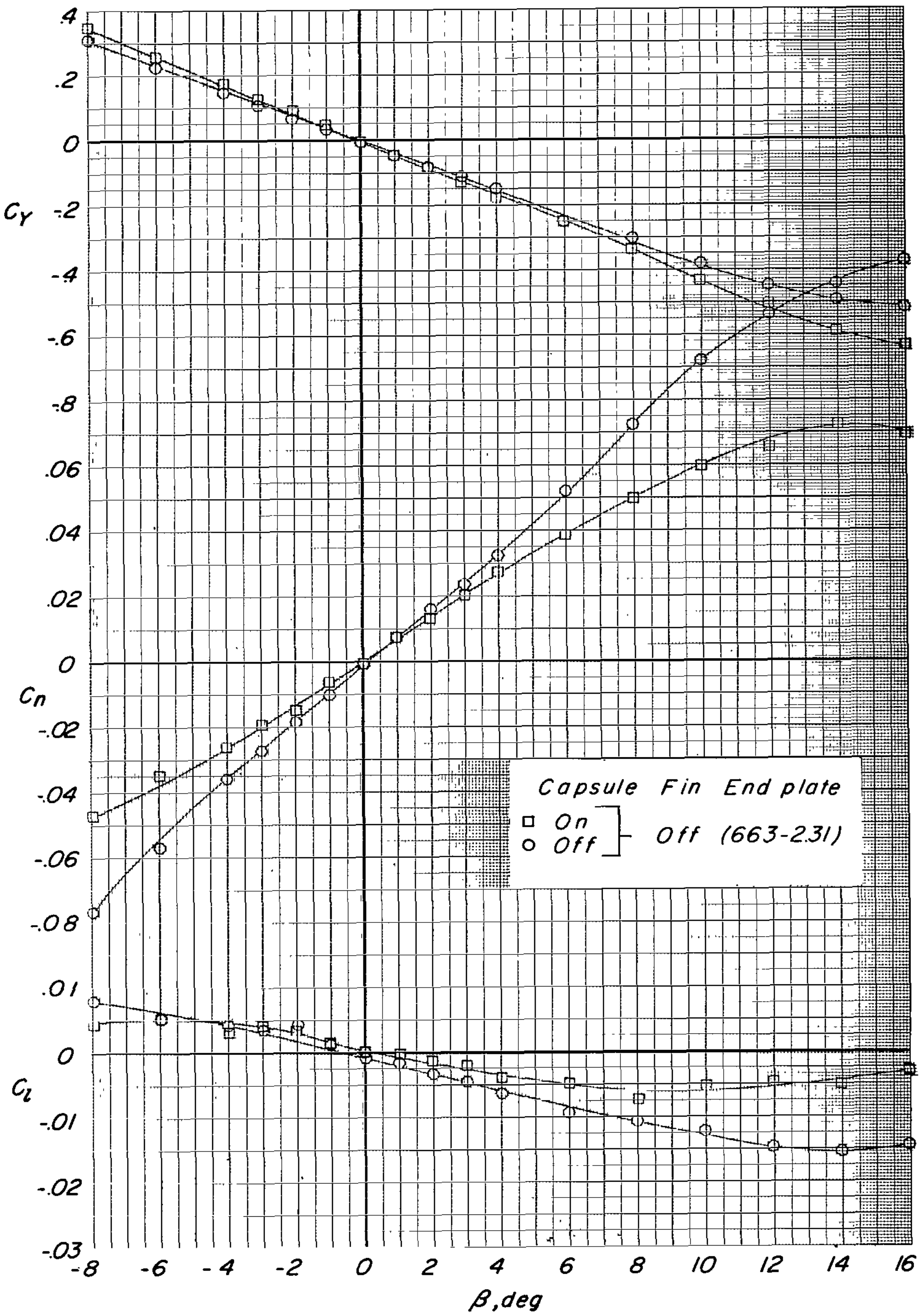

Figure 25.- Effect of capsule on aerodynamic characteristics in sideslip. Constant-chord stabilizer; elliptical tail fairing; rear capsule position; round struts; $\delta_f = 40^{\circ}$; $\alpha = 1.20^{\circ}$.

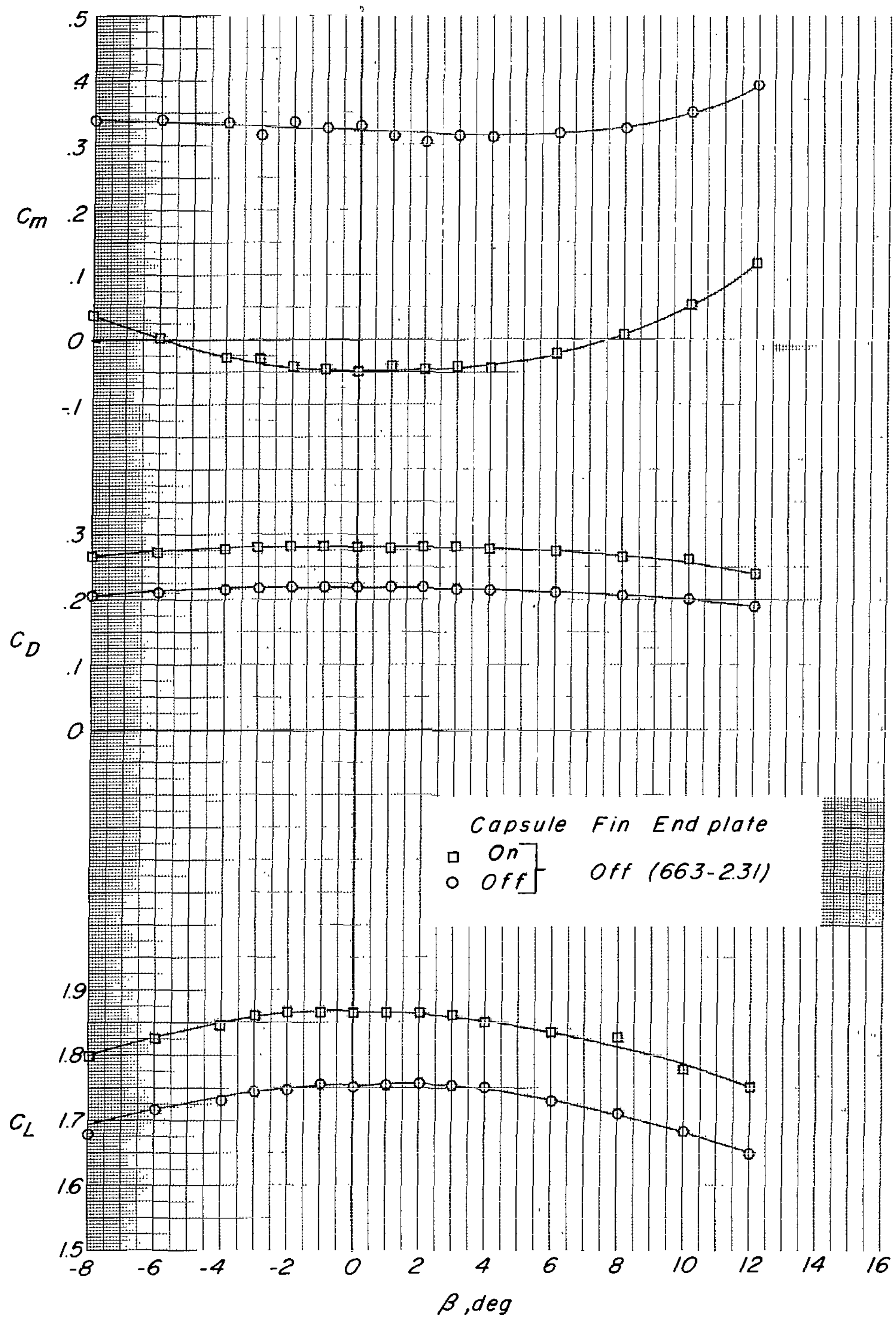

Figure 25.- Concluded.

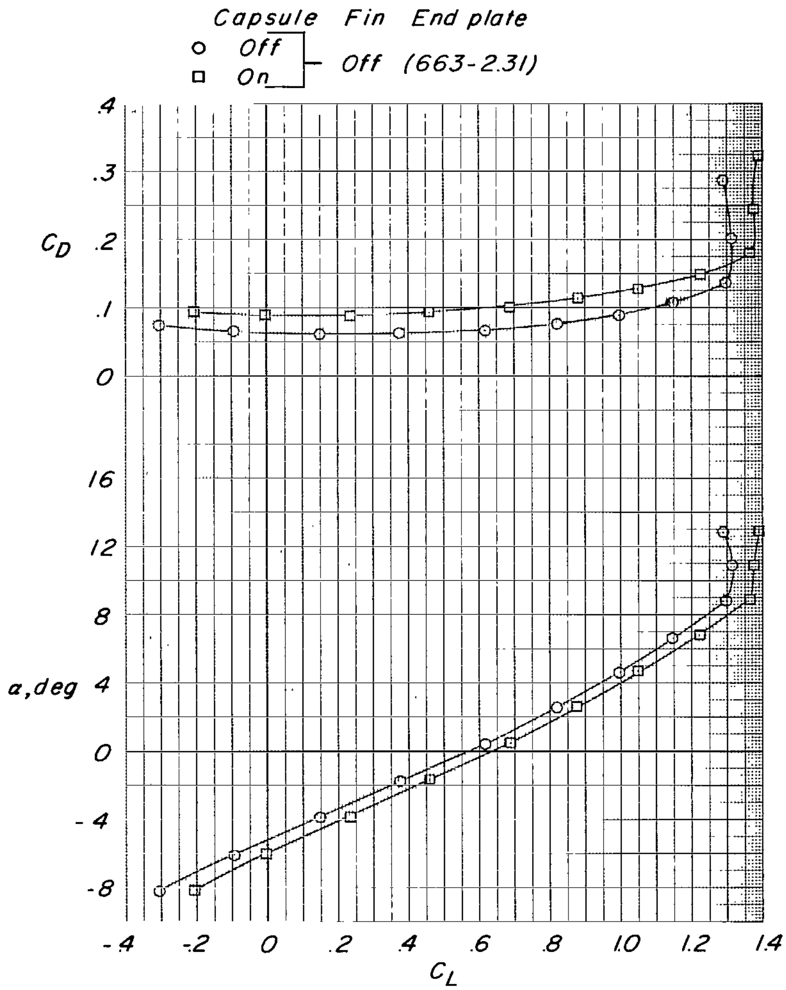

Figure 26.- Effect of capsule on aerodynamic characteristics in pitch. Constant-chord stabilizer; elliptical tail fairing; rear capsule position; round struts.

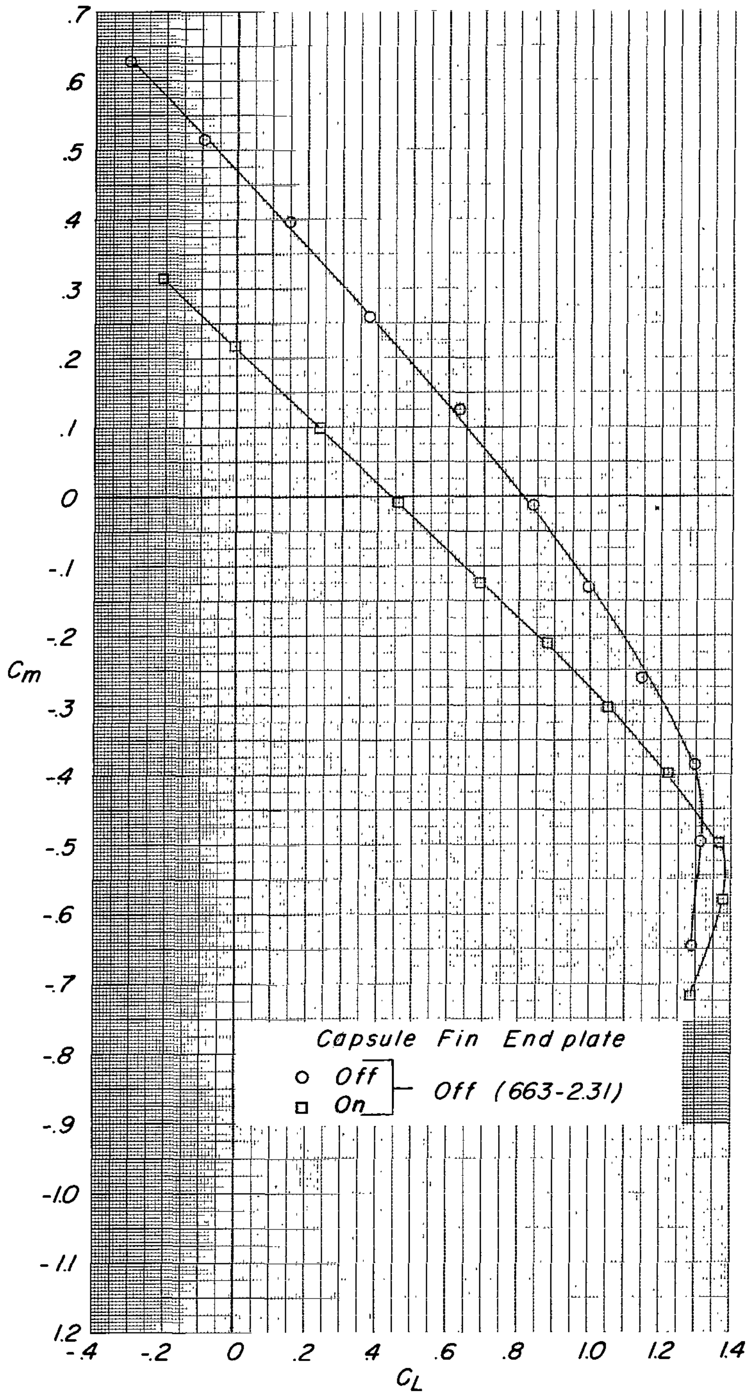

Figure 26.- Concluded.

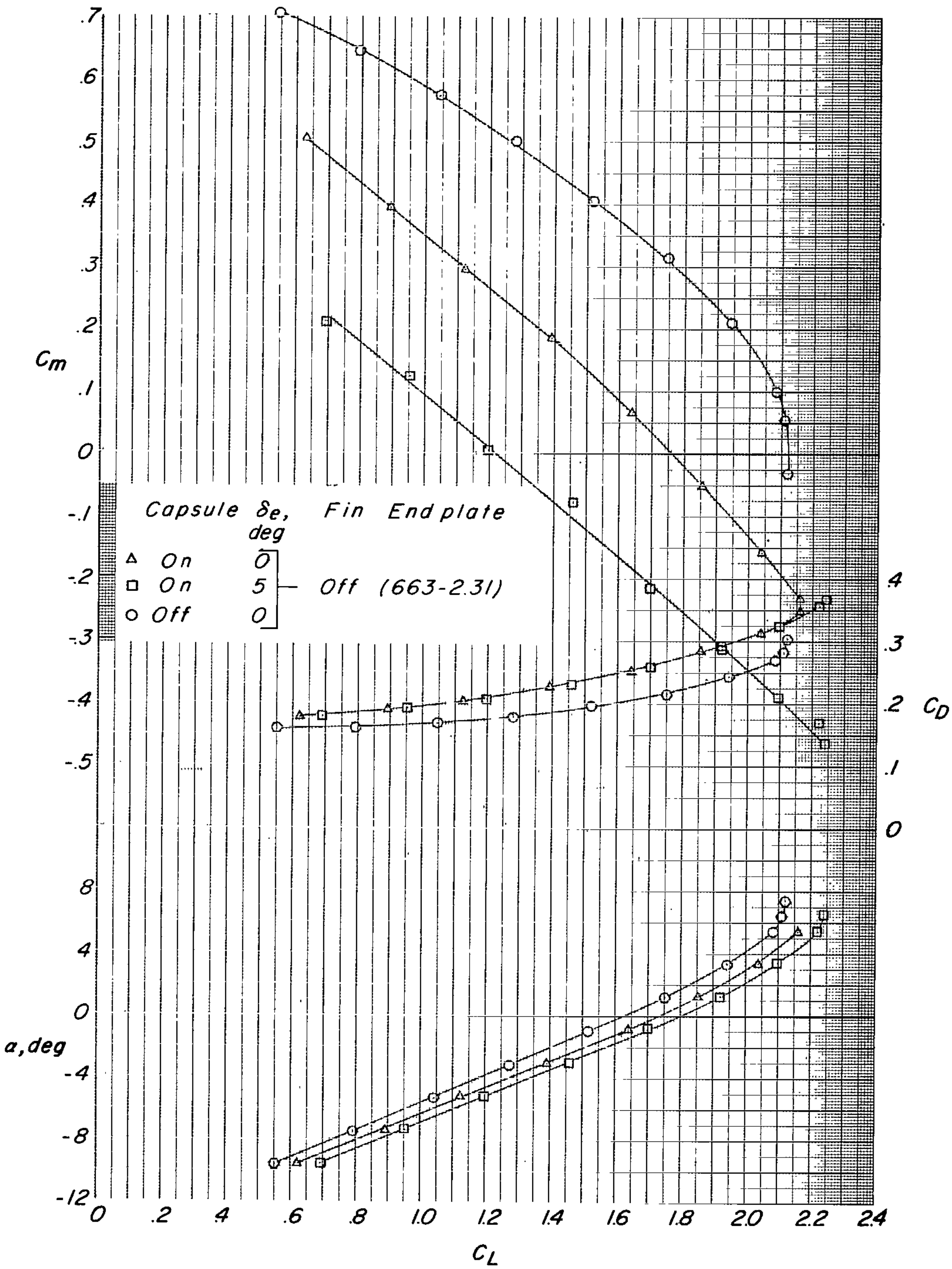

Figure 27.- Effect of capsule and elevator deflection on aerodynamic characteristics in pitch. Constant-chord stabilizer; elliptical tail fairing; rear capsule position; round struts; $\delta_f = 40^{\circ}$.

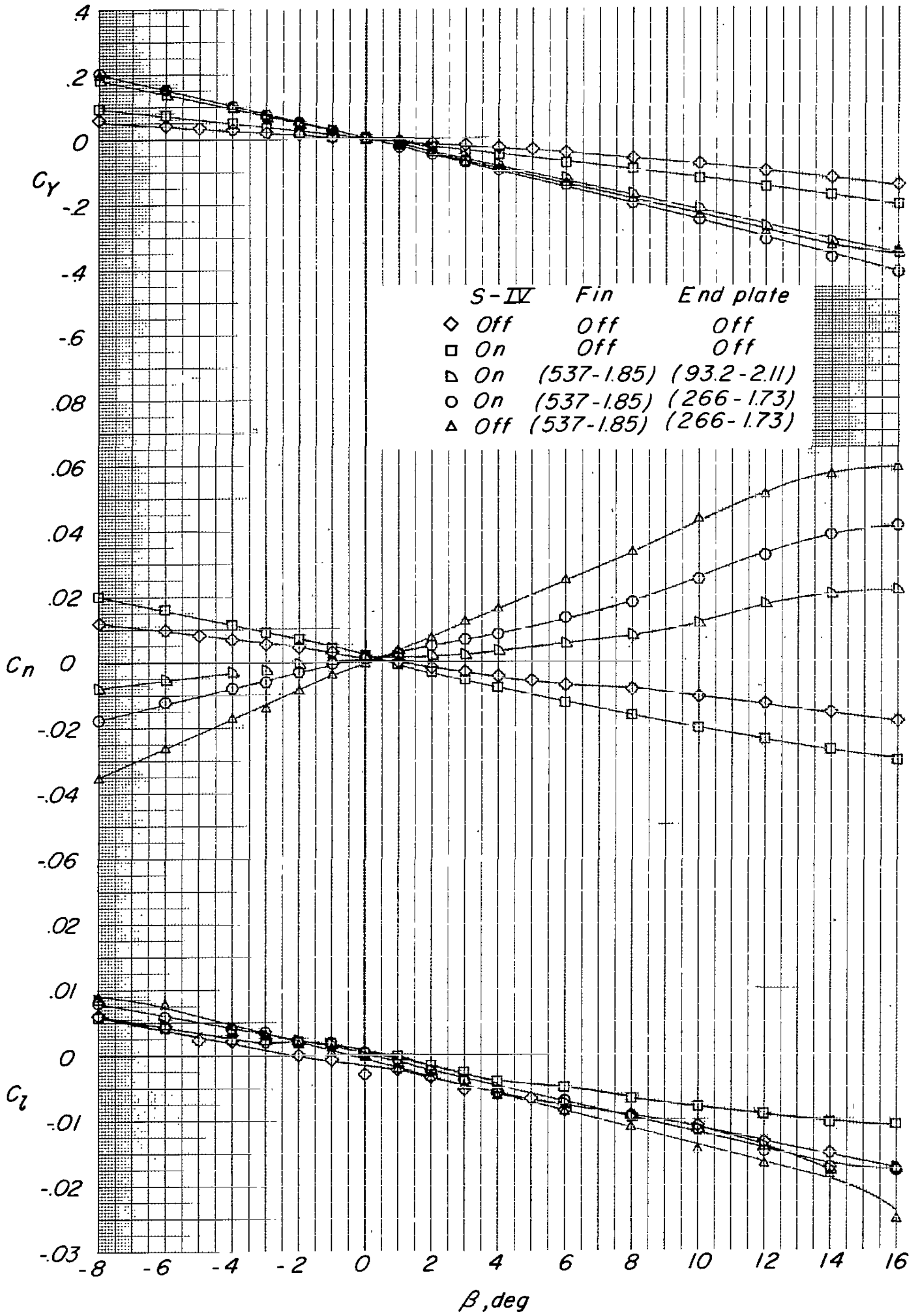

Figure 28.- Effect of S-IV and vertical-tail configuration on aerodynamic characteristics in sideslip. Basic stabilizer; $\alpha = 0.41^{\circ}$.

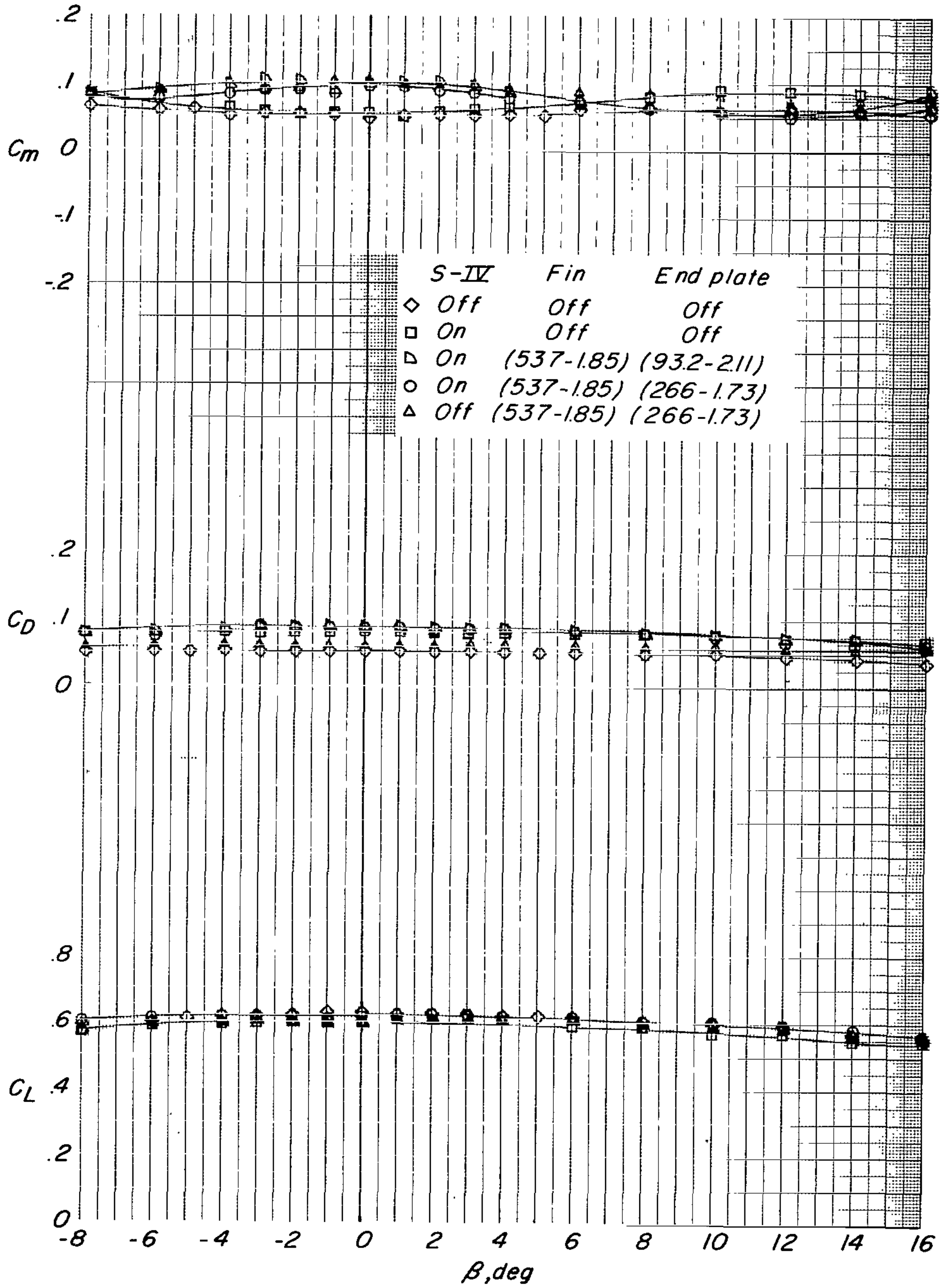

Figure 28.- Concluded.

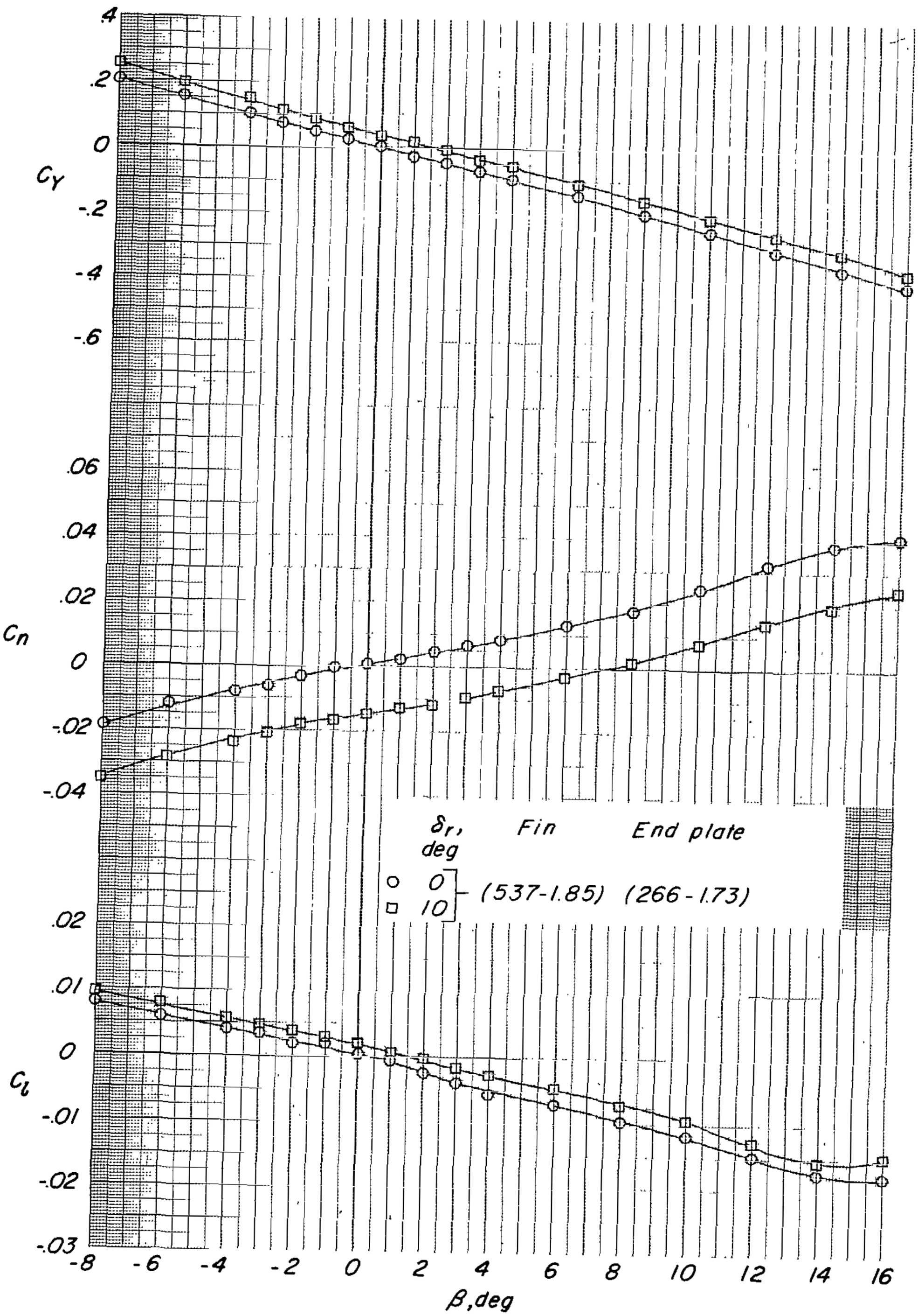

Figure 29.- Effect of rudder deflection on aerodynamic characteristics in sideslip. Basic stabilizer; S-IV on; $\alpha = 0.41^\circ$.

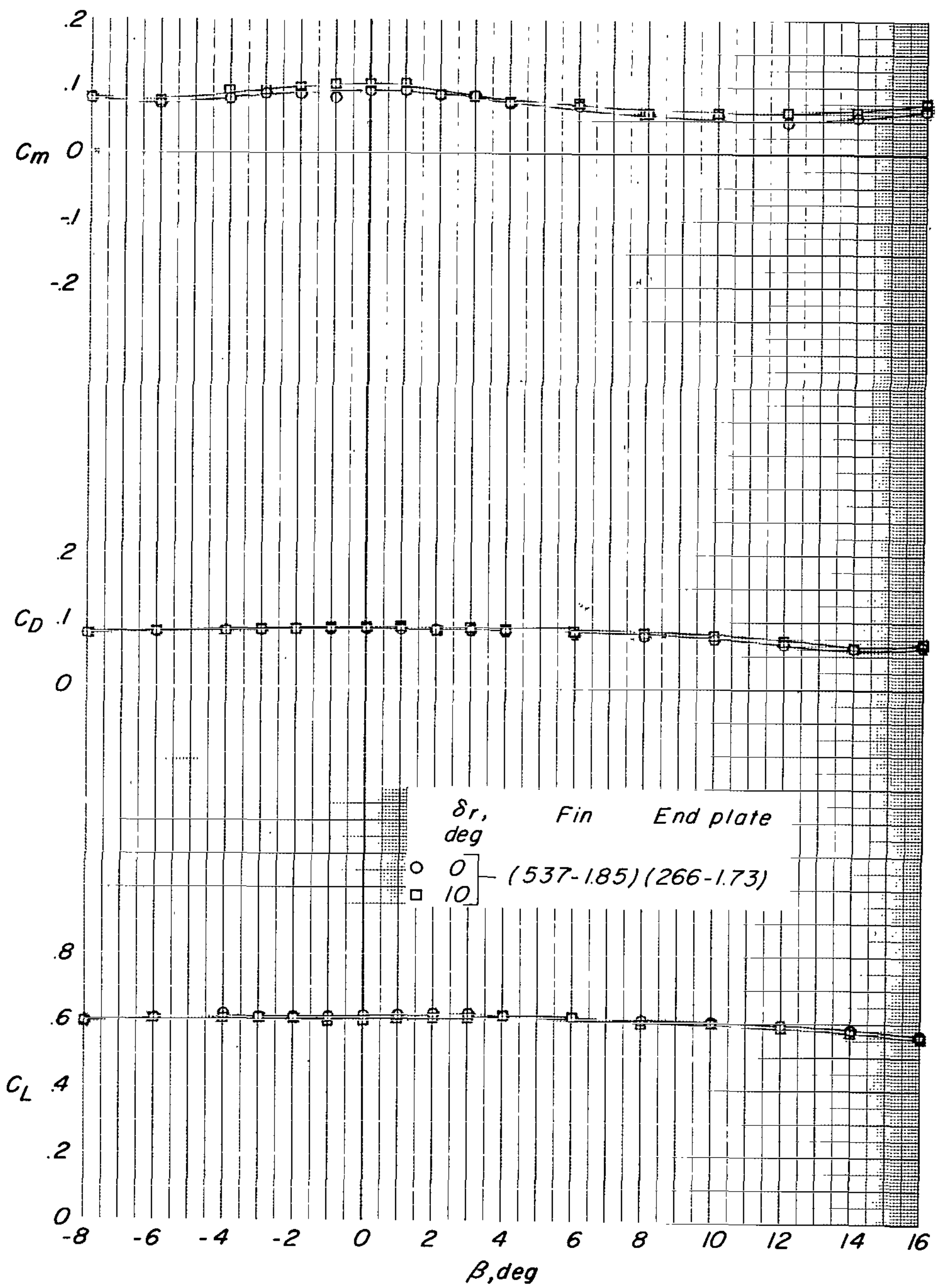

Figure 29.- Concluded.

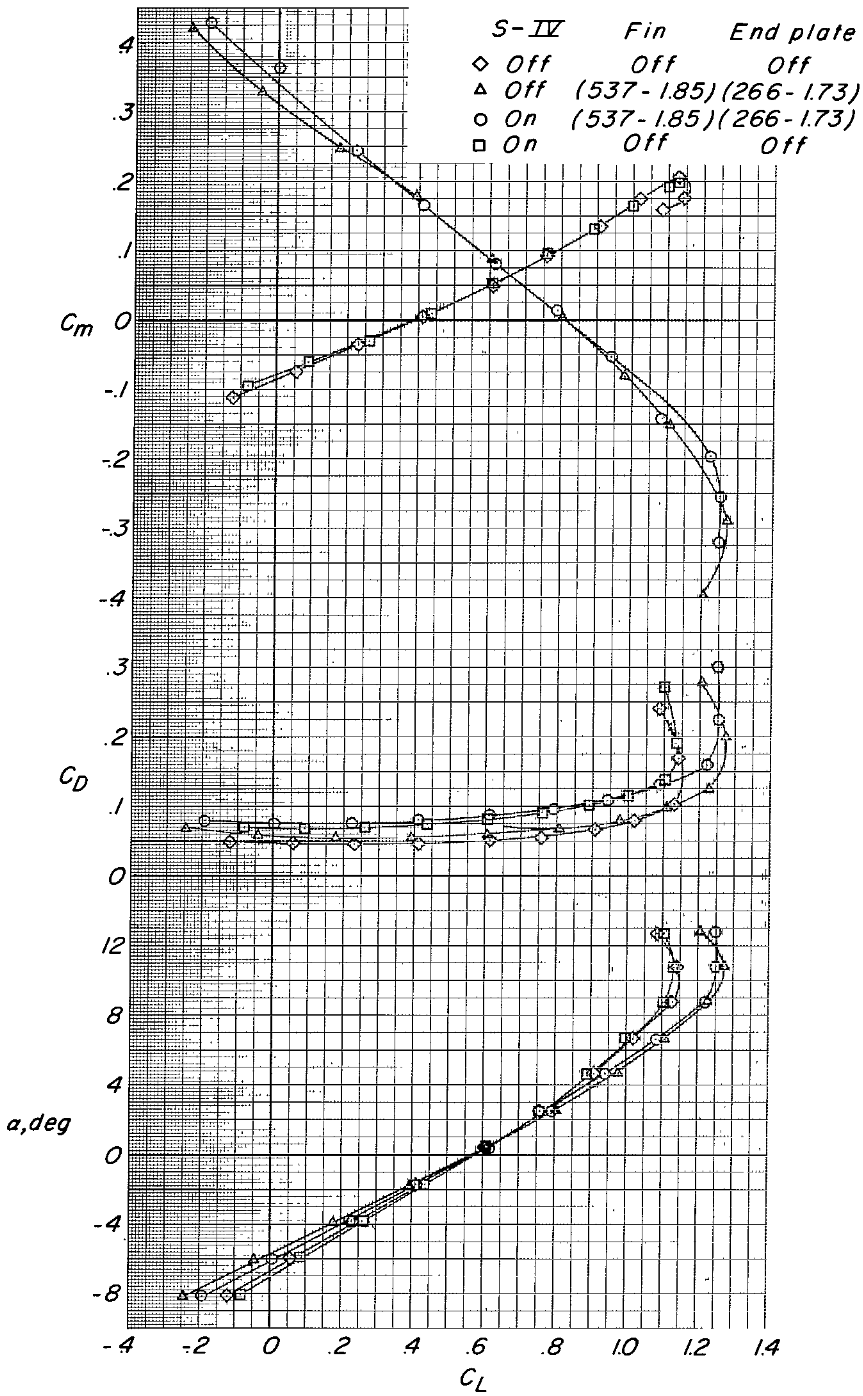

Figure 30.- Effect of S-IV and vertical-tail configuration on aerodynamic characteristics in pitch. Basic stabilizer.

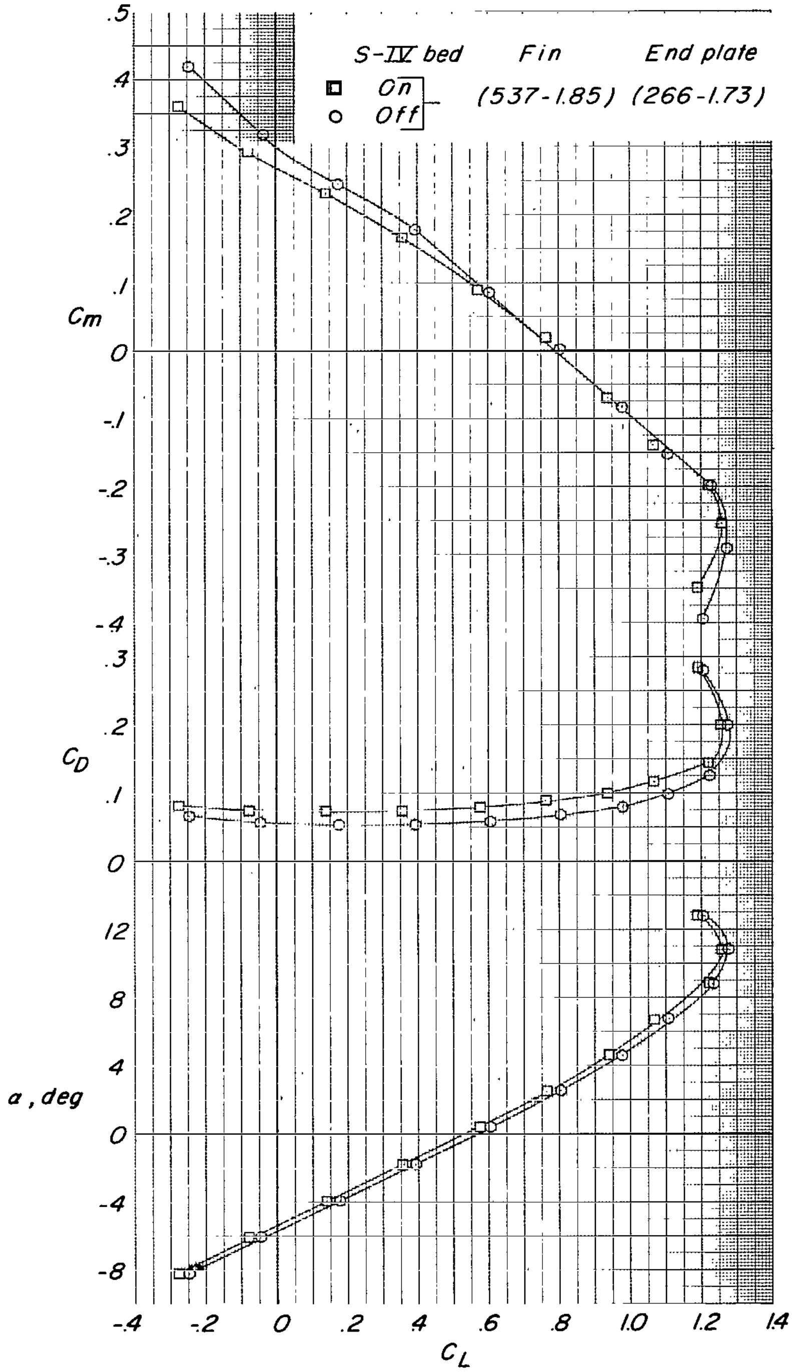

Figure 31.- Effect of S-IV bed on aerodynamic characteristics in pitch. Basic stabilizer.

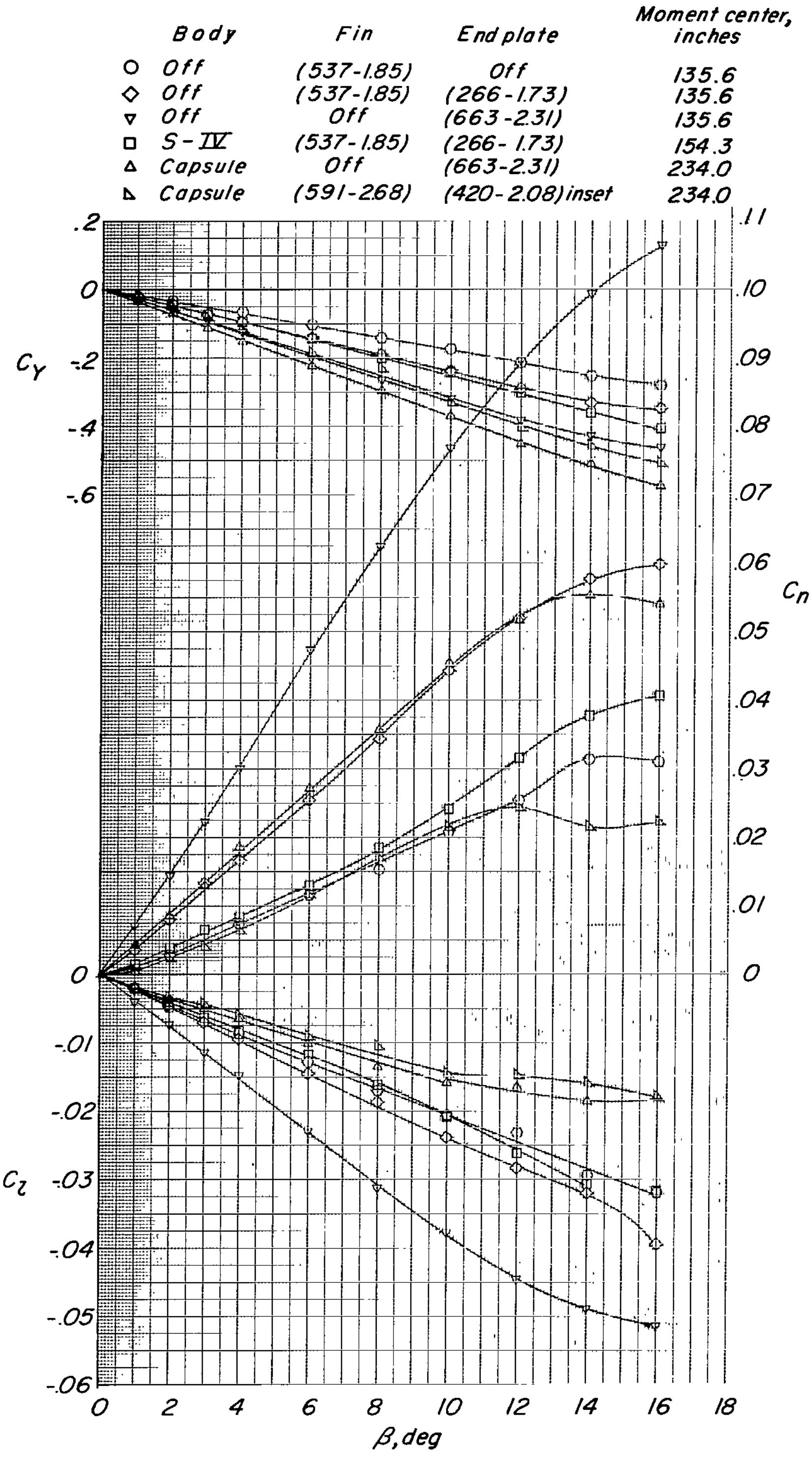

Figure 32.- Summary of effect of body and vertical-tail configuration on lateral aerodynamic characteristics. Elliptical tail fairing; rear capsule position; round struts; $\alpha = 0.42^{\circ}$. Moment centers are given with respect to bottom of fuselage.

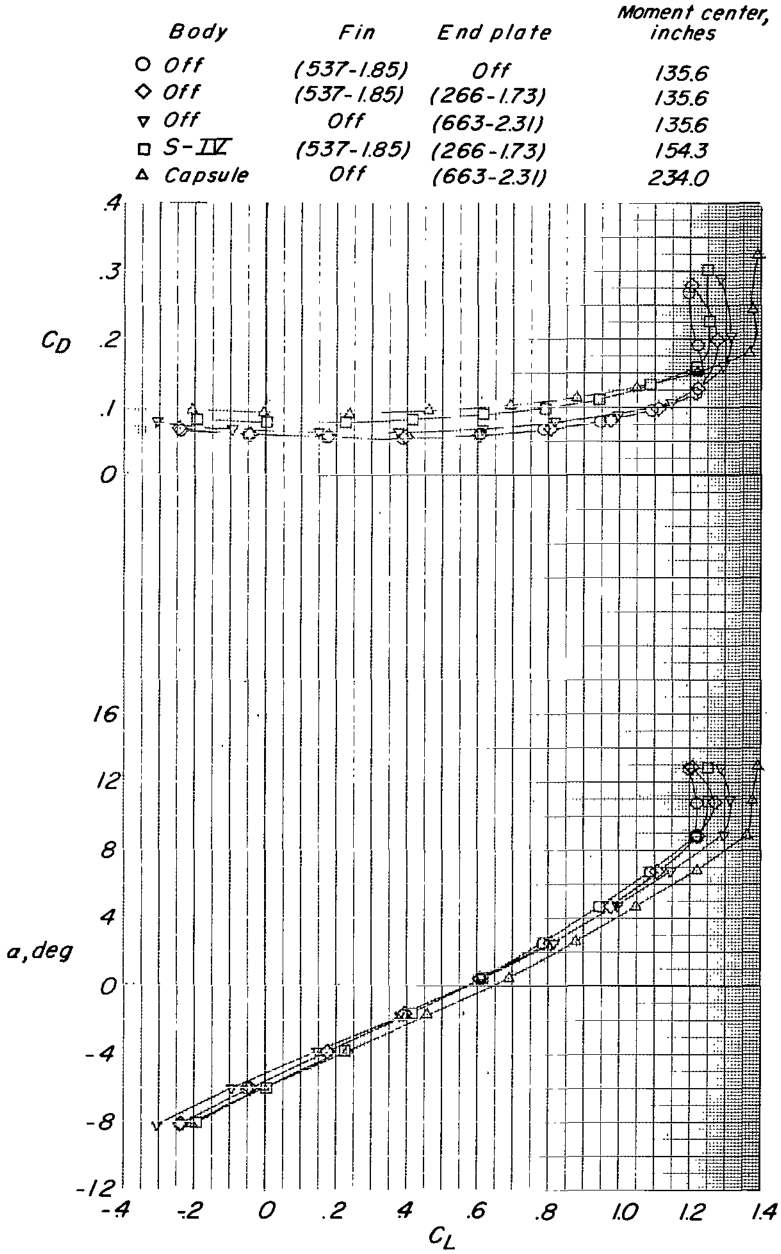

Figure 33.- Summary of effect of body and vertical-tail configuration on aerodynamic characteristics in pitch. Elliptical tail fairing; rear capsule position; round struts; $\beta = 0^{\circ}$. Moment centers are given with respect to bottom of fuselage.

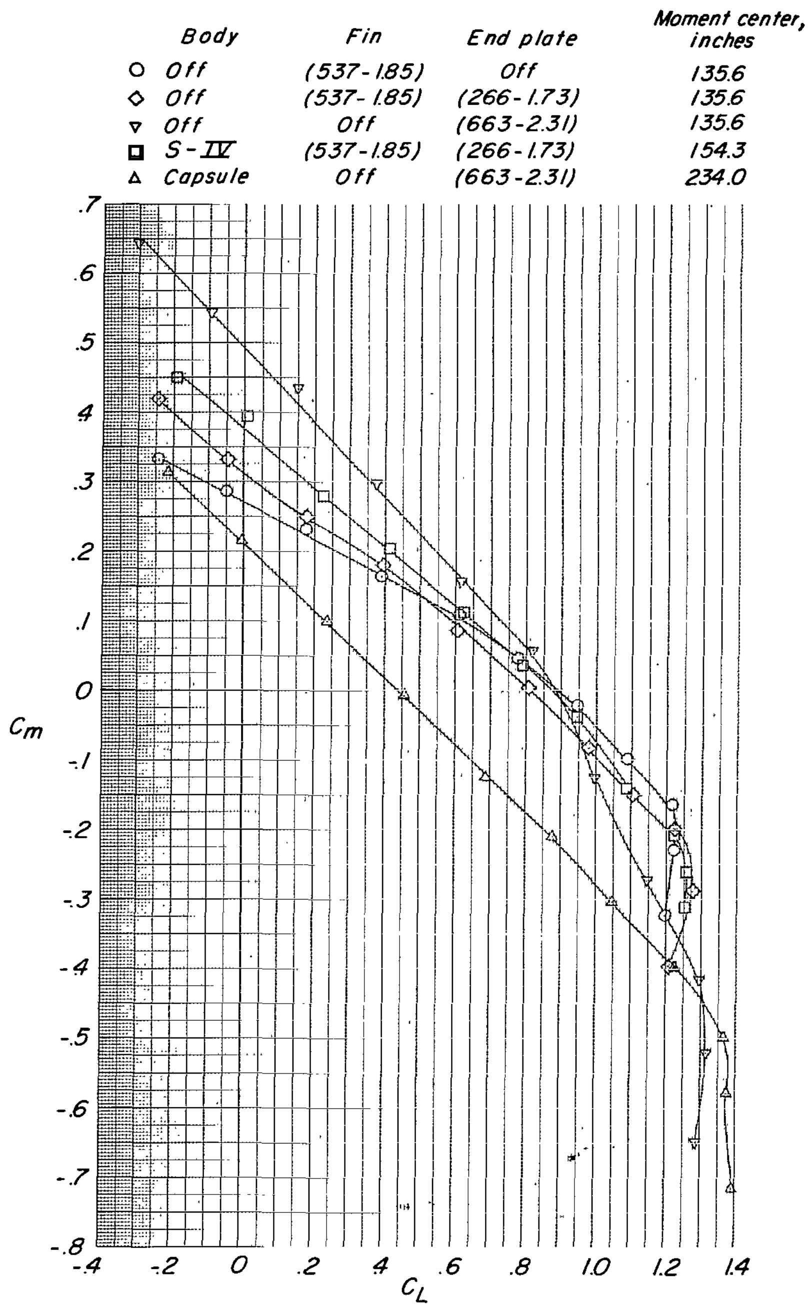

Figure 33.- Concluded.

NASA-Langley, 1964 L-3579

2/7/85